CELL-AUTONOMOUS AND NON-AUTONOMOUS ROLES FOR TGF-BETA SIGNALING IN PANCREATIC CANCER METASTASIS

by

Anne M. Macgregor-Das

A dissertation submitted to Johns Hopkins University in conformity with the requirements for the degree of Doctor of Philosophy

Baltimore, Maryland
March 2015

ABSTRACT

Pancreatic cancer is an almost universally lethal disease, with five-year survival rates approaching 6%. Its dismal prognosis is a consequence of several factors, including a lack of early detection methods, the inherent aggressive nature of this disease, and largely ineffective therapeutic regimens. Moreover, an overwhelming majority of patients are diagnosed at an advanced stage after their tumor has already metastasized. Decades of research have shed light onto the genes and signaling pathways that drive pancreatic carcinogenesis and progression. The transforming growth factor-beta (TGFβ) signaling pathway is often perturbed in pancreatic cancer, with alterations to the key transcription factor SMAD4 being observed in over half of all tumors. Paradoxically, TGFβ exerts both tumor suppressive and tumor-promoting influences. TGFβ suppresses tumor formation by regulating cell cycle progression and promoting apoptosis. However, it can also promote tumor progression by both cell autonomous and non-autonomous signaling mechanisms, namely, by promoting epithelial-mesenchymal transition, stromal deposition, and immune evasion. In pancreatic cancer, SMAD4 loss portends a worse prognosis and is correlated with widely metastatic disease. The goal of this thesis was to further understand the relationship between TGFβ signaling and metastatic efficiency in pancreatic cancer, with a particular interest on how TGFβ signaling in the tumor epithelium influences the tumor microenvironment. Using a novel conditional mouse model of pancreatic cancer, we show that reduced TGFβ signaling in invasive PDA results in the oligometastatic phenotype whereas oncogenic TGFβ signaling promotes widely metastatic disease. Additionally, inactivation of either TGFβR2 or SMAD4 in

pancreatic cancer cells alters the immune response in invasive disease by mediating the accumulation of regulatory immune cell subsets. It will be important to further investigate how TGFβ signaling facilitates the recruitment and polarization of these cells into tumors and the extent to which it influences their function in order to fully appreciate their contributions to progression and metastasis in pancreatic cancer.

Thesis Readers

Christine Iacobuzio-Donahue, M.D., Ph.D. (Thesis Advisor)
Professor of Pathology
Memorial Sloan Kettering Cancer Center

Michael Goggins, M.D. (Thesis Committee Member)
Professor of Pathology, Medicine and Oncology
The Johns Hopkins University School of Medicine

Acknowledgments

First, I want to give a special thank you to my thesis advisor Dr. Christine Iacobuzio-Donahue. Her passion for science is inspiring, and her constant support and encouragement over the years are much appreciated. I want to thank her for her mentorship, for allowing me to work on a project that combined my personal interests with the research interests of the lab, and for helping me to grow as an independent scientist. Additionally, I would like to thank Dr. James Eshleman, who has served as my co-mentor for the last year as I completed my thesis. Thank you for all your advice and support. I would also like to thank former and current lab members: Richard Morgan, Tyler Saunders, Cate White, Shinichi Yachida, Karen Matsukuma, Salva Naranjo-Suarez, Yi Zhong, Justin Poling, Vicente Valero, Alvin Makohon-Moore, and Jackie Brosnan-Cashman for thoughtful scientific discussions, for fun and relaxing lunches, dinners, happy hours and birthdays, and for making the lab an absolutely wonderful place to work for the last six years. A special thank you to the entire GI Pathology Group for everything they have done to support me during graduate school. Thank you to Dr. Nick Roberts and Dr. Laura Wood for their guidance over the last year. Additionally, special thanks to Dr. Robert Anders for spending countless hours looking over histology slides with me, and for all your advice.

I would also like to thank my thesis committee members: Dr. Elizabeth Jaffee, Dr. Chuck Drake, Dr. Michael Goggins, and Dr. Angelo DeMarzo for their insight, encouragement, and suggestions. Additionally, a special thank you to Dr. Goggins for his efforts in reviewing my dissertation. I would also like to thank the Pathobiology Graduate Program, especially our program director Dr. Noel Rose, co-director Dr. Ed Gabrielson,

former Program Coordinators Wilhelmena Braswell and Nancy Nath, and current Program Coordinator Tracie McElroy. To all my fellow Pathobiology classmates: Alyssa Walker, Sarah Croessmann, Joy Wu, Saniya Fayzullina, RenChin Wu, WeiWen Teo, and Sungyul Lee, thank you for your friendship, for keeping a smile on my face through problems sets and exams, and for your advice and insight over the last six years. To the rest of the Pathobiology students, I want to thank you for all the laughs, inside jokes, and support that each of you has offered. To Melek Sunay and Jackie Brosnan-Cashman – you are the best friends anyone could ever ask for. Thank you for being there when I needed you, for all your helpful suggestions, for the laughs and support. It means more to me than you can imagine.

Finally, to my family: I have been and always will be grateful for your love and support. A huge thank you to my parents Tom and Mary Lou, my brother Andy and sister Kali. Thank you for understanding my crazy work schedule, for listening to me talk about science and experiments, and for always inspiring me to keep going. And lastly, to my husband Sam – thank you for your amazing support and encouragement. Thank you for keeping me sane, for all the little things you do that you think go unnoticed (they do not!), and for being my best friend.

Table of Contents

List of Figures

List of Tables

Chapter 1 : Pancreatic Adenocarcinoma Background

Portions of this chapter have been published in a review and are reprinted here with permission from Wiley Periodicals, Inc.

Macgregor-Das AM and Iacobuzio-Donahue CA. 2013. Molecular pathways in pancreatic carcinogenesis. J Surg Oncol. 107(1):8-14.

Every year in the United States, approximately 44,000 people are diagnosed with pancreatic adenocarcinoma (PDA). It is among the most lethal of all cancers, with nearly 38,000 deaths per year and five-year survival rates of 6%. To date, pancreatic cancer remains the 4th leading cause of cancer deaths among both men and women (1).

A number of genetic studies have proven instrumental in elucidating the key genes, and more recently molecular pathways, that drive the formation and progression of pancreatic cancer. Early studies identified several genes that are frequently altered in pancreatic cancers (2). Subsequent analysis of the precursor lesions giving rise to pancreatic cancer indicated the temporal accumulation of these genetic alterations during pancreatic carcinogenesis (3). Most recently, next generation sequencing technologies have revealed the genetic landscape of neoplasms that arise from preinvasive neoplasms of the pancreas. Such surveys are helping to shape the development of new, personalized approaches to clinical management and therapy for pancreatic cancer patients.

Pancreatic Carcinogenesis

Precursors to Pancreatic Cancer. Three precursors to pancreatic cancer have been described (4; 5). The vast majority of pancreatic cancers develop from microscopic precursors called pancreatic intraepithelial neoplasia (PanIN), that originate in small terminal (<5 mm) pancreatic ducts (4) (Figure 1.1). PanINs are further classifiable based on their degree of morphologic atypia. In PanIN-1 lesions transformation of the normal ductal epithelium into tall columnar cells with intracellular mucin is seen, whereas PanIN-2 lesions are notable for the development of cytologic atypia and nuclear crowding. PanIN-3 lesions are characterized by extensive nuclear crowding and nuclear atypia, pseudopapillary growth, mitotic figures and intraluminal necrosis (4; 6).

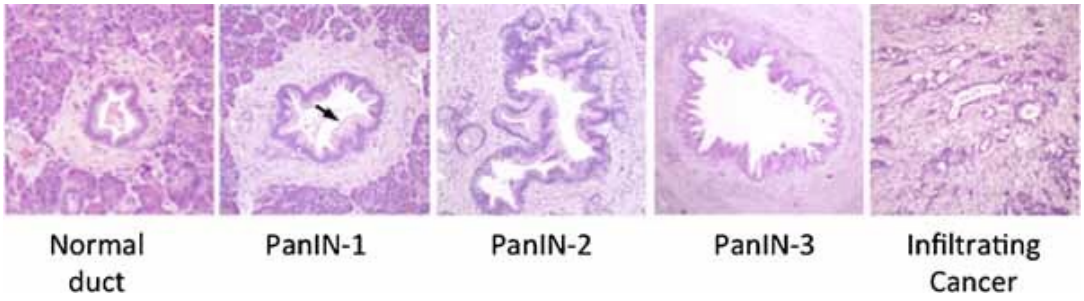

Figure 1-1: Morphologic Progression Model of Pancreatic Intraepithelial Neoplasia

Shown from left to right are histological examples of a normal pancreatic duct, pancreatic intraepithelial neoplasia (PanIN), and pancreatic cancer. Normal ducts are characterized by a low cuboidal epithelium surrounded by a periductal fibrotic cuff. PanIN-1 lesions are differentiated from normal ductal epithelium by the presence of mucinous hyperplasia of the ductal cells (arrows) but without cytological atypia. PanIN-2 lesions are notable for the presence of nuclear enlargement, atypia, crowding and papillary infoldings of the epithelium. PanIN-3 lesions, synonymous to high-grade dysplasia/carcinoma in situ, show a complete loss of cell polarity (arrows) and marked cytological atypia in association with frequent mitotic figures and pseudopapillary growth of the neoplastic epithelium. PanIN-3 lesions may progress to invasive cancer that is characterized by poorly formed neoplastic glands with an infiltrative growth pattern admixed with abundant desmoplastic stroma.

By contrast, intraductal papillary mucinous neoplasms (IPMNs) and mucinous cystic neoplasms (MCNs) are macroscopically visible cystic neoplasms. IPMNs arise in the mucin-producing main pancreatic duct or one of its branches (Figure 1.2A; 1.2B) where they distend the duct system by intraductal growth of the neoplasm and by copious mucin production. MCNs are typically intraparenchymal and do not communicate with the pancreatic duct system (Figure 1.2C; 1.2D). Histologically, MCNs are characterized by a mucinous epithelial lining in association with an underlying ovarian-like stroma (Figure 1.2D). A detailed discussion of the morphologic features of dysplasia in cystic precursors is beyond the scope of this review, but both IPMNs and MCNs also show a range of morphologic features ranging from low grade, to moderate, to high grade dysplasia (5). Ultimately, pancreatic cancer may arise from any of these above precursor lesions yet cancers arising in association with PanINs are much more common (7).

The Genetic Progression Model. The genetic events that accumulate during carcinogenesis have been best described for PanINs (Figure 1.3). Genetic events detected in PanIN-1 lesions include telomere shortening and activating mutations in *KRAS* (8; 9). PanIN-2 lesions exhibit *CDKN2A* loss while PanIN-3 lesions demonstrate genetic inactivation in *TP53*, *SMAD4* and *BRCA2* (8). Of course, exceptions to these scenarios have been shown with occasional PanIN-1 having *CDKN2A* loss or PanIN-2 having *TP53* inactivation (10). While the morphological progression of IPMNs and MCNs from low to moderate to high grade dysplasia is well known, the relationship of these morphologies to accumulating genetic abnormalities is less well characterized. However, as discussed later in this review the genetic events underlying IPMN and MCN formation are now being determined.

KRAS. One of the earliest and most universal genetic alterations observed in pancreatic cancer is activating mutations in the oncogene *KRAS* (11). At least 99% of PanIN-1 lesions harbor mutations in *KRAS*, suggesting its activation is an important initiating step in carcinogenesis of most pancreatic cancers (10). *KRAS* encodes a guanosine triphosphate (GTP)-binding protein, which functions as a key mediator in a variety of cellular processes, including cell survival, proliferation, and cell motility. In its inactive state, Ras is bound to GDP. Extracellular signaling through growth factor receptors triggers the removal of GDP from Ras, allowing GTP to bind. Inactivation of these active Ras-GTP complexes is accomplished when GTP is hydrolyzed. Activating mutations in the *KRAS* gene result in a loss of the intrinsic GTPase activity of the Ras protein, and consequently, constitutive signaling occurs even in the absence of extracellular signals (12). Activated Ras feeds into a number of signaling pathways, including the RAF/mitogen activated protein (MAP) kinase pathway, as well as into the phosphoinositide-3-kinase (PI3K)/AKT signaling pathway. Activating mutations in *BRAF* are observed in a subset of pancreatic cancers lacking *KRAS* mutations, resulting in aberrant Ras-Raf-MAPK signaling (13).

CDKN2A. The tumor suppressor gene *CDKN2A* is inactivated in over 90% of pancreatic ductal adenocarcinomas, with the vast majority of alterations arising as early as the PanIN-2 stage (14; 15). The *CDKN2A* gene possesses alternative splicing sites that result in the formation of several protein products. For example, the p14/ARF protein sequesters MDM2 helping to stabilize TP53 whereas the p16/INK4A protein acts to inhibit the formation of complexes between cyclins and cyclin-dependent kinases (CDKs) thus regulating progression through the G_1 checkpoint in the cell cycle (16-18).

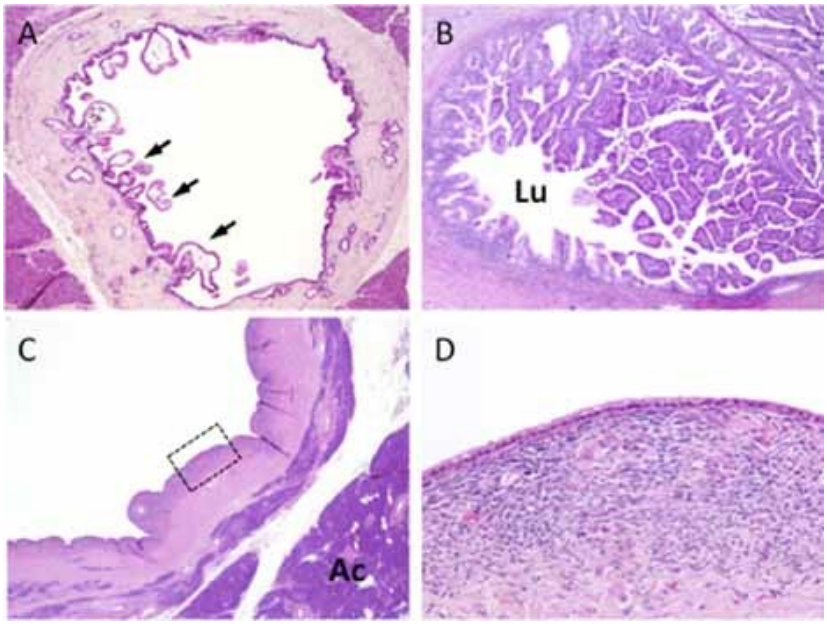

Figure 1-2: Morphologic Features of Cystic Neoplasms of the Pancreas

A: Intraductal papillary mucinous neoplasm (IPMN) of the main pancreatic duct. In this example the IPMN shows low-grade dysplasia, with scattered papillae seen at low power (arrows). **B**: IPMN with high-grade dysplasia. The neoplasm shows exuberant papillary growth that fills the lumen (Lu) of the main pancreatic duct. **C**: Low power view of a mucinous cystic neoplasm (MCN). The neoplasm is distinct from the surrounding pancreatic acinar tissue (Ac). **D**: High power view of the region outlined in panel C showing low cuboidal mucinous epithelial lining and underlying ovarian-like stroma.

In about 40% of cases, inactivation of *CDKN2A* occurs through homozygous deletion. Intragenic mutation with subsequent loss of the second allele acts as a second mechanism for *CDKN2A* loss, accounting for another 40% of alterations. Methylation of the promoter region of *CDKN2A*, resulting in gene silencing, has also been observed (14).

TP53. Inactivation of the *TP53* gene is observed in higher-grade, PanIN-3 lesions (19). Up to 85% of pancreatic cancers have *TP53* inactivation, with the most frequent mechanism of inactivation being intragenic mutation with loss of the second allele (20; 21). TP53 functions as an essential regulator of many interrelated cellular processes including apoptosis, cell cycle progression and DNA repair. In response to DNA damage, TP53 can promote the transcription of *p21*, a CDK inhibitor that can bind to cyclin-CDK complexes, leading to cell cycle arrest in the G_1 phase. TP53 can also regulate transcription of both pro and anti-apoptotic genes. Loss of *TP53* results in an overall increase in genomic instability, as cells are permitted to proliferate in the setting of otherwise catastrophic DNA damage (22).

SMAD4. As is seen with *TP53*, *SMAD4* loss is observed in high-grade PanIN-3 lesions (23). Inactivation of *SMAD4*, either by homozygous deletion or intragenic mutation with the loss of the second allele, occurs in ~55% of pancreatic ductal adenocarcinomas (24). The Smad4 protein plays a key role in propagating extracellular signals through the transforming growth factor β (TGFβ) signaling pathway. TGFβ regulates cell proliferation and differentiation, and thus acts as a critical tumor suppressor in normal cells. Activation of this pathway begins with binding of a TGFβ ligand to type I and type II serine/threonine kinase cell surface receptors. This results in receptor dimerization and activation of the type I receptor leading to its phosphorylation of the

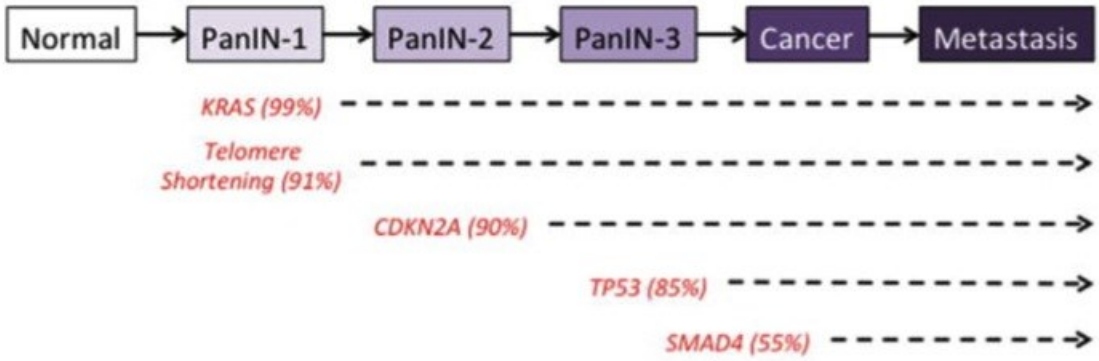

Figure 1-3: Genetic Progression Model of Pancreatic Carcinogenesis

The molecular alterations that accumulate during pancreatic carcinogenesis can be classified into early (telomere shortening and activating mutations in *KRAS2*), intermediate (inactivating mutations or epigenetic silencing of *CDKN2A*) and late (inactivating mutations of *TP53* and *SMAD4*) events. Mutations in additional genes may also occur during PanIN formation but are not illustrated in this example.

Smad2 and Smad3 proteins. Smad4 complexes with phosphorylated Smad2/3 proteins and together they translocate into the nucleus where, in association with transcriptional cofactors, regulate the expression of genes involved in a variety of important cellular processes including cell cycle control, cell differentiation and growth (25). Loss of *SMAD4* and hence canonical TGFβ signaling in pancreatic ductal adenocarcinomas results in the loss of TGFβ-induced growth inhibition (26), and correlates with both poor prognosis and the development of widespread metastases in patients (25; 27; 28).

Observations from Exomic Sequencing Approaches

Genetic alterations in *KRAS*, *CDKN2A, TP53*, and the TGFβ family were initially elucidated using candidate gene approaches, namely dideoxy (Sanger) sequencing. However, in recent years next generation sequencing methodologies have been used to examine the entire coding fraction of the genome (i.e. the "exome") with the goal of identifying the entire compendium of somatic alterations in this tumor type (20). This, in turn, has contributed to creating a more comprehensive genetic landscape by uncovering both gene "mountains" and "hills", i.e. genetic alterations that are observed in a high and low frequency of tumors, respectively (29).

The Landscape of Pancreatic Cancer. A total of 20,661 protein-coding genes have been analyzed in 24 pancreatic cancers (20), leading to identification of a total of 1562 somatic alterations. The majority of these changes were found to be base substitutions; however, small insertions and deletions as well as alterations within the untranslated regions (UTRs) and at splice sites were also observed. Over 1300 genes were found to contain at least one genetic alteration, with 148 genes containing two or more alterations. Copy number analysis was also utilized to interrogate gene deletion and

amplification events, and revealed a total of 198 homozygous deletions and 144 focal high-copy amplifications in the 24 tumors analyzed. Genes within these regions of deletion or amplification included well-established tumor suppressors and oncogenes, respectively; however, additional genes that had not been previously associated with pancreatic ductal adenocarcinoma were also found.

A list of candidate cancer genes ("CAN" genes) was generated based on the set of genes harboring somatic alterations (20). This analysis was based largely on passenger mutation rates, gene mutation type and frequency. Importantly, this list included each of the previously identified genes known to play a role in pancreatic carcinogenesis (*KRAS*, *CDKN2A*, *TP53* and *SMAD4*) indicating the robustness of this approach. Genes not previously appreciated in this tumor type were also identified, for example *MLL3*. The significance and roles of each of these CAN genes remains to be determined in functional systems; however, new studies of these genes in various tumor types is shedding light onto emerging processes and pathways involved in tumorigenesis (30-32).

Core Signaling Pathways of Pancreatic Cancer. Further categorization of the somatic alterations data generated by whole exome sequencing revealed that they correspond to 12 core signaling pathways (Figure 1.4). Many of these pathways consist of genes that have already been appreciated as players in pancreatic cancer formation and progression, such as DNA damage control (*TP53*), cell cycle regulation (*CDKN2A*) and TGFβ signaling (*SMAD4*). Most importantly, the authors were able to show that while most patients' carcinomas exhibited a genetic alteration corresponding to each of the 12 core pathways, the specific gene mutated for a given pathway in each patient often varied. This finding may help account for both the heterogeneous nature of tumors, as

well as offer insight into why agents targeting a specific gene in a pathway rarely result in a therapeutic advantage in more than a minor percentage of patients.

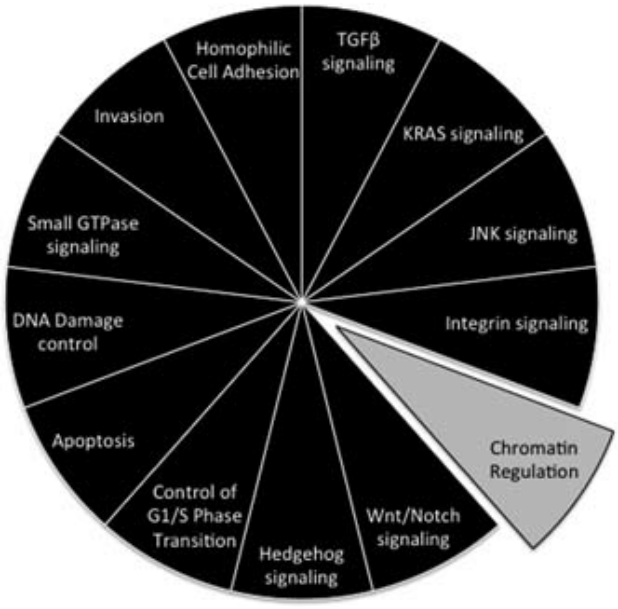

Figure 1-4: Core Signaling Pathways in Pancreatic Cancer

The 12 pathways and processes whose component genes were genetically altered in most pancreatic cancers based on whole exome sequencing 20 are shown in black, and the pathway more recently identified in pancreatic cancer in gray 31–34. Therapeutic targeting of one or more of these pathways, rather than specific gene alterations that occur within a pathway, provides a new paradigm for treatment of pancreatic cancer. GTPase, guanosine triphosphatase; TGF-β, transforming growth factor β.

The TGFβ Signaling Pathway

As depicted in Figure 1.4, the TGFβ signaling cascade is one of the 12 pathways and processes whose constituent genes are mutated in pancreatic cancers (20). SMAD4 alterations (as discussed above) are the most frequently observed mutations in this pathway in PDA; however, loss of other components of the cascade have been noted (24). These include the upstream receptors TGFβ receptor 1 (TGFβR1), TGFβ receptor 2 (TGFβR2), and bone morphogenetic protein receptor 2 (BMPR2) (20; 33; 34). Additionally, alterations in the receptor-regulated SMAD (R-SMAD) gene SMAD3 have been described, albeit infrequently (35). Upregulation of the inhibitory SMADs (SMAD6 and SMAD7), which negatively regulate pathway signal transduction by competitively binding with upstream receptors, has also been shown (36; 37). Pancreatic tumors have also been found to overexpress TGFβ ligands, which can act directly on tumor cells if the receptors have not been inactivated, as well as on neighboring stromal and immune cells (38).

Canonical and Non-canonical TGFβ Signaling. The TGFβ superfamily of proteins consists of bone morphogenetic proteins (BMPs), TGFβs and activins (39). The pleiotropic nature of the pathway is a direct result of the number of different ligands that can activate the signaling cascade and the equally diverse set of transcription factors that complex with the SMAD proteins within the nucleus (40). Classical TGFβ signaling is initiated when TGFβ ligands bind to serine/threonine kinase receptors. The signal is propagated through SMAD transcription factors that form a complex prior to entering the nucleus to regulate gene transcription. As described above, TGFβ ligand-mediated signaling is mediated by the SMAD2/SMAD3 R-SMADs associating with the co-SMAD,

SMAD4. In the case of the BMP-mediated branch of the pathway, signaling is carried out by a different set of R-SMADs (SMAD1 and SMAD5), which complex with SMAD4 prior to entering the nucleus. Pathway activation results in the transcription of target genes important in the regulation of critical cellular processes including the cell cycle, cell differentiation, apoptosis, extracellular matrix formation, and immunoregulation (39-41).

In addition to the SMAD-dependent signaling cascade, TGFβ ligand binding triggers the activation of other signaling pathways within the cell. These include the p38 MAPK, Erk, JNK, and Rho-like GTPases (39). TGFβ-mediated signaling through Rho-like GTPases is known to be important in actin polymerization and cell adhesion, both of which are critical for cancer cell metastasis (39; 42; 43). Interestingly, these SMAD-independent pathways have also been shown to regulate key components of the canonical arm. For example, JNK and Erk signaling can facilitate the activation of different SMAD family members (44). Additionally, Ras/Erk MAPK signaling through TGFβ-ligand binding results in the production of more TGFβ ligand, allowing for continued pathway activation even when canonical signaling is lost (i.e. SMAD4 mutation) (45).

The Dual Role of TGFβ in Cancer. As described above, the TGFβ signaling pathway is responsible for regulating critical tumor suppressive mechanisms in normal cells (40). TGFβ regulates the expression of important inhibitors of cell cycle progression, p15 and p21, resulting in cell cycle arrest in the G1 phase (46; 47). TGFβ signaling is also important for inducing apoptosis; however, the mechanisms of this regulation are not fully characterized. Signaling through the pathway has been reported to mediate the expression of several pro-apoptotic (Bmf and Bim) and anti-apoptotic factors

(Bcl-2) (48-50). In addition to these cell-autonomous mechanisms of tumor suppression, TGFβ also exerts paracrine effects that aid in preventing tumor formation (40). Using a mouse model with targeted deletion of TGFβR2 in fibroblasts, Bhowmick et al. was able to demonstrate increased proliferation of neighboring prostate epithelial cells and the eventual formation of intraepithelial neoplasia. TGFβR2-deficient fibroblasts secreted excess hepatocyte growth factor, which could then act on adjacent prostate epithelial cells, facilitating their proliferation (51). In addition to paracrine signaling that suppresses epithelial cell proliferation, TGFβ signaling can indirectly prevent tumor formation by limiting inflammation (40). Rudolf Virchow first hypothesized a link between chronic inflammation and the development of tumors in the 1860s (52). Today, it is well accepted that a subset of cancers arise from chronic infections, with inflammation being a defining characteristic of such processes (52; 53). Immune cells are potent producers of cytokines, chemokines, reactive oxygen and nitrogen species, and digestive enzymes, which together provide a supportive milieu for tumorigenesis (53). TGFβ is a key regulator of immune cell migration, differentiation, and survival, and as such, can inhibit tumor formation by suppressing chronic inflammation (40; 54).

In addition to the tumor suppressive capabilities of the TGFβ signaling pathway, many studies have highlighted the importance of this pathway in progression and metastasis (40; 55). As was noted with the tumor suppressive aspects of TGFβ signaling, these tumorigenic mechanisms occur within the tumor cells themselves as well as via paracrine signaling between tumor and stromal cells. TGFβ is known to promote epithelial-mesenchymal transition (EMT), a process thought to be critical for invasion and metastasis. During EMT, epithelial tight junctions are lost, and the actin cytoskeleton

is reorganized (56). This process is governed by several transcription factors that control the expression of epithelial and mesenchymal genes, including Twist, Zeb-1, Snail and Slug (57). While canonical TGFβ signaling is known to regulate the expression of these transcription factors, several SMAD-independent pathways have been implicated in TGFβ-driven EMT, including Erk/MAPK, mTOR, and RhoA GTPase activity (58-60). Coupled to its role in EMT, TGFβ reshapes the extracellular matrix by increasing levels of key digestive enzymes such as matrix metalloproteinases (MMPs) (61).

The paracrine effects of TGFβ produced from tumor cells have prominent consequences on the tumor microenvironment. As already noted, TGFβ is a potent immunosuppressive cytokine that regulates immune cell recruitment, differentiation, and survival (62; 63). Important for tumor progression, TGFβ can directly impede T-cell mediated tumor cell killing by inhibiting the production of perforin and granzymes (64). Moreover, it is known to suppress MHC I and II expression on cells, further contributing to a loss in immunosurveillance (65). Equally important, TGFβ is indispensible for the differentiation of T regulatory cells (66). T regulatory cells in the tumor microenvironment further contribute to immune tolerance by inhibiting cytotoxic T cell function (54). The immunoregulatory effects of TGFβ are not limited to the lymphoid compartment. Several groups have demonstrated increased myeloid cell recruitment to tumors where TGFβ signaling has been abrogated (67; 68). Additionally, TGFβ influences neutrophil chemotaxis, macrophage differentiation, and inhibits macrophage-mediated tumor cell killing (69).

Another way TGFβ signaling influences the tumor microenvironment is by contributing to stromal cell deposition (40). Specifically, TGFβ is responsible for

myofibroblast differentiation (70). Myofibroblasts are critical for tumor cell invasion, and are also notable for producing enzymes necessary for extracellular matrix remodeling, and cytokines and chemokines that facilitate tumor and immune cell migration and angiogenesis (71).

In summary, a number of studies lend support to a dual role for TGFβ signaling in carcinogenesis. In normal cells and during early tumor formation, the suppressive arm of this pathway works to inhibit proliferation and inflammation, and promotes apoptosis (40; 69). Tumors are able to override these tumor suppressive capabilities, often by activating oncogenic signaling pathways such as Ras/Erk (72). After deactivating the tumor-suppressive arm, tumors can subsequently harness the tumor-promoting functions of TGFβ to facilitate invasion and metastasis (40). Tumors that acquire mutations to upstream receptors effectively abolish pathway signaling; however, they can still utilize TGFβ ligand to promote progression via paracrine signaling that alters the surrounding tumor microenvironment (54). In contrast, some tumors are able to selectively inhibit the tumor suppressive arm of the pathway, retaining metastasis-promoting functions (73; 74). Additionally, as was the case in the former example, these tumors can utilize TGFβ paracrine signaling to further facilitate invasion and metastasis. The mechanistic basis for the dual role of TGFβ in carcinogenesis has garnered further attention in recent years, and a more complete understanding is necessary if we hope to be able to target this pathway in patients.

The Immune Reaction in PDA

In recent years, a number of studies have shed light on the complex interdependence of the primary tumor and its surrounding microenvironment (75-77).

The tumor microenvironment consists of a vast array of cells, including fibroblasts, endothelial cells, and infiltrating immune cells (78). One of the defining features of PDA, desmoplasia, illustrates the importance of tumor-stromal interactions in tumor formation and progression (79). This widespread stromal deposition, which can constitute nearly 80% of the tumor, is a direct consequence of mediators secreted from tumor cells (including TGFβ-mediated factors, as described above). In turn, this dense stromal network of cells impacts tumor proliferation and invasion through secretion of digestive enzymes and chemokines and cytokines that are instrumental in the recruitment and polarization of immune cells within the tumor (79-81).

The role the immune system plays in cancer development and progression is complex. For one, as already mentioned chronic inflammation is thought to play a tumor-promoting role in a variety of cancers (54). However, it is also well established that the immune system is an essential tumor-suppressive mechanism as it can recognize and eliminate altered neoplastic cells (82). Additionally, research has demonstrated that various immune cells are present within precursor lesions and primary tumors, although the exact composition varies tremendously from one patient to the next (83-85). In PDA, many groups have been able to demonstrate that progression from precursor lesions to invasive carcinoma is characterized by notable changes in immune infiltrate (86; 87). Moreover, immune infiltrate in PDA tumors has been correlated with clinical outcome, with patients possessing increased numbers of infiltrating CD8+ cytotoxic T cells faring better than patients with a more immunosuppressive infiltrate (T regulatory cell dominant) (88; 89). These differences in immune infiltrate require special recognition when considering the potential benefits of immune-based therapies in patients. Below, we

will review the two major subsets of immune cells, lymphoid and myeloid, highlighting their roles in PDA initiation, progression and metastasis.

Tumor-Infiltrating Lymphocytes. Effector lymphocyte populations largely mediate the anti-tumor immune response. Major cell types include CD4+ and CD8+ T cells, B cells, and natural killer (NK) cells. Each of these major subsets can exert anti-tumor and pro-tumor functions, and the predominant response is largely shaped by the cytokines present in the surrounding milieu (90). In PDA, a sizeable CD4+ T cell infiltrate has been observed; however, the majority of these cells tend to be tumor-promoting, immunosuppressive T regulatory cells. T regulatory cells have been shown to infiltrate in early, precursor stages in both human tissue samples and animal models of PDA (86; 88; 91). These cells serve as significant inhibitors of the anti-tumor immune response as they can directly suppress CD8+ T cell-mediated tumor killing and contribute to immune tolerance. They further enhance tumor progression via secretion of key cytokines, including TGFβ (66). In contrast, PDA tumors often have few effector CD8+ T cells, NK or classical B cells, with the highest numbers often being seen in early precursor lesions (86; 92; 93).

Tumor-Infiltrating Myeloid Cells. The predominant infiltrate observed in PDA tumors is myeloid in nature. This includes infiltrating macrophages, neutrophils, and immature myeloid-derived suppressor cell (MDSC) populations (86). As was described with lymphoid cells, myeloid immune populations can either be classically activated (anti-tumor) or alternatively activated (pro-tumor), with polarization being dictated by the local cytokine environment (94). Monocytes that arrive in the tumor microenvironment often differentiate into alternatively-activated macrophages (M2) or MDSCs. Animal

models of PDA indicate that M2 macrophages infiltrate tumors in precursor stages, and can contribute to tumor progression by facilitating angiogenesis and invasion (86; 95). Additionally, macrophages secrete various cytokines and chemokines responsible for recruitment and polarization of other infiltrating immune cells (96). MDSCs are a heterogeneous population of immature myeloid cells. In mice, they are marked by expression of Gr-1 and CD11b (97; 98); however, in humans it appears that various subsets of these cells exist, each with their own set of markers (84; 85; 99; 100). MDSCs are characterized by their ability to produce anti-inflammatory cytokines. Their presence in tumors contributes to the tumor's ability to evade the immune system from attacking and destroying altered cells. Additionally, like T regulatory cells, MDSCs function as a significant barrier to effective immunotherapies (101). In addition to their respective effects on shaping the local tumor microenvironment, macrophages and MDSCs work to promote immune tolerance by inhibiting effector lymphocyte-mediated tumor cell killing. In support of this idea, studies in animal models have indicated a reciprocal relationship between infiltrating lymphocytes and infiltrating myeloid cells exists. In precursor lesions, lymphocytes are more abundant but their numbers and functionality are compromised as myeloid cells accumulate within the tumor stroma (86).

Neutrophil infiltration in PDA tumors has been correlated to decreased survival in patients (102). Normally, neutrophils function to kill invading pathogens – a process mediated by their ability to secrete reactive nitrogen and oxygen species and digestive enzymes (103). In the context of tumor progression, these same factors are important in extracellular matrix remodeling and tumor invasion (104; 105).

Tumor infiltrating immune cells have the potential to suppress and/or kill tumor cells; however, in PDA they are often linked with tumor-promoting functions (106). As was described above, the TGFβ signaling pathway has profound effects on skewing immune cell infiltrate in tumors (69; 81). Importantly, the predominant myeloid and T regulatory cell infiltrate found in PDA tumors can also strongly influence autocrine and paracrine TGFβ signaling networks (further exacerbating tumor progression, invasion and metastasis) as these cells are significant producers of TGFβ ligand (40).

Animal Models of PDA

As has been alluded to throughout this chapter, researchers have utilized mouse models of PDA to answer fundamental questions about the biology of this disease. Detailed histological and genetic studies of human tumor tissues resulted in the progression model of PDA described in Figure 1.3 (3; 107). Using the information gleaned from this model, many groups have worked to generate mouse models that could faithfully recapitulate various aspects of human PDA (108). The types and numbers of models has grown over the years, each possessing advantages and limitations, but all have offered invaluable insight into PDA carcinogenesis. As a brief summary, these mouse models can be divided into one of two broad categories, including genetically engineered models and cell line/tissue implantation models (109). The following chapters utilize a combination of conditional genetic mouse models and orthotopic implantation of murine PDA cell lines.

Implantation Models of PDA. Various implantations models of PDA exist, with the factors defining them including the type of tissue used (cell line versus tissue; human versus mouse) and the location of implantation (subcutaneous, orthotopic, splenic, or tail-

vein) (109). The use of human tissue and cell lines in implantation models has been carried out extensively over the years; however, a major limitation of this model is that it requires the use of immunodeficient mice. Thus, comprehensive studies of the immune response to tumor growth are not feasible (110). To overcome this problem, a number of tumor-derived murine cell lines have been generated from genetically engineered mice bred to the same genetic background, allowing for implantation in immunocompetent animals.

The different sites of implantation offer unique advantages and disadvantages. Subcutaneous models are relatively easy to perform; however, they often fail to recapitulate human PDA and infrequently metastasize (111). Tail-vein implantation is an especially good model for metastasis, but studies on primary tumor biology are not possible. Orthotopic and splenic implantation models recapitulate human PDA and frequently metastasize, but intraabdominal cell leakage, bleeding and infections are possible complications with this technique (109; 112).

Genetically Engineered Models of PDA. Genetically engineered mouse models offer important advantages over the implantation models described above. Notably, they allow for studies of all stages of pancreatic carcinogenesis, including early precursor lesions that can otherwise not be studied using cell lines or tumor tissues. They also allow for defined expression of mutant alleles to the pancreas, allowing for histologically-relevant models that possess both tumor and stromal components. With that said, these models take considerably more time and resources to generate and maintain. Additionally, genetic manipulations of target genes occur in every cell within the

pancreas that expresses the chosen promoter, a phenomenon that does not occur in human PDA (108; 109).

To conditionally activate or inactivate genes within the pancreas, Cre-mediated recombination utilizing one of two pancreas-specific promoters is often employed. Pancreatic and duodenal homeobox 1 gene (Pdx1) or pancreatic transcription factor 1a (Ptf1a) are required for pancreatic development and differentiation. Both endocrine and exocrine cell types express Pdx1, while Ptf1a expression is confined to exocrine cells (113; 114). One of the first genes to be targeted using this approach was *Kras*. Mice expressing the Cre-activated KrasG12D allele, hereafter referred to as KC mice, develop precursor ductal lesions that model human pancreatic intraepithelial neoplasia (PanIN). A small fraction of these animals (about 10%) go on to develop invasive adenocarcinoma with metastasis; however, latency can span 9-15 months (115).

From here, many groups coupled Kras activation with inactivation of various tumor suppressor genes. One of the most commonly used PDA mouse models used today is known as the KPC mouse, which combines Kras activation with a mutant allele of *p53* ($p53^{R172H}$). As was the case with the KC model of PDA, KPC mice develop PanIN lesions that progress to invasive ductal adenocarcinoma. Importantly, shorter latency (4-6 months) and higher rates of metastasis are observed in the KPC model (116).

Of particular interest for subsequent chapters, several groups have inactivated components of the TGFβ signaling cascade in the context of *Kras* activation. Izerdjene et al. generated LSL-*KrasG12D*/+;*Dpc*4*flox*/+;Ptf1a*Cre*/+ (KDC mice), which interestingly developed mucinous cystic neoplasms that infrequently progressed to PDA (117). However, inactivation of TGFβR2 (either one or both alleles) resulted in the more typical

PanIN-to-PDA histological progression. KTC mice (LSL-*KrasG12D*/+;*Tgfbr2flox/flox*;*Ptf1aCre*/+) develop aggressive, metastatic PDA within a few months of birth. Latency is slowed to 6-8 months when only one allele of TGFβR2 is targeted (118).

Taken together, animal models of PDA provide important tools for researchers to study the initiation, progression, invasion and metastasis of PDA. Each model system possesses its own set of unique limitations, but they allow for the comprehensive analysis of tumor-stromal interactions, the immune reaction in PDA, and importantly, they offer a platform from which different treatment modalities can be extensively tested (108).

Chapter 2 : Rationale and Aims

Rationale

Pancreatic ductal adenocarcinoma (PDA) is among the most lethal of all cancers: five-year survival rates are only around 6% (119). Great strides have been made in understanding the genetic alterations that give rise to PDA, which include activating mutations in the KRAS oncogene, and inactivating mutations in genes that play critical roles in cell cycle control, apoptosis, and TGFβ signaling (11; 14; 15; 21; 24). The TGFβ signaling pathway, one of twelve pathways/processes known to be altered in PDA carcinogenesis, has both tumor suppressive and tumor-promoting capabilities (40). The complexity of this signaling cascade, with both canonical and SMAD-independent arms, is likely contributing to the dual roles of TGFβ in tumor prevention and progression. In PDA, greater than half of patients will lose SMAD4 function, which has been correlated to worse prognosis and a widely metastatic pattern of failure (27; 28; 120). In contrast, less than 5% of patients will acquire inactivating mutations in TGFβ receptor 2 (TGFβR2) (34); however, alterations in this upstream component of the pathway are not associated with a decrease in overall survival (35).

While the genetic alterations that occur within tumor cells undoubtedly contribute to its metastatic potential, it is becoming increasingly apparent that the surrounding tumor microenvironment plays an important role in invasion and metastasis (67; 121; 122). The tumor microenvironment consists of a vast array of cells including fibroblasts, stellate cells, endothelial cells, and a variety of immune cells (123). A diverse immune infiltrate, consisting of both lymphoid and myeloid populations of cells, has been noted in patient

tumor samples as well as within tumors of murine models of PDA (86; 88; 91). These immune cells can have both anti-tumor and tumor promoting functions, with the proportions and nature of infiltrating immune cells largely being shaped by the surrounding milieu (124-126). In particular, TGFβ ligand acts within the tumor microenvironment by regulating immune cell recruitment to tumors and by polarizing immature immune cells when they infiltrate lesions (81). Tumor infiltrating immune cells have been shown to secrete factors such as matrix metalloproteinases (MMPs), which aid in tumor invasion and metastasis (67; 98; 127; 128). Additionally, populations of immunosuppressive cells, namely T regulatory and myeloid-derived suppressor cells, contribute to tumor progression by promoting an immune tolerant environment (75; 76).

Given that TGFβ signaling is associated with cancer cell and microenvironmental changes that can influence tumor progression, and that alterations in TGFβ signaling components are prevalent in PDA, we sought to understand how different TGFβ pathway mutations in tumor cells influence tumor microenvironmental changes, and in turn, how these changes within the stromal compartment of the tumor promote metastatic efficiency in PDA. The major goals of this thesis were to address how mutations in TGFβR2 and SMAD4 alter metastatic progression, and what immune infiltrate changes occur in the context of these mutations. ***We hypothesized that levels of TGFβ signaling underlie the differing metastatic propensities of PDA, and more specifically, that the patterns of metastatic failure seen in some patients may be explained by differences in immune infiltrates that are regulated by TGFβ.***

Specific Aim 1

Determine how inactivation of TGFβR2 alters metastatic efficiency in PDA.

Rationale

SMAD4 loss is common in PDA, and is associated with widely metastatic disease and decreased survival (28; 35). In contrast, TGFβR2 mutations are observed in only a small subset of patients, and are associated with better survival compared to patients with SMAD4 mutations (34; 35). Additionally, the effects of TGFβR2 inactivation on PDA metastasis have not been comprehensively studied, and such inactivating mutations can have different consequences than those observed with SMAD4 loss. To better our understanding of how TGFβ signaling promotes metastasis in PDA, we coupled histological analysis of human tissues with functional studies in a novel genetically engineered mouse model of PDA.

Specific Aim 2

Identify how immune populations are skewed in response to TGFβR2 inactivation in PDA.

Rationale

Aberrant TGFβ signaling has profound consequences on tumor progression (40; 63). Within tumor cells, TGFβ pathway inactivation results in the loss of tumor suppressive functions, including regulation of cell cycle progression and apoptosis. Importantly, the effects of loss of signaling in the tumor epithelium extend to the surrounding stroma. These include changes in stromal architecture as well as in the proportions and polarization of immune cells (63; 78). To identify which immune cell populations are altered in response to defects in TGFβ signaling, we used our novel genetically engineered mouse model of PDA

(Specific Aim 1) to interrogate infiltrating leukocytes via flow cytometric analysis.

Specific Aim 3

Determine what effect SMAD4 loss has on immune infiltrate in PDA, and whether immunosuppressive cells in SMAD4-deficient tumors alter metastatic propensity.

Rationale

Activation of TGFβ receptors initiates both SMAD-dependent (canonical) and SMAD-independent (non-canonical) signaling networks. Loss of TGFβR2 function (examined in Specific Aims 1 & 2) results in abrogation of both canonical and non-canonical cascades whereas in the context of SMAD4-deficiency, SMAD-independent signaling is retained (39; 40). To determine whether SMAD-independent signaling networks influence the immune infiltrate in PDA tumors, we generated SMAD4-deficient tumor cells and implanted them directly into the pancreata of mice. Additionally, given that SMAD4 loss is correlated with widely metastatic PDA, we explored whether immunosuppressive cells from SMAD4-deficient tumors contribute to metastatic efficiency.

Significance

Pancreatic cancer is among the most lethal of all cancers. In 2014, the National Cancer Institute estimates that 46,420 people in the United States will be diagnosed with pancreatic cancer and 39,590 patients will die from the disease (119). An overwhelming majority of these patients, as high as 80%, are diagnosed when the primary tumor has already metastasized either locally or to distant sites (119). Treatment options for these advanced-stage patients are severely lacking. Surgical resection is rarely offered to patients with metastatic disease (129), and the accepted combination therapies of either FOLFIRINOX or Gemcitabine coupled with Abraxane extend survival by less than six months compared to Gemcitabine alone (130; 131).

Improving the bleak prognosis inherent to PDA requires a more comprehensive understanding of the mechanisms of metastasis. Overall, this study aims to answer how perturbed TGFβ signaling influences progression and metastasis in PDA, as well as offer insight into the complex tumor cell-stromal cell interactions that work to mediate these processes.

Chapter 3 : Cell-Autonomous TGFβ Signaling in Pancreatic Cancer Uncouples Primary Tumor Growth from Organ-Specific Colonization Through Secretion of Prometastatic Mediators.

This work is submitted for publication.

Y Zhong, A Macgregor-Das, T Saunders, A Makohon-Moore, J Poling, L Cope, S Leach, and C Iacobuzio-Donahue. Cell-Autonomous TGFβ Signaling in Pancreatic Cancer Uncouples Primary Tumor Growth from Organ-Specific Colonization Through Secretion of Prometaststic Mediators.

Introduction

Abundant epidemiologic and clinical data indicate that pancreatic ductal adenocarcinoma (PDA) is a highly lethal disease with a current five-year survival rate that barely surpasses 6% (132). Most diagnoses are made well after the tumor has invaded into surrounding vital structures or disseminated at which time there is a paucity of treatment options (133). The current understanding of PDA metastasis, like other solid tumors, is that cells from the primary tumor intravasate into vessels, disseminate within the circulation and extravasate into distant sites where a minority may establish secondary lesions (134). Genomic studies and computational models also indicate that clinical metastasis is a late event in the clonal evolution of PDA (135; 136), although compelling data in transgenic models suggests that some aspects of this process occur before the advent of invasive ability (137). However, beyond this framework, the actual mechanisms by which PDA metastasizes remains unknown. Ultimately, the dismal survival statistics faced by newly diagnosed patients can only be improved with a more complete understanding of the biology of PDA metastasis.

Comprehensive analyses of PDA indicate that it is a genetically complex disease (20; 138). Like other epithelial cancers, PDA arises from the accumulation of somatic alterations in a distinct set of driver genes (139) upon which additional somatic alterations occur over time and geographic space (136). These driver genes, *KRAS, CDKN2A, TP53,* and *SMAD4*, arise during pancreatic intraepithelial neoplasia (PanIN) from which an infiltrating carcinoma may develop (140). Additional cell-autonomous mechanisms that contribute to PDA behavior include aberrant activation of developmental signaling pathways (141; 142), alterations in cellular metabolism (143;

144) or a dependence on autophagy (145). The dynamic stromal reaction characteristic of PDA and associated immunosuppressive environment may further contribute to its aggressive biology (reviewed in (146)).

In previously reported autopsy series of patients with documented infiltrating PDA of the pancreas, a subset were identified that had low metastatic burdens, and in some cases no metastases despite prolonged survival, suggesting the existence of a form of pancreatic cancer with low metastatic propensity (28). In an effort to understand this phenomenon, we used a combination of classical morphologic studies of human tissues, transgenic mouse models and functional metastasis assays as a platform for delineating the mechanisms of metastatic efficiency of PDA.

Materials and Methods

Antibodies

Primary antibodies raised against CD31 were purchased from Life Span Biosciences (LS-B1932); Keratin 17/19 (#3984), pHH3 (#9701), P-p44/42 MAPK (pERK, #4376) were purchased from Cell Signaling Technology; SHH was purchased from R&D Systems (AF464); Muc5AC (Sc-21701), TGFBR2 (L-21, SC-400), COL6A1 (H200, sc-20649), NGAL (M-145, sc-50351), E-cadherin (G-10, sc-8426) was purchased from Santa Cruz Biotechnology; Fibronectin was purchased from Abcam (ab23750); SMA was purchased from Dako (1A4); CD10 (PA5-23701) was purchased from Thermo Fisher Scientific); LGAL53BP (Bs-5729R) was purchased from Bioss Antibodies.

Human Tissues

Postmortem primary and metastatic pancreatic cancer tissues from consenting patients were obtained following IRB approved protocols previously described in detail (Embuscado et al., 2005).

Mouse strains

The conditional *LSL-KRAS*^{G12D} mice (147), *129S4-Trp53tm2Tyj* (148), *B6.129S6-Tgfbr2tm1Hlm* (149) *and Ptf1a*$^{tm1.1(cre)Cvw}$ mice (150) were previously described. The *LSL-Kras*^{G12D} knock-in strains *129S4-Trp53*^{tm2Tyj} and *B6.129S6-Tgfbr2*^{tm1Hlm} were obtained from Jackson Laboratories. The *Ptf1a*$^{tm1.1(cre)Cvw}$ mice were purchased from MMRRC (Mutant Mouse Regional Resource Centers). Mice were genotyped by PCR using primers specific to transgenic alleles (conditions available on request). This study was approved by the Animal Care and Use Committee.

Mouse Histology and Immunohistochemistry

Normal tissues, pancreata and metastatic cancer tissues of moribund mice or mice at specific age timepoints (4, 8, 12 weeks) were fixed with 10% buffered formalin solution overnight and embedded into paraffin by the Johns Hopkins Reference Histology Laboratory. Sections cut from each paraffin block were stained with hematoxylin and eosin following standard protocols and observed under a light microscope for diagnoses. For immunolabeling, unstained 5-μm sections were cut from paraffin blocks and the slides deparaffinized by routine techniques followed by incubation in 1x sodium citrate buffer (diluted from 10 x heat-induced epitope retrieval buffer, Ventana-Bio Tek Solutions, Tucson, AZ) before steaming for 20 minutes at 80 °C. Slides were cooled 5 minutes and incubated for two hours to overnight with primary antibody. Immunolabeling was detected using the Ventana IVIEW Kit per kit instructions and sections were counterstained with hematoxylin.

Cell Staining for Immunofluorescence Microscopy

Cells grown on coverslips were fixed in 3.7% or 4.0% paraformaldehyde solution for 30 minutes at 37°C. All subsequent steps were carried out at room temperature. Coverslips were incubated with E-cadherin monoclonal antibodies (1:100 dilution; Santa Cruz) in PBS-1% BSA for 1 h and followed by incubation together with FITC-conjugated goat anti-mouse secondary antibody (Sigma). Coverslips were mounted in Prolong Gold Antifade reagent with DAPI (Molecular Probes), and images were captured with a Zeiss fluorescence microscopy system.

Cell proliferation assay

All cells were cultured in DMEM (GIBCO, Invitrogen Life Technologies, Carlsbad, CA, USA) supplemented with 10% fetal bovine serum (FBS), 100 units/ml penicillin, 100 □g/ml streptomycin and 2 mmol/L L-glutamine at 37 ^{o}C and 5% CO2. Cell proliferation assay was performed using cell counting Kit-8 (Dojindo Molecular Technologies, Inc., Gaithersburg, MD, USA) according to manufacturer protocols. Absorbance was measured at 490 nm using a microplate reader. Each experiment was carried out in triplicate.

Experimental Metastasis Assays

KPC and KPTC cell cultures were dissociated into single cell suspensions in PBS, counted, and injected into the tail veins of C57/B6 mice (5 x 10^5 cells per mouse). After three weeks the animals were euthanized and their lungs removed, rinsed in PBS and the number of gross (surface) pulmonary nodules counted using a dissecting microscope.

Quantitative Secretome Analysis

KPC and KPTC cells were grown to confluence in tissue culture dishes, washed with serum-free media eight times and incubated in serum-free media for 24 hours. The conditioned media (CM) was harvested and centrifuged to eliminate any intact cells and the supernatants were then concentrated and desalted by centrifugation in Amicon Ultra-15 tubes (molecular weight cutoff 3000 Da; Millipore, Billerica, MA). Protein samples were quantified and analyzed by the Proteomics Core Facility of Johns Hopkins. The protein concentrations of KPC and KPTC CM samples were labeled with the iTRAQ reagent (Applied Biosystems, Foster City, CA, USA) according to the manufacturer's protocol, and then subjected to MS/MS analysis. Data analysis on the data files from the LC-MS/MS were performed with the Thermo Scientific™ Proteome Discoverer™

Software (Thermo Fisher Scientific, Inc., Waltham, MA). The identified proteins were further subjected to bioinformatic analysis. Proteomics data have been deposited in the Peptide Atlas Database with the accession number PASS00575.

Quantitative Real Time PCR

Total RNA was extracted from tissue samples using RNeasy mini Kit (Cat. No., 74104; Qiagen). RNA was treated with DNase I (Invitrogen) to digest remnant genomic DNA. cDNA was synthesized from 0.5 □g of total RNA by the SuperScript Preamplification System (Invitrogen) according to the protocol recommended by the manufacturer. For quantitative PCR, one microgram of RNA per sample was reverse transcribed into cDNA using SuperScriptTMIII Platinum® Two-Step qRT-PCR Kit (Invitrogen) according to the protocol recommended by the manufacturer. Real-time quantitative RT-PCR analysis was performed using an automated sequence detection instrument (7300 Real Time PCR System, Applied Biosystems, CA, USA) for the real-time monitoring of nucleic acid green dye fluorescence (SYBR®Green, Invitrogen Inc, CA, USA). Relative fold-changes of analyzed gene expression compared to the housekeeping gene β-actin were determined by calculation of the $2^{\Delta\Delta Ct}$. All analyses were performed in triplicate at least 2 times. Primer sequences will be provided upon request.

Western Blotting Assay

Cell lysates were prepared by suspending cell pellets in RIPA buffer (20 mM Tris, 0.1% SDS, 1% Triton X-100, 1% sodium deoxycholate, pH 7.4) supplemented with protease inhibitor cocktail tablets (Roche diagnostics GmbH, Mannheim, Germany). Equal amounts of proteins were separated on SDS-polyacrylamide gel and transferred onto PVDF membranes (DuPont NEN, Boston, MA). Each membrane was hybridized with

primary antibody followed by horseradish peroxidase (HRP)-linked IgG and visualized by the enhanced chemiluminescence (ECL) system (Amersham). Expression of β-actin or GAPDH were used as internal controls.

Stable shRNA knockdowns and Stable over-expression

COL6A1 shRNA (TF500404, Origen) and cDNA plasmid (MG223027, Origen) LCN2 shRNA (TG511895, Origen) and cDNA plasmid (MG226233, Origen) were purchased from Origen. KPC and KPTC cells were cultured in Dulbecco's modified medium containing 10%FBS. Plasmid DNA transfection of cells was performed by using Attractene reagent (Cat. No., 301005, Qiagen) following the Reverse transfection protocol. 48 hours after transfection, passage the cells into the appropriate selection medium, maintain the cells in selective culture medium until colonies appear. Inhibition of gene expression by shRNA and over-expression of target gene were determined by Western blot analysis.

Results

Expression of TGFβ Pathway Components Correlates with Metastatic Behavior in Human Pancreatic Cancer

To determine the extent to which there are morphologic features that define oligometastatic PDA (patients with 0-10 gross metastases) (28) we reviewed histologic sections prepared of the primary carcinoma for six patients with this phenotype at autopsy (Table 3.1). Nine primary carcinomas from patients from the same autopsy series who had widely metastatic PDA (>10 gross metastases) were similarly studied. All 15 patients were untreated, largely an unfortunate consequence of their late diagnosis, allowing us to definitively exclude treatment related changes to the tumor tissues examined.

Primary tumor tissues from oligometastatic PDAs showed evenly dispersed well to moderate differentiated neoplastic glands with organized lumina and basally located nuclei (Figure 3.1A, 3.1B and Figure 3.2A). Infiltration by single cancer cells into the surrounding stroma was uncommon and when seen was localized to discrete microscopic foci (Figure 3.2A). None of the PDAs were mucin producing (colloid carcinomas). The stromal response was robust and contained abundant collagen deposition admixed with glycosaminoglycans as evidenced by a Movats pentachrome stain; αSMA, a marker of activated stellate cells (151) was also diffusely positive throughout the stromal compartment (Figure 3.2C). While metastases in these patients were relatively uncommon (Table 3.1), when present their histologic features were similar to that of the matched primary carcinoma, indicating the morphologic characteristics of the neoplastic epithelium were persistent in the secondary sites (Figure 3.2D). By contrast, tissues from

the primary tumors of widely metastatic disease revealed a predominance of neoplastic glands with poorly formed lumina, syncytial growth, intraluminal necrosis and apoptotic debris (Figure 3.1A, 3.1B and Figure 3.2B). Single cell infiltration into the surrounding stroma was frequent and in some carcinomas the predominant morphology (see A132, Figure 3.2B). However, the stromal response was similarly prominent in widely metastatic PDAs based on αSMA and pentachrome stains (Figure 3.2C). Perineural and/or vascular invasion was also identified in both oligometastatic and widely metastatic PDA indicating this feature was not discriminatory of metastatic propensity in this sample set (Table 3.1 and Figure 3.2E). Given these differences, we next wondered if PDA cells in each phenotype have differences in expression of E-cadherin and vimentin, two general markers of epithelial versus mesenchymal phenotypes. An immunolabeling survey of each carcinoma indicated that E-cadherin was expressed by all carcinomas, and in virtually all it was mislocalized to the cytoplasm (Figure 3.1C). By contrast, vimentin was strongly expressed in 6 of 9 widely metastatic PDAs but in none of the oligometastatic PDAs, indicating a gain of vimentin was correlated with higher metastatic propensity ($p=0.027$, Fisher Exact Test).

The TGFβ signaling pathway is a master regulator of cell differentiation, growth, adhesion and migration during embryogenesis and in response to inflammation, including within the pancreas (25). Given the pronounced disparities in neoplastic cell morphology, cohesion and expression of vimentin between the two cohorts of samples, we hypothesized that levels of TGFβ signaling may account for these differences. We therefore labeled tumor tissues of each PDA for TGFβ1 ligand expression, revealing a marked difference in overall TGFβ1 within oligometastatic and widely metastatic PDA

(Figure 3.1D). Oligometastatic PDAs showed low expression within both the epithelial and stromal compartment; however, scattered positive labeling stromal cells were seen (insets A70 and A56, Figure 3.1D). By contrast, primary carcinoma tissues associated with widely metastatic disease showed positive expression throughout the tumor tissues (A43 and A93, Figure 3.1D). A semi-quantitative review of one complete cross-section of each carcinoma in a blinded manner confirmed these differences with none of five evaluable oligometastatic PDAs showing positive TGFβ1 labeling compared to seven of nine widely metastatic PDAs (p=0.021, Fisher Exact Test; see also Table 3.2). Because TGFβ1 ligand exerts its effects through binding to the TGFβRI/II receptor complex (41) we next evaluated the expression of TGFβR2 in serial sections of these same tumors (Figure 3.1E). Similar to that of its ligand there was a significant disparity of TGFβR2 expression between oligometastatic and widely metastatic pancreatic cancers, with the latter subset having significantly greater expression levels within the neoplastic epithelium (p=0.014, Fisher Exact Test; see also Table 3.2). Collectively, these data indicate that a relative loss of TGFβ signaling components within PDA cells is correlated with the low metastatic propensity observed in some patients.

Reduced TGFβ signaling Accelerates Carcinogenesis in a Conditional Mouse Model of Pancreatic Ductal Adenocarcinoma

To determine the mechanisms by which reduced levels of TGFβ signaling in PDA affect oncogenic behavior, we generated *LSL-KRAS*$^{G12D/+}$*;LSL-Trp53*$^{R172H/+}$*;Tgfbr2*$^{flox/-}$ mice by interbreeding them with *Ptf1a*$^{Cre/+}$ transgenic animals (hereafter referred to as *KPTC* mice). The co-occurrence of each rearranged allele was detected in the pancreas but not kidneys of each compound mutant animal by allele-specific PCR (Figure 3.3A

and Figure 3.4). *KPTC* mice were phenotypically normal at birth and born at expected Mendelian ratios.

KPTC mice (n=34) exhibited a median survival of 4.4 months with 100% mortality occurring by 7.4 months, which was significantly shorter than their littermate controls (*LSL-KRAS*$^{G12D/+}$*;LSL-Trp53*$^{R172H/+}$*; Ptf1a*$^{Cre/+}$ mice, *KPC*, p<0.0001; *LSL-KRAS*$^{G12D/+}$*;LSL-Trp53*$^{R172H/+}$*; Tgfbr2*$^{lox/+;}$ *Ptf1a*$^{Cre/+}$ mice, *KTC*, p<0.0001; and others) (Figure 3.3B). Necropsy of these mice indicated the presence of abundant hemorrhagic ascites in association with a fibrotic pancreatic mass (Figure 3.3C), which obstructed the small bowel or was infiltrative into surrounding organs (Figure 3.3D). A subset of animals (n=12) also had gross evidence of metastasis to the liver, lung, peritoneum or abdominal lymph nodes (Table 3.3) similar to the spectrum of disease encountered in human PDA. With one exception all quadruple mutant animals succumbed to infiltrating PDA (Figure 3.3E and Tables 3.3, 3.4). Histologic review of the pancreata from cohorts of *KPTC* mice sacrificed at predetermined intervals also revealed preinvasive lesions consistent with murine PanIN (mPanIN) (140). Moreover, the latency to development of cancer was significantly shorter in *KPTC* mice compared to *KPC* controls (Figure 3.3F). In *KPTC* mice mPanIN2 lesions were seen as early as four weeks of age; by 12 weeks of age 89% of mice developed mPanIN3 with a subset (22%) also developing infiltrating PDA. By contrast, only 30% of *KPC* mice had mPanIN3 at the 12 week timepoint (p=0.012). Based on these observations we conclude that TGFβ signaling restrains pancreatic carcinogenesis, and loss of one *Tgfbr2* allele abrogated this restraint in *KPTC* mice.

Loss of TGFβ signaling Restrains Cell-Autonomous Oncogenic Properties of Invasive PDA

We next compared the histology of the PDAs arising in *KPTC* mice to those arising in *KPC* mice. Regions of ductal (well or moderately differentiated) and solid (poorly differentiated) growth were seen in both *KPTC* and *KPC* tumors (Figure 3.5A). However, infiltrating PDAs in *KPTC* mice were highly enriched for ductal morphology as supported by an increased overall frequency of well to moderate differentiation (85% of *KPTC* carcinomas versus 59% of *KPC* carcinomas, p=0.029, Table 3.4) and in the proportion of well or moderate differentiation per individual carcinoma (median 75% versus 50%) (p=0.0053, Figure 3.5B and Table 3.4). Areas of ductal morphology were largely accompanied by a relative increase in stromal density as well based on routine histologic stains and labeling for αSMA (Figure 3.5A). The presence of undifferentiated (sarcomatoid) carcinoma was also seen in a minority of *KPTC* and *KPC* mice, as was the presence of high-grade neoplasms of the cerebellum or spinal cord that caused hindlimb paralysis in some animals (Figure 3.6). These latter findings are likely related to neural $Ptf1a^{Cre/+}$ expression as recently described (152).

To confirm that the differences in morphology were not due to transgene variegation and/or mosaic Cre activity, we microdissected areas of coexistent poorly differentiated and well/moderately differentiated PDA from a subset of *KPTC* and *KPC* tumors (Figure 3.7A). In all cases the identical genotype was present in both morphologies within the same carcinoma, confirming that somatic mosaicism for transgene activation did not account for these effects. Furthermore, all PDAs irrespective of genotype or morphology showed nuclear accumulation of Trp53 protein indicating

universal loss of the wild type allele (Figure 3.7B). Smad4 expression was also retained in primary cells prepared from *KPTC* and *KPC* PDA tissues (Figure 3.7C,D).

To understand why *KPTC* carcinomas showed a shift towards more differentiated tumors, we immunolabeled a subset of *KPTC* and *KPC* PDA for Tgfβr2 and Tgfβ1. Tgfβr2 was expressed in all *KPTC* tumors although at low power labeling was heterogeneous with regions of both strong and weak positive expression seen within the same tissue section (Figure 3.5C). At higher power, these differences in labeling intensity showed a striking correlation to the extent of ductal differentiation present within a single PDA. For example, areas of poor differentiation showed positive labeling of the neoplastic epithelial cells (Figure 3.5D) whereas geographically distinct areas of well to moderate differentiation in the same carcinoma showed weak to negative expression of Tgfβr2 within the epithelial compartment (Figure 3.5E). Labeling was retained in the stromal compartment of both well to moderately and poorly differentiated areas (Figure 3.5E & I). A qualitative difference in Tgfβr2 expression was noted as well in that labeling was cytoplasmic in poorly differentiated regions whereas in well to moderate differentiated regions it was localized to the apical cytoplasm (inset, Figure 3.5E) suggesting a degree of posttranslational processing in accounting for differences in Tgfβ signaling as well. By contrast, there were no quantitative or qualitative differences for Tgfβ1 labeling in *KPTC* PDA tissues (Figure 3.5F & G). We next determined the extent to which variability of Tgfβr2 labeling occurs in *KPC* PDAs. Similar to *KPTC* tumors, Tgfβr2 was heterogeneous in labeling intensity throughout *KPC* PDAs and this intensity also corresponded to the extent of ductal differentiation (Figure 3.5H & I). Labeling for Tgfβ1 was also uniform in *KPC* PDAs although in one carcinoma a relative

loss of Tgfβ1 was noted in the region of well-differentiated morphology that also had a complete loss of Tgfβr2 expression (*KPC2*, Figure 3.5J & K).

These data suggest that there is an inherent geographic variation to the levels of cell-autonomous Tgfβ signaling in a single PDA, and the consequence of *Tgfbr2* haploinsufficiency in the *KPTC* model is a shift towards a greater proportion of neoplastic cells having reduced Tgfβ pathway activity. To support this hypothesis, we labeled each *KPTC* and *KPC* PDA for fibronectin, a known Tgfβ target gene (153). Fibronectin expression within the neoplastic epithelium paralleled that of Tgfβr2, with higher levels of fibronectin detected in regions of poor differentiation (Figures 3.5L & N) and low levels of fibronectin in regions of well/moderate differentiation (Figures 3.5M & O) in both *KPTC* and *KPC* mice. Labeling for fibronectin was nonetheless observed within the adjacent stroma of all PDAs, buttressing our observation that Tgfβ signaling within the neoplastic compartment serves as the basis for these observations. To further support our hypothesis, we treated primary *KPTC* and *KPC* cells with vehicle or Tgfβ1 ligand (Figure 3.5P). *KPC* cells underwent a profound loss of E-cadherin expression and transformed from tight epithelial clusters to loose aggregates in the presence of Tgfβ1, whereas no effect was seen for *KPTC* cells. Thus, unlike carcinogenesis in which Tgfβ signaling exerts a restraining influence, in invasive PDAs Tgfβ signaling promotes oncogenic behavior, thereby phenocopying our observations in human PDA.

Reduced TGFβ signaling Limits the Efficiency of Lung Metastasis

To determine the extent to which Tgfβ signaling affects metastatic propensity, we characterized the metastatic burdens in both cohorts of mice. Despite their reduced median survival, *KPTC* mice had a paradoxical reduction in the rate of metastasis with

only 12 of 34 *KPTC* mice (35%) having any gross or microscopic evidence of metastasis compared to 15 of 22 *KPC* mice (68%) (Figure 3.8A). However, among mice with metastasis there was no significant difference in their observed metastatic burden. Moreover, in both cohorts of mice the distribution of metastases was similar with the lung and liver the most common sites of spread, respectively.

As *KPTC* mice developed PDA at a reduced latency compared to *KPC* mice (Figure 3.3B), we asked whether earlier death due to the primary tumor was the cause of the lower rates of metastasis. If so, primary cells from *KPTC* and *KPC* carcinomas would be expected to have similar rates of metastasis in experimental assays. To address this question, we injected primary tumor cells prepared from individual *KPTC* or *KPC* mice into the tail veins of $CD1^{nu/nu}$ mice followed by quantification of lung metastases. While these cell lines had no significant differences in cell proliferation (Figure 3.8B) or mRNA expression of Snail, Slug or Twist (data not shown), *KPTC* cell lines showed a markedly lower efficiency at generating lung metastases in this assay (Figures 3.8C & D, $p<0.0001$) indicating the earlier time to death of *KPTC* mice was not the cause of decreased metastasis. These findings suggested to us that loss of Tgfβ signaling in the primary site reduces the fitness of disseminated cells rather than reducing the rate of dissemination per se, and those cells with retention of Tgfβ activity are selected for during colonization of the lung. Consistent with this notion, the immunolabeling patterns for Tgfβr2 and Tgfβ1 were similar in spontaneous lung metastases from *KPTC* and *KPC* mice (Figure 3.8E).

Reduced TGFβ signaling Limits the Ability to Form Invasive Liver Metastasis

We next assessed the liver metastases in these same mice, the next most common site of metastasis in our model, to determine if this interpretation holds. There was a profound difference in the morphologic features of liver metastases in *KPTC* and *KPC* mice (Figure 3.9A). In *KPTC* mice, neoplastic cells were frequently identified within vascular spaces of the portal drainage system as evidenced by luminal red blood cells or lymphocytes (arrow, Figure 3.9B) and immediately adjacent bile ducts (Figure 3.9C & D). CD31 labeling confirmed the observation of intravascular carcinoma as well as indicated that colonization of the portal veins by the PDA led to a replacement of the endothelial cells (Figure 3.9D). The intravascular cells were confirmed to be PDA by both CK19 expression (Figure 3.9E) and nuclear accumulation of Trp53 protein (Figure 3.9F).

A number of features indicated that intravascular metastases were not simply a reflection of dissemination caught in an early phase. First, intravascular metastases greater than >1 mm in diameter were identified that nonetheless had no stromal reaction (Figure 3.9G & H) giving the appearance of a cystic mass with pseudopapillary features (Figure 3.9H); such metastases would have required numerous cell divisions to reach this size. Second, intravascular metastases were uncommon in *KPC* mice whereas invasive metastases were frequent, with invasion recognized by the associated stromal response and infiltrative growth into the liver parenchyma (Figure 3.9I). Finally, in *KPC* mice with intravascular liver metastases, invasive metastases were also present and outnumbered the former by at least 10-fold (Figure 3.9J). A quantitative assessment of the presence of intravascular versus invasive metastases confirmed the difference

between the two genotypes (eight of nine *KPTC* mice, 89%, with only intravascular metastases versus two of nine *KPC* mice, 22%, p=0.0076, Figure 3.9K). Further review of liver metastases in these mice revealed that the one *KPTC* mouse with invasive liver metastases (*KPTC18*) had a metastatic sarcomatoid carcinoma and one of the *KPC* mouse with intravascular liver metastases (*KPC17*) only had three total gross metastases identified at necropsy. We next reviewed the labeling patterns of fibronectin, indicating that intravascular metastases were uniformly negative for fibronectin, whereas invasive metastases were uniformly positive (Figure 3.9L). Collectively, these data suggest that the ability of PDA cells to colonize the liver is also dependent on Tgfβ signaling.

TGFβ Signaling Promotes Secretion of Pro-Metastatic Mediators

The Tgfβ signaling pathway plays an important role in the crosstalk between cancer cells and their tumor microenvironment at the metastatic niche, which is required for metastatic growth in secondary sites (154). We were interested in the extent to which cell-autonomous Tgfβ signaling may modulate growth in secondary sites by its effects on the secretion of prometastatic proteins. We therefore collected the 24 hour conditioned media from Tgfβ stimulated *KPTC* and *KPC* cells and subjected it to iTRAQ-based quantitative proteomic analysis (Figure 3.10A). More than 3000 proteins were identified by this approach including known Tgfβ-target genes such as Tgfβ1 and VEGF (155). Bioinformatic analyses to screen for the most differentially secreted proteins between *KPTC* and *KPC* cells resulted in a high-confidence list of 391 proteins with a false-discovery rate ≤0.001 and a p-value ≤0.001 (subset of proteins shown in Table 3.5).

The secretome of *KPTC* and *KPC* cells were dramatically different, as evidenced by the 343 proteins secreted in abundance from *KPTC* cells versus 48 proteins that were

more abundant in the secretome of *KPC* cells (Figure 3.10B, Table 3.5). *KPC* secreted proteins included Sdf1r and Cxcl1, both reported to promote breast cancer metastasis by providing cell-survival paracrine signals to disseminated tumor cells (156; 157), and Vcam1 that promotes organ-site specific breast and melanoma metastasis via IL-18 dependent upregulation of endothelial growth factors or integrin α4β1 (156; 158). Biologically interesting proteins, some of which have putative roles in pancreatic cancer, were also identified including the mitochondrial protein HSP60 (156; 159) or the nonmuscle myosin protein MYH9 (160). We selected two proteins, Col6A1 and Lcn2, for further evaluation and functional validation in *KPTC* and *KPC* cells. Col6A1 is a short chain collagen involved in cell migration and differentiation related to embryologic development; it has also been described to be a Tgfb1 target gene in fibroblasts (161). Lcn2, also known as neutrophil gelatinase, plays a role in cytosolic iron-delivery in association with bacteriostasis and has been associated with aggressive features in several tumor types (162).

Western blotting for these two proteins in total protein extracts prepared from *KPC* and *KPTC* cells confirmed the results of the secretome analysis, with *KPC* cells showing greater levels of expression for both Col6A1 and Lcn2 (Figure 3.10C); spontaneous lung metastases were also confirmed to express Col6A1 and Lcn2 (Figure 3.10D). However, mRNA expression of Col6A1 and Lcn2 was upregulated to a similar magnitude by Tgfβ1 stimulation in both KPC and KPTC cells. This indicates that the Tgfβ downstream pathways responsible for promoting PDA metastasis may be different from those that control Col6A1 and Lcn2 expression (Figure 3.11). To determine if these two proteins have a causal effect on metastasis, we tested their ability to modulate

experimental lung metastases. Stable knockdown of Col6A1 in both *KPC2* (Figure 3.10E) and *KPC9* (Figure 3.10F) primary cells led to significant reductions in lung colonization (Figure 3.10G, p=0.001; Figure 3.10H, p=0.047) compared to mice injected with primary cells stably transfected with a scrambled shRNA. Despite efficient knockdown of Lcn2 in *KPC2* cells (Figure 3.10E) only a modest effect on lung colonization was seen (Figure 3.10G). This supports the view that prometastatic proteins work as a collective unit such that knockdown of any individual protein may not have a robust effect (156). By contrast, stable overexpression of Col6A1 or Lcn2 in *KPTC4* cells (Figure 3.10I) caused a marked increase in metastatic lung colonization compared to mock expressing cells (Figure 3.10J, $p<0.0001$ and $p<0.0001$, respectively). Together, these observations indicate that the prometastatic effects of Tgfβ1 include secretion of soluble mediators that can enhance the efficiency of distant metastasis in pancreatic cancer.

Discussion

The TGFβ pathway has long been known to exert both tumor suppressive and tumor promoting properties (40; 69). The tumor suppressive functions of this pathway stem from its role in cytostasis, apoptosis and differentiation; loss of these suppressive influences may occur through genetic or epigenetic mechanisms thus allowing the cancer cell to co-opt TGFβ responses for invasion, dissemination and metastatic colonization (40). Our data indicate that aggressive PDAs follow this paradigm, in keeping with findings of restrained PanIN progression in an *EL-Kras/Tgfbr1*$^{+/-}$ pancreatic cancer mouse model (163). However, we now show strong evidence that for a subset of PDA the tumor suppressive effects of the TGFβ pathway are retained after carcinogenesis, the phenotypic consequences of which are oligometastatic pancreatic cancer (Figure 3.12).

Evidence suggesting the tumor-promoting role of the TGFβ pathway were shown by Ijichi et al in a model of aggressive pancreatic ductal adenocarcinoma based on conditional inactivation of *Tgfβr2* in association with *Kras*^{G12D} expression (118). While our data are entirely in keeping with their findings, they also clarify the role of *Tgfβr2* by demonstrating that aggressive growth at the primary site is not synonymous with metastatic propensity, and may even have an inverse correlation, consistent with observations by Ostapoff using a neutralizing Tgfβr2 antibody (164). In this regard the KPTC model faithfully recapitulates clinical stage III patients who are diagnosed with locally advanced disease in the absence of metastases, some of who may never progress systemically but who die from complications of infiltration into adjacent vital structures (28). The extent to which patients with locally advanced PDA are enriched for the oligometastatic phenotype or for inactivating mutations in *TGFβR2* may be worthwhile to

determine. Of interest, Blackford et al showed that surgically resected patients whose carcinomas have *TGFβR2* mutations have an improved overall survival compared to those with *SMAD4* inactivation (35) although the patterns of failure of these patients were unknown.

These findings do not minimize the roles of other critical pathways for this disease, including TGFβ, in the stromal compartment. In fact, the pronounced stromal response in regions of low cell-autonomous TGFβ suggest an enhancement of paracrine regulation with potentially important consequences for stromal modulating therapies (165-167). These consequences relate to not only the heterogeneity of the stromal reaction within a single PDA, but to the heterogeneity of the stromal reaction across different PDAs as well.

The mechanisms by which the TGFβ pathway converts from tumor suppressive to tumor promoting appear to vary by tumor type (40). In pancreatic cancer, this shift may be mediated by mutation of the *TP53* tumor suppressor gene given its occurrence in late carcinogenesis that coincides with the acquisition of TGFβ oncogenic activity (107), its known role in promoting metastasis (168-170), that somatic mutation of *TP53* occurs at much higher frequency that that of *SMAD4,* that loss of *SMAD4* is not required for the development of aggressive metastatic disease, and finally that patients with oligometastatic disease are more likely to have wild type *TP53* (171). In this regard SMAD4 loss compounds the tumor promoting effects of TGFβ to an even greater extent, resulting in the most virulent form of PDA. Given that *SMAD4* loss itself may promote metastasis of PDA (117), the tumor promoting properties of the TGFβ pathway in the

setting of mutant *TP53* can thus be classified as Smad4-dependent and independent (172; 173).

The above interpretation may also serve to explain the conclusion by Hezel et al that the TGFβ pathway is suppressive during progression; in that murine model a *Trp53* null allele was used and both cell-autonomous and non-cell autonomous TGFβ ligand was pharmacologically targeted (174). Regardless, the work by Hezel et al clearly demonstrates the complexities of targeting this pathway that should be taken into consideration.

Conditional mouse models of pancreatic cancer have proven invaluable in discerning the biologic events of significance for this disease (reviewed in (175)). Such events include the relevance of *KRAS* activation within different lineages of the pancreas that lead to pancreatic intraepithelial neoplasia formation, the combined effects of mutant *KRAS* and candidate tumor suppressor gene inactivation in PDA progression and metastasis (176), and the biological characteristics of this disease with relevance for clinical management (137; 145; 166; 167; 177; 178). However, notable efforts to represent the aggressive metastatic phenotype of pancreatic cancer have resulted in a paucity of models of the oligometastatic phenotype that are encountered in up to 10-20% of human pancreatic cancer patients (28; 179; 180). In the future, studies that incorporate information regarding metastatic burdens into both human outcome data and phenotypic analyses of conditional mouse models should generate additional insights into the biology of this complex tumor type.

Figures and Tables

Figure 3-1: Histologic and Molecular Features of Human Oligometastatic Pancreatic Cancer

(A) Examples of primary tumor tissues collected at autopsy from patient A56 with oligometastatic pancreatic cancer, and of patient A93 with widely metastatic pancreatic cancer. See also Figure 2. **(B)** Quantification of the percent tubular growth pattern (well to moderate gland differentiation) per histologic review of one complete cross section per PDA. Frequency distributions were compared by Fisher Exact Test. **(C)** Representative E-cadherin and vimentin immunolabeling in oligometastatic and widely metastatic PDA. **(D,E)** Representative TGFβ1 (D) and TGFβR2 (E) expression in two oligometastatic and two widely metastatic PDA. Insets in the A70 and A56 TGFβ1 stained tissues illustrate rare positive labeling stromal or immune cells. Arrows in TGFβ1 labeled sections of A43 and A93 illustrate positive labeling peritumoral stroma. *Scale bars, 100 μm.*

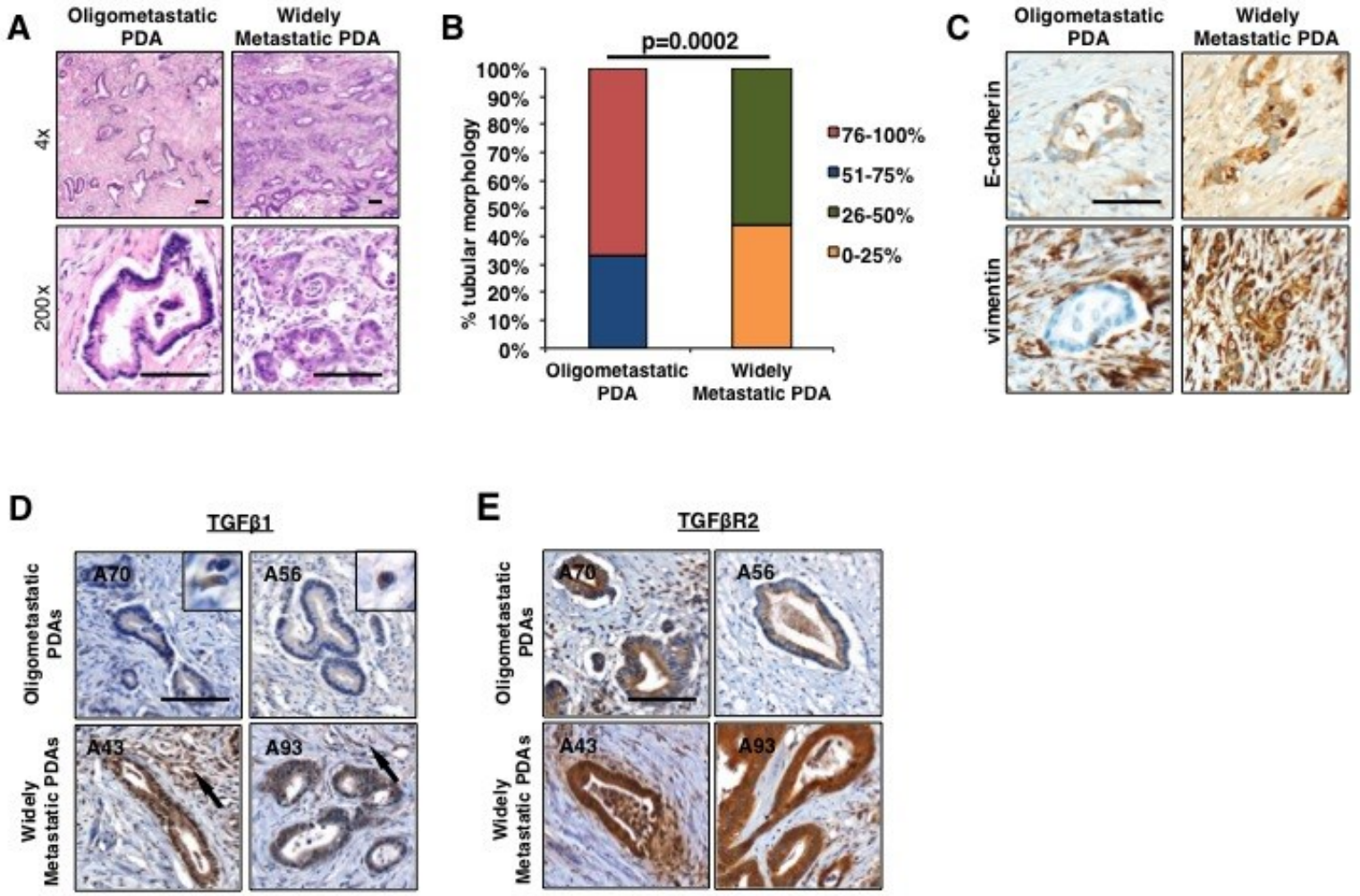
A
Oligometastatic PDA
Widely Metastatic PDA
4x
200x
B
p=0.0002
% tubular morphology
100%
90%
80%
70%
60%
50%
40%
30%
20%
10%
0%
Oligometastatic PDA
Widely Metastatic PDA
76-100%
51-75%
26-50%
0-25%
C
Oligometastatic PDA
Widely Metastatic PDA
E-cadherin
vimentin
D
TGFβ1
Oligometastatic PDAs
Widely Metastatic PDAs
A70
A56
A43
A93
E
TGFβR2
Oligometastatic PDAs
Widely Metastatic PDAs
A70
A56
A43
A93

Figure 3-2: Histologic Features of Oligometastatic and Widely Metastatic Pancreatic Cancers

(A) Examples of primary tumor tissues collected at autopsy from patients A77 and A70 with oligometastatic pancreatic cancer. The arrow in A70 illustrates a single cancer cell within the stroma, shown at higher power in the inset. **(B)** Examples of primary tumor tissues collected at autopsy from patients A17 and A132 with widely metastatic pancreatic cancer. **(C)** Movats pentachrome and α-smooth muscle actin staining representative oligometastatic and widely metastatic PDA. **(D)** Histomorphology of metastases to the lymph node and lung of patient A70 whose primary PDA tissue is shown in (A). **(E)** Perineural invasion in representative oligometastatic (A70) and widely metastatic pancreatic cancer (A125). *Scale bars, 100 μm.*

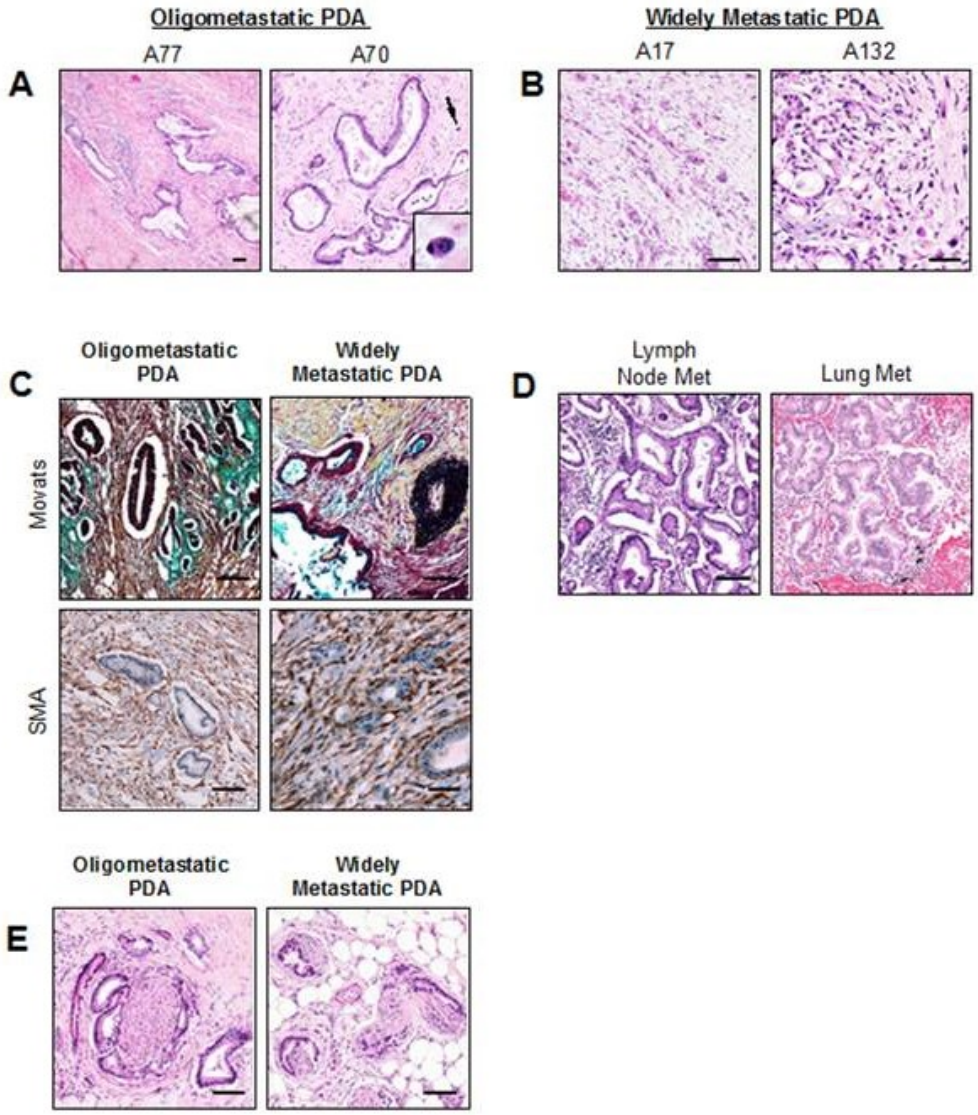
A
Oligometastatic PDA
A77
A70
B
Widely Metastatic PDA
A17
A132
C
Oligometastatic PDA
Widely Metastatic PDA
Movats
SMA
D
Lymph Node Met
Lung Met
E
Oligometastatic PDA
Widely Metastatic PDA

Figure 3-3: Generation and Characterization of KPTC Mice

(A) Recombination of the *LSL-Kras*$^{G12D/+}$ and *LSL-Trp53* $^{R172H/+}$ alleles in the pancreata but not kidneys of KPC and KPTC mice. Recombination of one conditional *Tgfbr2* allele is seen in KPTC mice specifically. **(B)** Kaplan-Meier survival curves of *KPTC, KPC, KTC, KC* and control mouse cohorts. KPTC mice have a significantly shortened median survival compared to both KPC ($p<0.0001$) and KTC mice ($p=<0.0001$). Medians survivals were compared by pair-wise log-rank tests. **(C)** Gross findings in a representative moribund KPTC mouse with hemorrhagic ascites and jaundice. **(D)** Representative KPTC tumor showing infiltration into the adjacent stomach wall (arrows). **(E)** Representative well to moderately differentiated PDA in KPTC mouse shown in C,D. **(F)** Frequency of ADM and mPanIN grades 1-3 in pancreata of KPC and KPTC mice at 4, 8 and 12 weeks timepoints. The frequency of high grade PanIN (mPanIN3) is significantly higher in KPTC mice at 12 weeks (Chi-squared test), a subset of which also had infiltrating PDA. Nine-ten mice per genotype were used at each timepoint. *Scale bars, 100 μm*

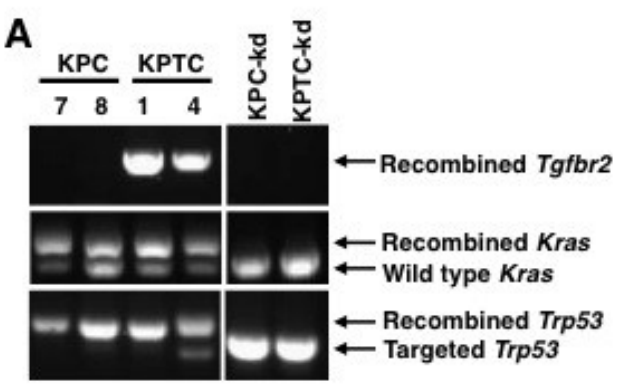
A
KPC
KPTC
7 8 1 4
KPC-kd
KPTC-kd
Recombined Tgfbr2
Recombined Kras
Wild type Kras
Recombined Trp53
Targeted Trp53

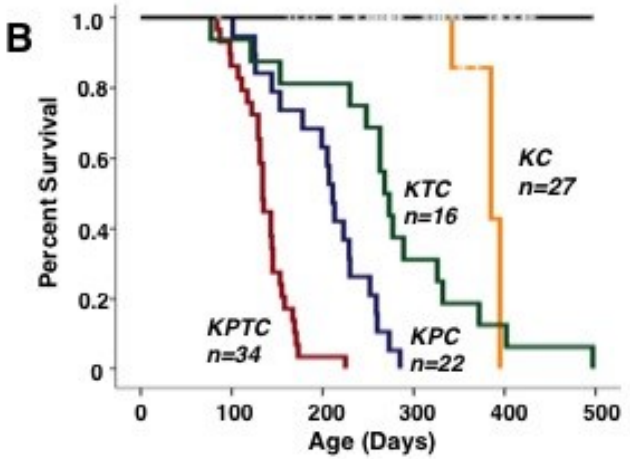
B
Percent Survival
1.0
0.8
0.6
0.4
0.2
0
0
100
200
300
400
500
Age (Days)
KPTC
n=34
KPC
n=22
KTC
n=16
KC
n=27


C

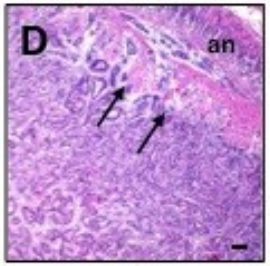
D
an

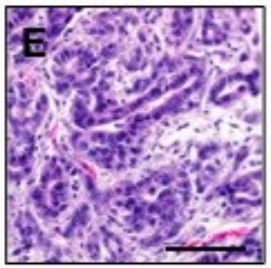
E

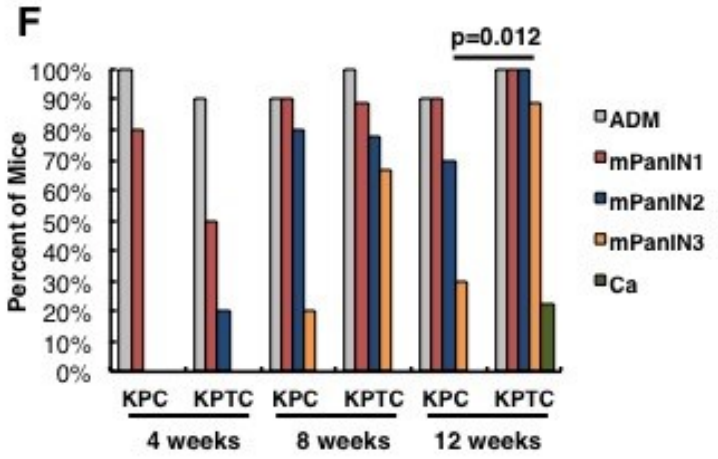
F
p=0.012
Percent of Mice
100%
90%
80%
70%
60%
50%
40%
30%
20%
10%
0%
KPC
KPTC
KPC
KPTC
KPC
KPTC
4 weeks
8 weeks
12 weeks
ADM
mPanIN1
mPanIN2
mPanIN3
Ca

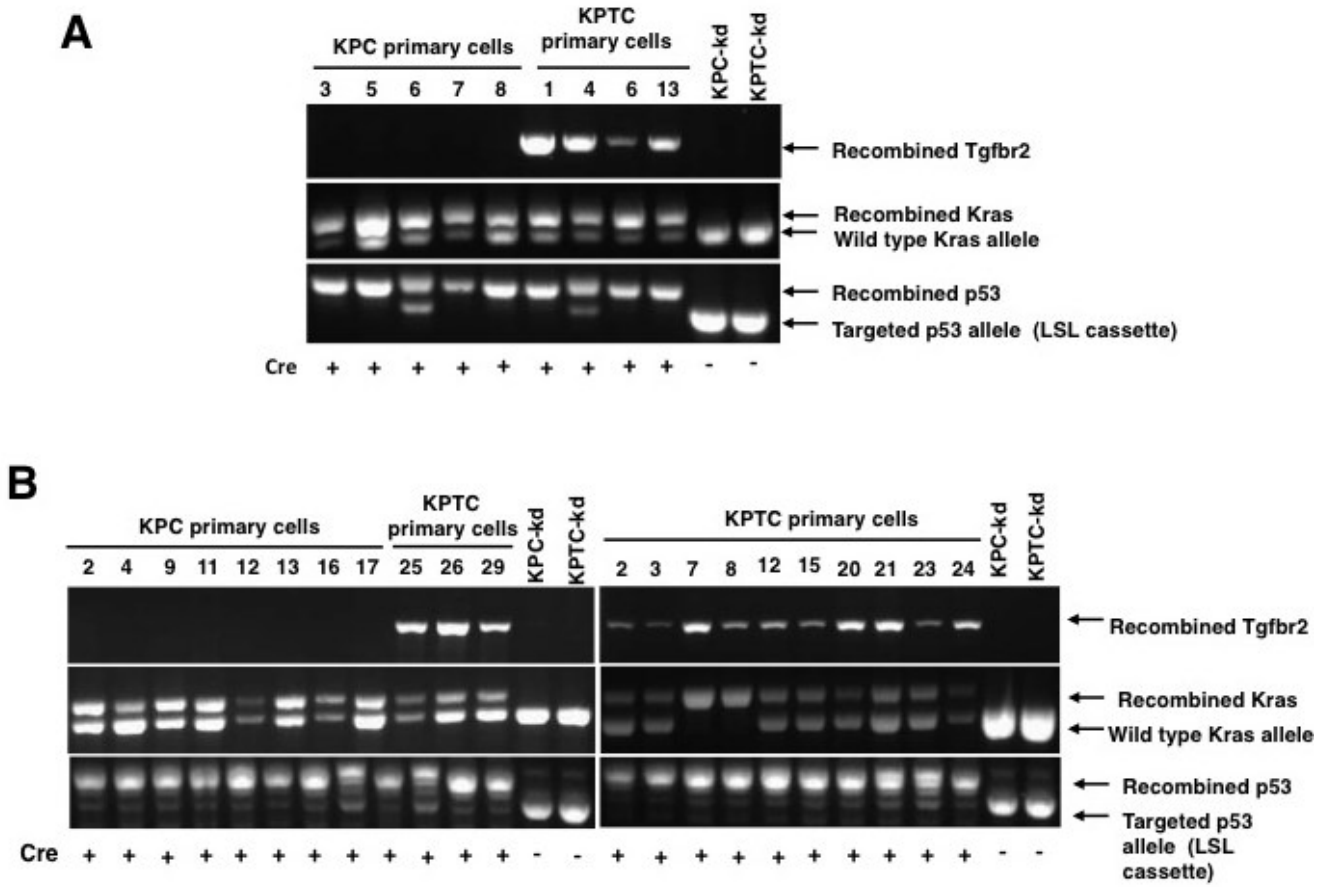

Figure 3-4: Genotyping of Primary KPTC and KPC PDA Cells

Recombination of the *LSL-Kras*$^{G12D/+}$ and *LSL-Trp53* $^{R172H/+}$ alleles in the pancreata but not kidneys of *KPC* and *KPTC* mice. Recombination of one conditional *Tgfbr2* allele was also demonstrated in *KPTC* mice specifically. *KPC7, KPC8, KPTC1* and *KPTC4* are also shown in Figure 3.3.

Figure 3-5: Loss of Cell-Autonomous *Tgfbr2* Leads to a Loss of Metastatic Traits in KPTC Tumors

(A) Representative histologic features of poorly-differentiated versus well-differentiated regions of the same PDA in KPTC22. Smooth muscle actin (SMA) highlights the greater abundance of stroma in the well-differentiated component. **(B)** Quantification of the percent tubular morphology of KPTC or KPC PDA based on histologic review of one complete cross section per PDA. KPTC tumors show a significant shift towards a more differentiated (tubular) morphology compared to KPC tumors. Frequency distributions were compared by Fisher Exact Test. **(C-G)** Heterogeneity for immunolabeling of TgfβR2 and Tgfβ1 in representative KPTC3 PDA. At scanning power **(C)** regions of both positive and negative labeling can be seen. These regions are shown at higher power in D and E, illustrating TgfβR2 positive labeling corresponds to poorly differentiated morphology **(D),** whereas loss of TgfβR2 labeling is present in the well-differentiated morphology of this same tumor (indicated by dashed outline, **(E)**. The inset in E demonstrates membranous labeling for TgfβR2. By contrast, no difference in labeling for Tgfβ1 expression is seen among poor **(F)** and well-differentiated regions **(G)** of this same PDA. **(H-K)** Heterogeneity for immunolabeling of Tgfβr2 and Tgfβ1 in representative KPC2 PDA. Similar to KPTC3, there is heterogeneity in intensity of Tgfβr2 labeling among the poor **(H)** and well-differentiated (indicated by dashed outlines, **(I)** regions of this PDA. Tgfβ1 expression is seen among poor **(J)** and well-differentiated regions **(K)** of this same PDA, although there is focal loss in the well-differentiated region (arrow, K). **(L-O)** Representative fibronectin immunolabeling in KPTC3 **(L,M)** and KPC2 **(N,O)** PDA tissues. Dashed lines outline well-differentiated PDA in M and O respectively. **(P)** Immunofluorescence labeling for E-cadherin in representative KPC and KPTC primary cells treated with vehicle or TGFβ1. DAPI was used as a counterstain to visualize nuclei. *Scale bars, 100 μm.*

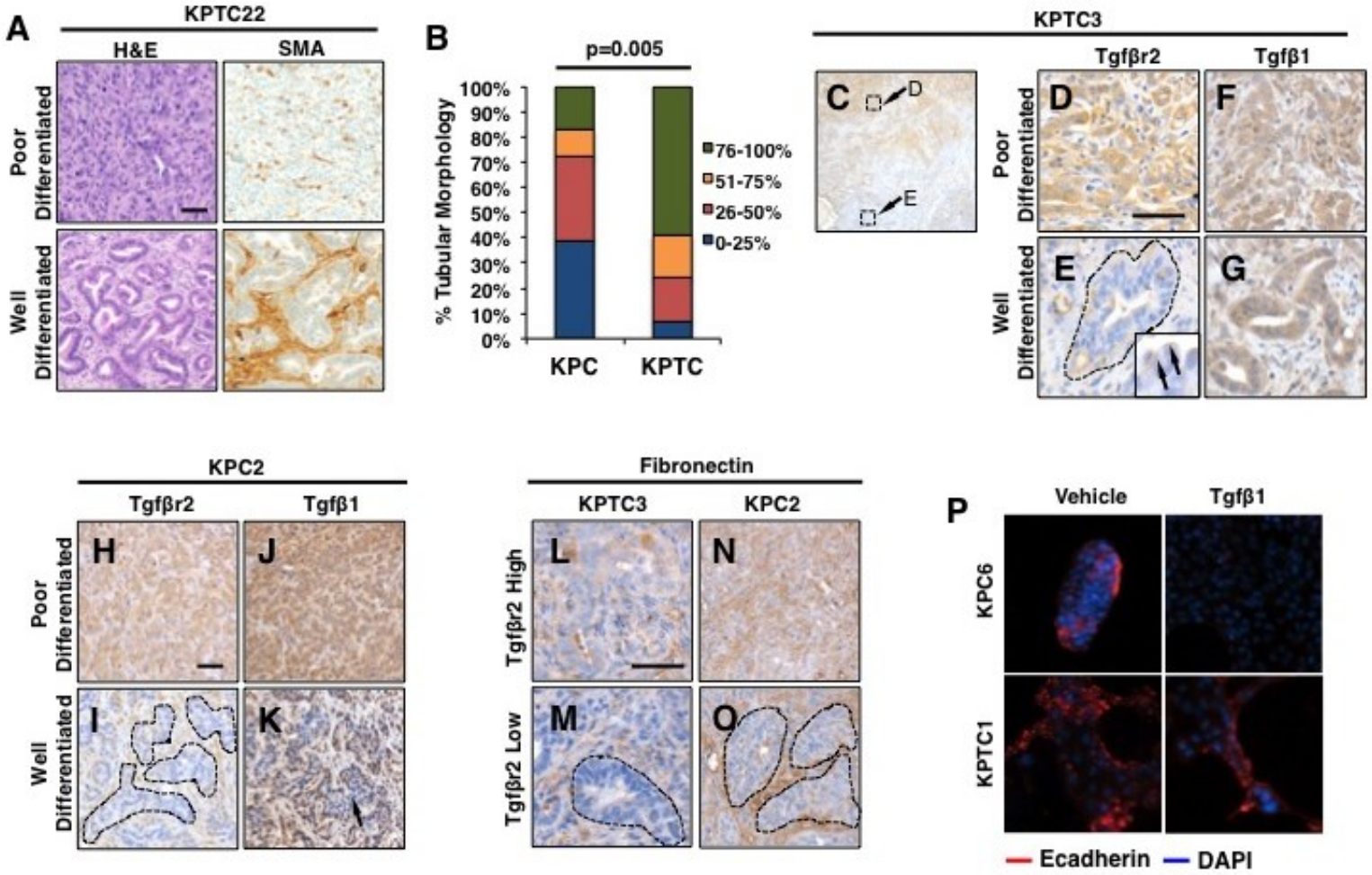
A
KPTC22
H&E
SMA
Poor Differentiated
Well Differentiated
B
p=0.005
% Tubular Morphology
100%
90%
80%
70%
60%
50%
40%
30%
20%
10%
0%
KPC
KPTC
76-100%
51-75%
26-50%
0-25%
KPTC3
C
D
E
Tgfβr2
Tgfβ1
F
G
KPC2
H
J
I
K
Fibronectin
KPTC3
KPC2
Tgfβr2 High
Tgfβr2 Low
L
N
M
O
P
Vehicle
Tgfβ1
KPC6
KPTC1
Ecadherin
DAPI

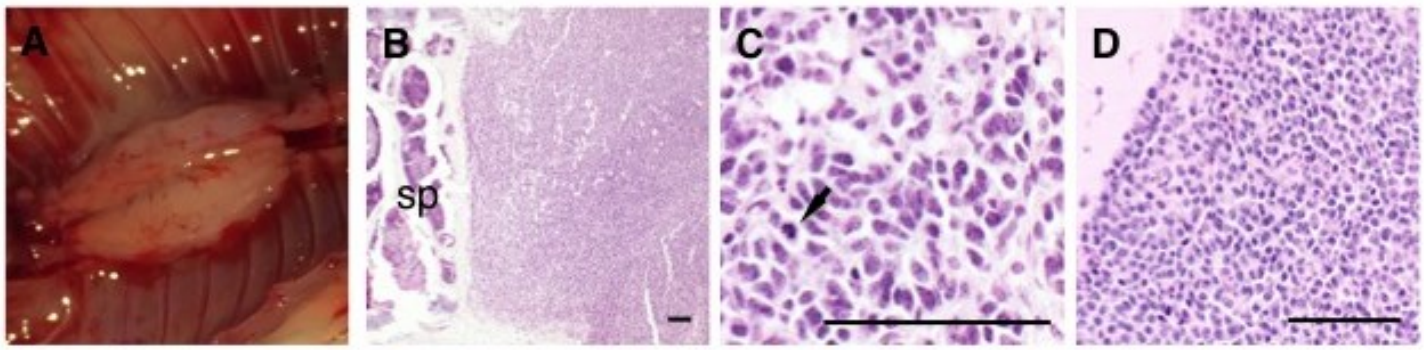

Figure 3-6: Extrapancreatic Tumors in KPC and KPTC Mice

(A) Gross example of spinal tumor in KPC mouse. **(B)** Low power histologic view of the tumor shown in A. The spine (sp) is shown at the left of the image. **(C)** Higher power histologic view of tumor shown in A, demonstrating features of a high-grade neoplasm with mitotic figures (arrow). **(D)** Cerebellar tumor in representative KPC mouse. *Scale bars, 100 μm.*

Figure 3-7: Molecular Features of KPTC PDAs

(A) Genotyping for *Kras*, *Trp53* and *Tgfbr2* recombination events in co-existent well differentiated (W) and poorly differentiated (P) PDA in KPTC mice. **(B)** Immunolabeling for Trp53 in primary KPTC and KPC PDA tissues. **(C,D)** Western blots of Smad4 and p16 expression in representative KPC and KPTC primary cells. Labeling of actin is used as a loading control.

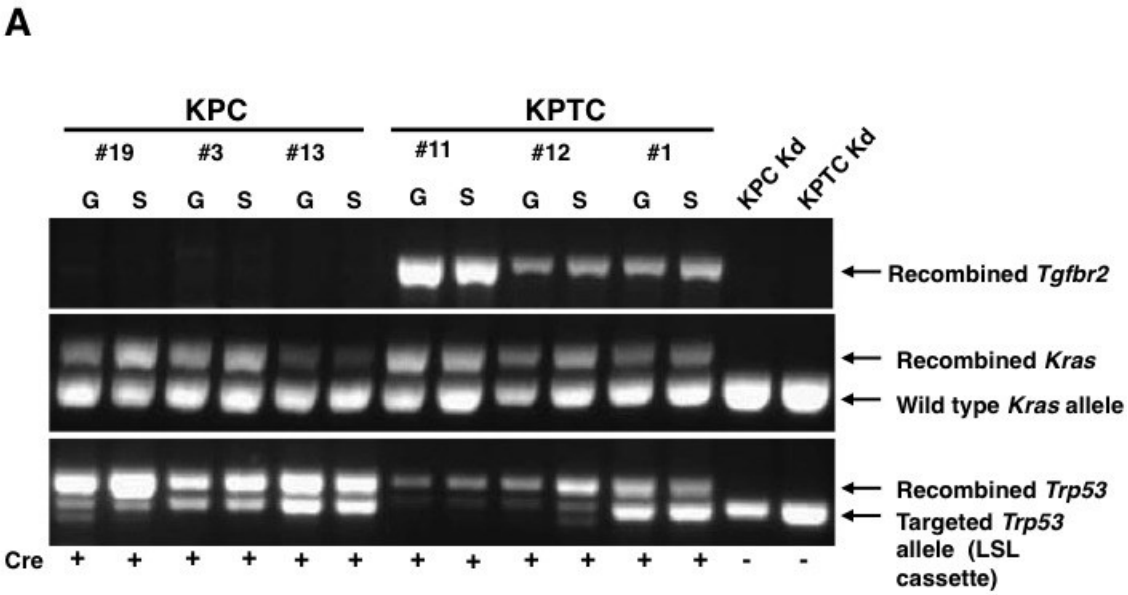
A
KPC
KPTC
#19
#3
#13
#11
#12
#1
G S G S G S G S G S G S
KPC Kd
KPTC Kd
Recombined Tgfbr2
Recombined Kras
Wild type Kras allele
Recombined Trp53
Targeted Trp53 allele (LSL cassette)
Cre + + + + + + + + + + + + - -

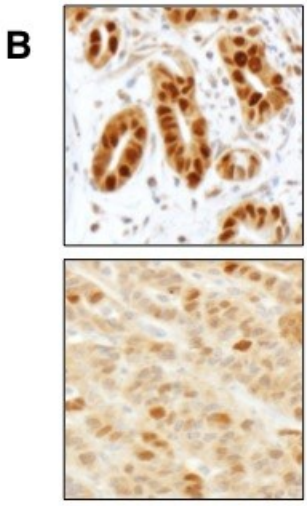
B

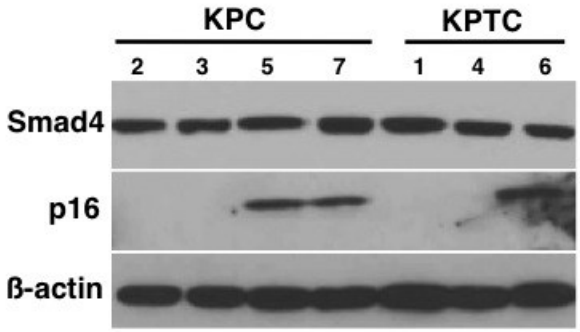
C
KPC
KPTC
2 3 5 7 1 4 6
Smad4
p16
ß-actin

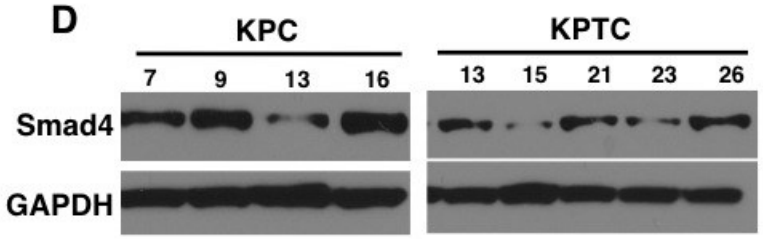
D
KPC
KPTC
7 9 13 16 13 15 21 23 26
Smad4
GAPDH

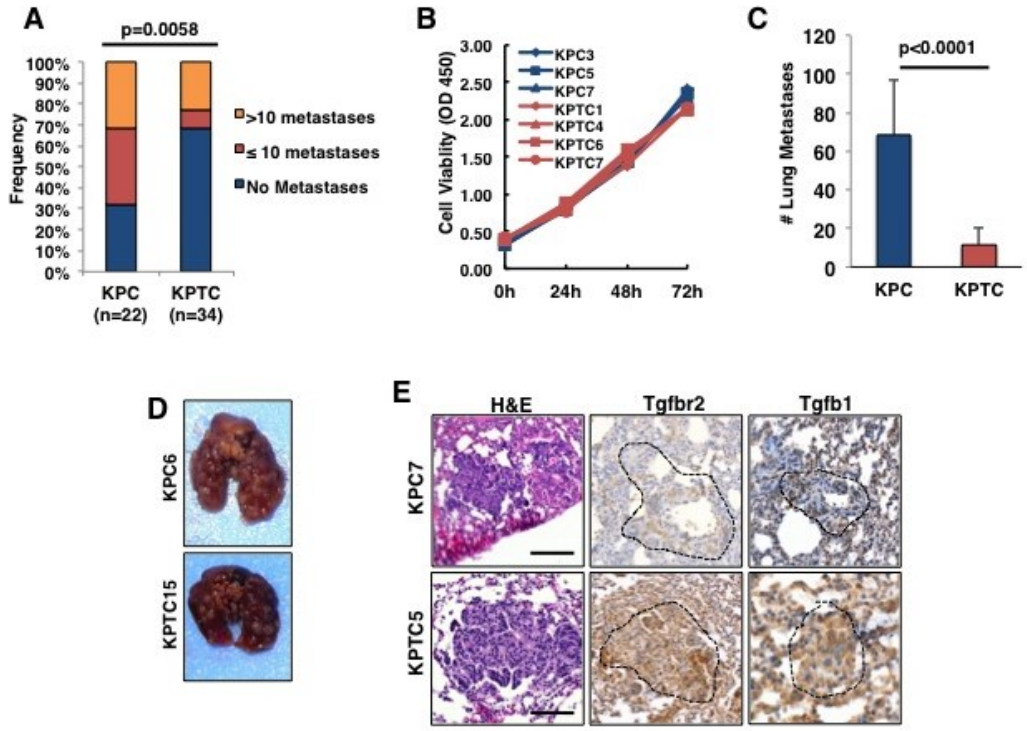

Figure 3-8: Cell-Autonomous Tgfβ Signaling Mediates the Efficiency of Metastatic Colonization of the Lungs

(A) Gross metastatic burdens at necropsy in KPC (n=22) and KPTC mice (n=34). Frequency distributions were compared by Chi-Square test. **(B)** Quantification of cell proliferation in primary KPC and KPTC cells. Data shown represent the mean ± standard deviation of three independent experiments per cell line. **(C)** Quantification of gross metastatic lung colonization at three weeks following tail vein injection of 1 x 10^5 primary KPC versus KPTC cells. Data shown represent the mean ± standard deviation of at least four primary cell lines per genotype, with each line injected into at least four mice per experiment. **(D)** Representative lungs in mice injected with KPC6 or KPC15 primary cells. Mice were sacrificed three weeks after injection of 1 x 10^5 primary cells. **(E)** Histologic and immunolabeling features of spontaneous lung metastases in representative KPC and KPTC mice. Compared to the background normal lung, there is no difference in labeling for Tgfβr2 or Tgfβ1 in the metastatic PDA cells. Scale bar, 100 μm.

Figure 3-9: Cell-Autonomous Tgfβ Signaling Mediates the Efficiency of Metastatic Colonization of the Liver

(A) Example of intravascular PDA in KPTC mouse liver. **(B)** Higher power of intravascular PDA illustrating intraluminal red blood cells and lymphocytes (arrow). **(C)** Higher power of intravascular PDA illustrating adjacent bile ducts (*bd*, arrows). **(D)** CD31 labeling of liver shown in A illustrating intravascular PDA involvement of the portal vein within a portal triad. *a*, artery; *v*, vein; *bd*, bile duct; *, lumen of intravascular PDA. **(E)** CK19 labeling of intravascular PDA. **(F)** p53 labeling of intravascular PDA. **(G,H)** Representative intravascular metastases with more complex growth features and size. **(I)** Representative invasive liver metastasis. Arrow indicates the reactive stromal response. **(J)** Intravascular (itv) and invasive (inv) liver metastases in KPC mouse. **(K)** Frequency of intravascular versus invasive liver metastases in KPC and KPTC mice. Frequency distributions compared by Fisher Exact Test. **(L)** Fibronectin labeling in intravascular and invasive liver metastases. *Scale bars, 100 μm.*

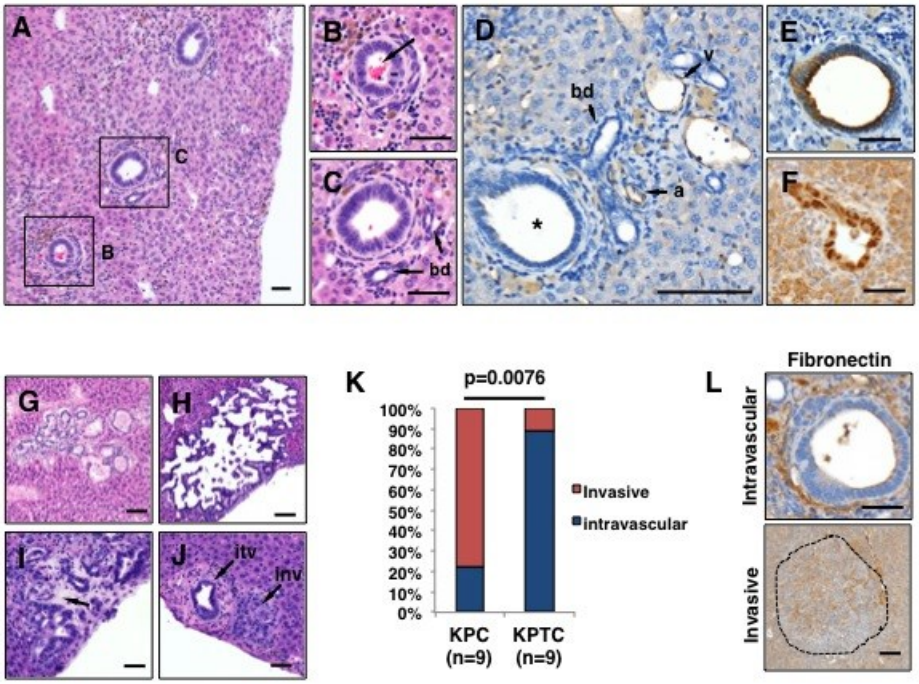
A
B
C
D
E
F
G
H
I
J
K
L
bd
v
a
itv
inv
p=0.0076
100%
90%
80%
70%
60%
50%
40%
30%
20%
10%
0%
Invasive
intravascular
KPC
(n=9)
KPTC
(n=9)
Fibronectin
Intravascular
Invasive

Figure 3-10: Tgfβ Signaling Promotes the Secretion of Novel Mediators of Distant Metastasis

(A) Schematic of experimental approach for identifying TGFβ-stimulated differentially secreted proteins using iTRAQ. **(B)** Hierarchical cluster analysis of the 48 secreted proteins identified as more abundant in the KPC secretome. See also Table S4. **(C)** Western blots of total protein extracted from KPC and KPTC primary cell lines and labeled for Col6A1 and LCN2 protein. Levels of GAPDH are shown as a loading control. **(D)** Immunolabeling for Col6A1 and Lcn2 in representative spontaneous KPC lung metastases. **(E)** Western blots demonstrating efficiency of knockdown of Col6A1 or Lcn2 in KPC2 cells. **(F)** Western blots demonstrating efficiency of knockdown of Col6A1 in KPC9 cells. **(G,H)** Quantification of lung colonization by KPC2 cells (G) or KPC9 cells (H) stably transfected with scrambled, Col6a1 or Lcn2 shRNAs. Data shown are the mean ± S.D of at least four animals per condition. Comparisons were made using a Student's T Test. **(I)** Western blots demonstrating overexpression of Col6A1 or LCN2 in KPTC4 cells. **(J)** Quantification of lung colonization by KPTC4 cells stably transfected with an empty or Col6a1 or Lcn2 expressing vector. Data shown are the mean ± S.D of at least four animals per condition. Comparisons were made using a Student's T Test.

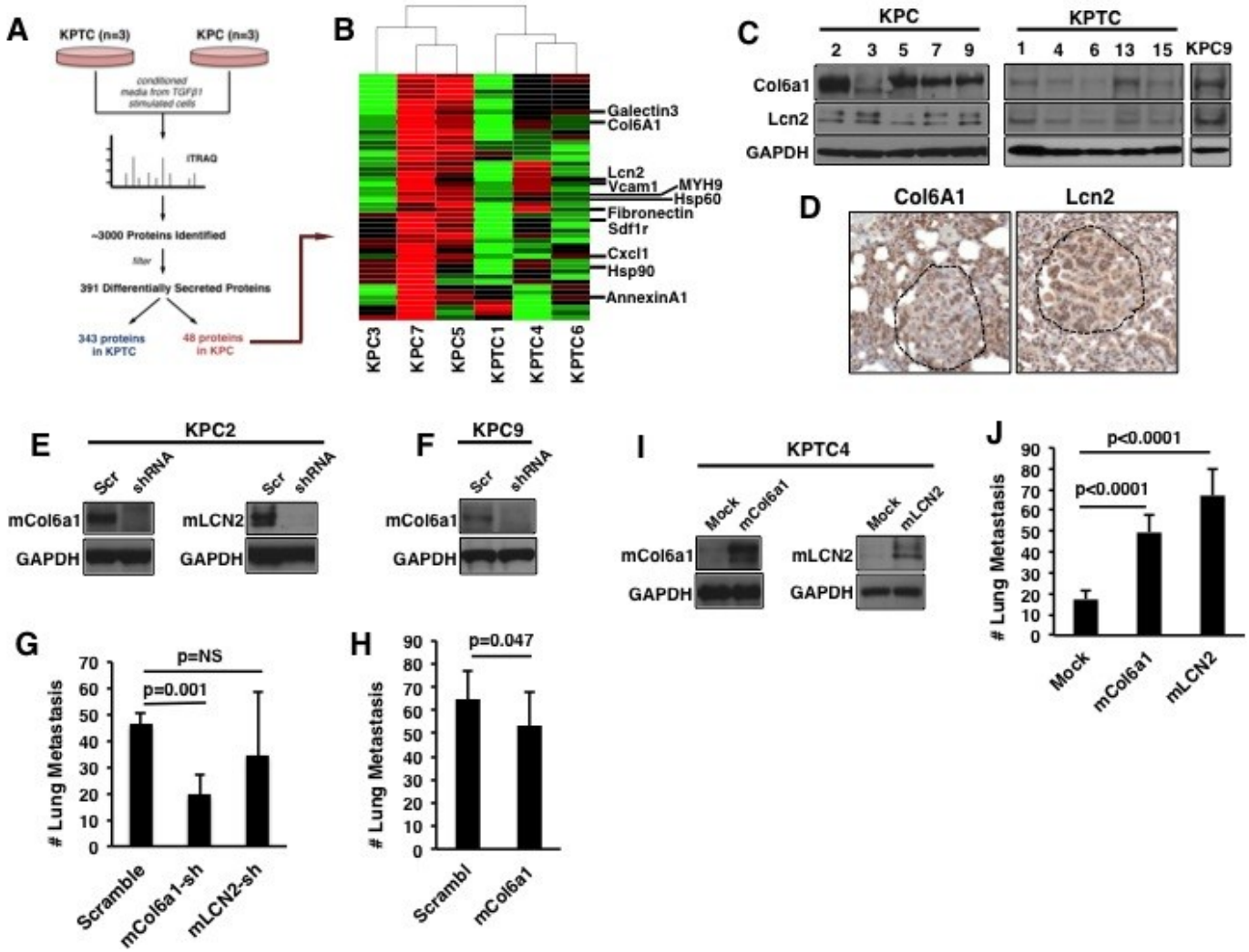
A
KPTC (n=3)
KPC (n=3)
conditioned media from TGFβ1 stimulated cells
ITRAQ
~3000 Proteins Identified
filter
391 Differentially Secreted Proteins
343 proteins in KPTC
48 proteins in KPC
B
Galectin3
Col6A1
Lcn2
Vcam1
MYH9
Hsp60
Fibronectin
Sdf1r
Cxcl1
Hsp90
AnnexinA1
KPC3
KPC7
KPC5
KPTC1
KPTC4
KPTC6
C
KPC
KPTC
2 3 5 7 9
1 4 6 13 15
KPC9
Col6a1
Lcn2
GAPDH
D
Col6A1
Lcn2
E
KPC2
Scr
shRNA
mCol6a1
GAPDH
mLCN2
F
KPC9
I
KPTC4
Mock
mCol6a1
mLCN2
J
p<0.0001
Lung Metastasis
Mock
mCol6a1
mLCN2
G
p=NS
p=0.001
Scramble
mCol6a1-sh
mLCN2-sh
H
p=0.047
Scrambl
mCol6a1

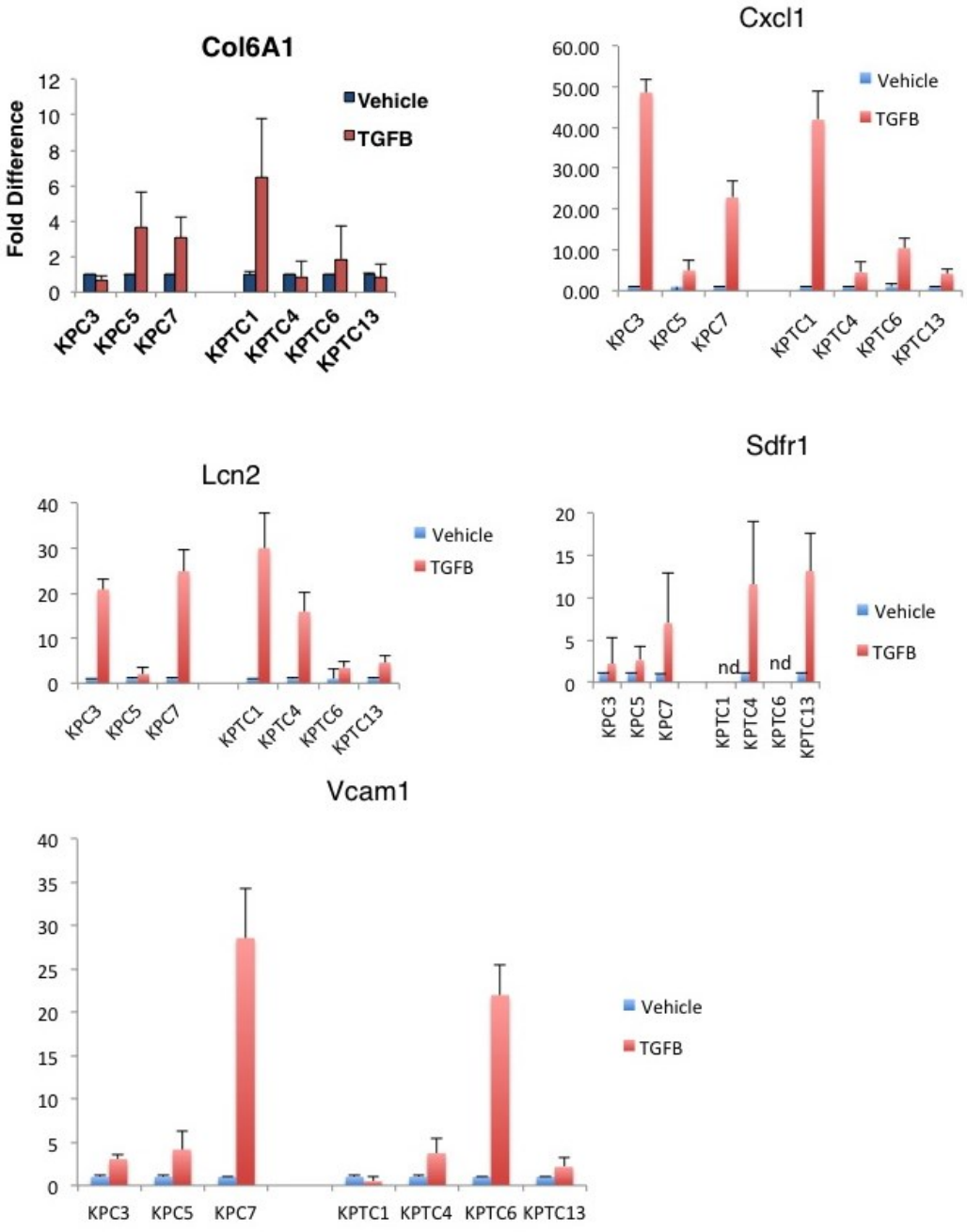

Figure 3-11: mRNA Expression of Candidate TGF-Associated Secreted Proteins

Quantitative PCR for expression of Col6A1, LCN2, SDF1r and VCAM1 genes whose protein products were identified as more abundant in the KPC secretome. Data shown represent the mean ± standard deviation of three independent PCRs per primary cell line. At least three cell lines per genotype were analyzed.

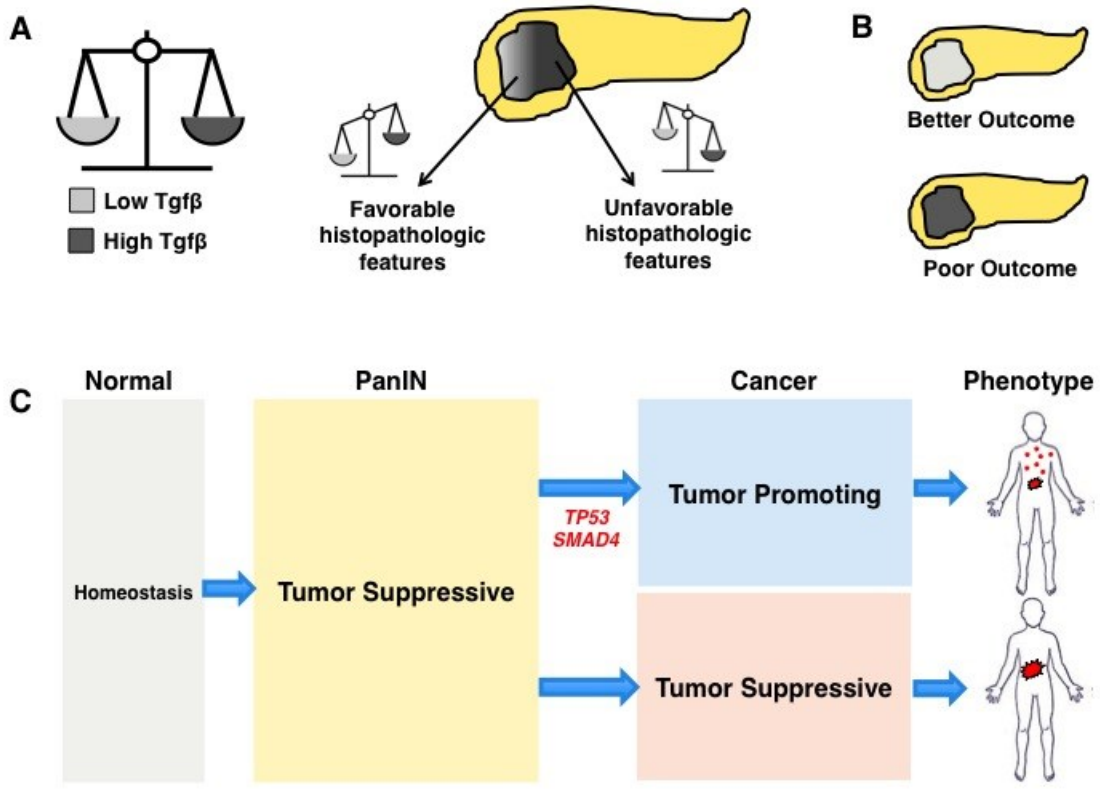

Figure 3-12: Integrated Model of TGFβ Signaling in Pancreatic Cancer

(A,B) Cell-autonomous TGFβ signaling in PDA exists varies across geographic sites within a single PDA (A) and across different PDAs (B). Low levels correspond to favorable histologic features and high levels correspond to unfavorable histologic features, aggressive behavior and worse outcome in patients. **(C)** TGFβ signaling in normal pancreatic epithelial cells maintains tissue homeostasis, and is suppressive during carcinogenesis. However, in PDA this pathway converts to a potent trigger of aggressive behavior and efficient metastasis to distant sites, potentially as a result of *TP53* and *SMAD4* mutations that occur in advanced stage PanINs. By contrast, PDAs that retain wild type *TP53* and *SMAD4* retain the suppressive properties of the TGFβ pathway leading to pronounced growth of the primary tumor but low metastatic efficiency.

Table 3.1: Clinicopathologic Features of Patients Studied

Case	Age/Sex	Race	Differentiation	Perineural Invasion	Vascular Invasion	Clinical Stage at Diagnosis	Overall Survival (months)	Metastatic Burden at Autopsy	Sites of Metastasis
25	59M	Caucasian	Moderate	N	N	I	23	0	
77	84F	Caucasian	Moderate	Y	Not seen	III	3	0	
13	59M	Caucasian	Poor	Y	Not seen	IV	7	≤10	Liver, Lung, Para-aortic Lymph Nodes
33	64M	Caucasian	Moderate	Y	Y	IV	1	≤10	Liver, Lung, Abdominal Lymph Nodes
56	54M	Caucasian	Well	Y	Not seen	III	4	≤10	Liver, Adrenal
70	78F	Caucasian	Well	Y	Y	IV	1	≤10	Liver, Lungs, Peritoneum, Abdominal Lymph Nodes
17	50F	Caucasian	Poor	Y	Y	IV	5	>100	Liver, Lung, Peritoneum
43	85F	Caucasian	Moderate to Poor	Y	Y	IV	2	>100	Liver
93	74M	Caucasian	Moderate to Poor	Y	Not seen	IV	4	>100	Liver, Lung, Peritoneum, Abdominal Lymph Nodes
124	74M	Caucasian	Moderate to Poor	Not seen	Y	IV	3	>100	Peritoneum
125	69F	Caucasian	Moderate to Poor	Y	Y	IV	0.5	>100	Liver
31	64F	Hispanic	Poor	Y	Y	IV	2	11-100	Liver, Lung
51	68M	Caucasian	Poor	Not seen	Y	IV	5	11-100	Liver
132	79M	Caucasian	Moderate to Poor	Not seen	Y	IV	10	11-100	Liver, Lung
57	64F	Caucasian	Moderate to Poor	Not seen	Y	IV	3	>100	Liver

Table 3.2: Immunohistochemical Analysis of Patients Studied

Case	TGFB1 Immunolabeling	TGFBR2 Immunolabeling
25	Not stained (tissues exhausted)	Not stained (tissues exhausted)
77	Negative (internal controls positive)	Weak positive
13	Negative (internal controls positive)	Negative (internal controls positive)
33	Negative (internal controls positive)	ND (autolysis)
56	Negative (internal controls positive)	Weak positive
70	Negative (internal controls positive	Strong positive
17	Positive	Strong positive
43	Strong Positive	Strong positive
93	Strong Positive	Strong positive
124	Positive	Positive
125	Negative (internal controls positive)	Positive
31	Positive	Strong positive
51	Negative (internal controls positive)	Positive
132	Positive	Strong positive
57	Positive	Strong positive

Solid black line separates oligometastatic patients (top; n = 6) from widely metastatic patients (bottom; n = 9).

Table 3.3: Metastatic Burden in KPC and KPTC Mice

The table shows clinical and metastatic burden data for KPC (n = 22) and KPTC (n = 34) mice. All mice were followed until moribund, at which time they were sacrificed and complete necropsies were performed. Sites of metastases are indicated for each animal.

ID	Genotype	Gender	Survival (Days)	Total Gross Mets	Peritoneal Mets	Diaphragm Mets	Liver Mets	Lung Mets	Lymph Node Mets
KPC10	KPC	Female	293.5	0					
KPC15	KPC	Female	270	0					
KPC16	KPC	Female	198	0					
KPC20	KPC	Male	128	0					
KPC4	KPC	Male	214	0					
KPC5	KPC	Male	100	0					
KPC11	KPC	Male	207	2			Yes		
KPC14	KPC	Female	230	2				Yes	
KPC19	KPC	Female	211	2				Yes	
KPC7	KPC	Female	252	5	Yes		Yes	Yes	
KPC1	KPC	Female	153	6	Yes		Yes		
KPC9	KPC	Male	125	9	Yes		Yes		Yes
KPC8	KPC	Female	126	24	Yes			Yes	Yes
KPC6	KPC	Male	205	>10	Yes		Yes	Yes	
KPC12	KPC	Female	262	Innumerable			Yes		
KPC13	KPC	Female	223	Innumerable	Yes		Yes	Yes	
KPC2	KPC	Male	178	Innumerable	Yes		Yes	Yes	Yes
KPC22	KPC	Female	389	Innumerable		Yes	Yes		Yes

KPC3	KPC	Male	229	Innumerable	Yes	Yes	Yes	Yes	Yes
KPC17	KPC	Male	144	>10				Yes	
KPC18	KPC	Male	259	>10		Yes			
KPC23	KPC	Female	287	0					
KPTC12	KPTC	Male	131	0					
KPTC13	KPTC	Female	122	0					
KPTC16	KPTC	Female	92	0					
KPTC17	KPTC	Female	92	0					
KPTC19	KPTC	Male	123	0					
KPTC20	KPTC	Female	145	0					
KPTC21	KPTC	Male	111	0					
KPTC24	KPTC	Female	173	0					
KPTC25	KPTC	Male	87	0					
KPTC26	KPTC	Male	158	0					
KPTC28	KPTC	Male	144	0					
KPTC29	KPTC	Male	158	0					
KPTC30	KPTC	Male	135	0					
KPTC31	KPTC	Male	112	0					
KPTC32	KPTC	Male	169	0					
KPTC33	KPTC	Female	275	0					

KPTC34	KPTC	Male	205	0						
KPTC35	KPTC	Male	137	0						
KPTC4	KPTC	Female	153	0						
KPTC22	KPTC	Male	90	1				Yes		
KPTC2	KPTC	Male	134	2				Yes		
KPTC7	KPTC	Female	225	2				Yes	Yes	
KPTC10	KPTC	Female	131	3				Yes		
KPTC3	KPTC	Male	143	10			Yes	Yes	Yes	
KPTC1	KPTC	Male	99	57	Yes					
KPTC15	KPTC	Female	164	>24				Yes	Yes	Yes
KPTC11	KPTC	Female	131	Innumerable			Yes	Yes	Yes	
KPTC14	KPTC	Male	130	Innumerable				Yes	Yes	Yes
KPTC18	KPTC	Female	129	Innumerable	Yes		Yes	Yes		Yes
KPTC23	KPTC	Male	118	Innumerable					Yes	
KPTC5	KPTC	Male	145	Innumerable				Yes	Yes	Yes
KPTC6	KPTC	Male	155	Innumerable	Yes		Yes	Yes	Yes	Yes
KPTC8	KPTC	Male	122	Innumerable				Yes	Yes	
KPTC9	KPTC	Female	98	Innumerable				Yes	Yes	

Table 3.4: Histopathology of Mouse Tumors

The table shows pathology data for KPC (n = 22) and KPTC (n = 34) mice, including tumor histology, degree of tumor cell differentiation, and percentage of tubular/ductal morphology. All mice were followed until moribund, at which time they were sacrificed and complete necropsies were performed. The corresponding survival and metastatic burden data is presented in Table 3.3.

ID	Genotype	Histology	Differentiation of PDA	Quantitation of Tubular (Ductal) Morphology per complete cross section
KPC10	KPC	Sarcomatoid	Undifferentiated	Not included
KPC15	KPC	PDA	Well	100% tubular
KPC16	KPC	PDA	Moderate/Poor	20% tubular
KPC20	KPC	PDA and sarcoma		Focus of PDA too small to quantify
KPC4	KPC	PDA	Poor	30% tubular
KPC5	KPC	PDA	Poor	30% tubular
KPC11	KPC	PDA	Poor	20% tubular
KPC14	KPC	PDA	Poor	20% tubular
KPC19	KPC	PDA	Moderate	95% tubular
KPC7	KPC	PDA	Poor	50% tubular
KPC1	KPC	PDA	Moderate/Poor	70% tubular
KPC9	KPC	PDA	Poor	30% tubular
KPC8	KPC	PDA	Moderate/Poor	10% tubular
KPC6	KPC	PDA (2 primaries)	Moderate and Moderate	70% and 80% tubular
KPC12	KPC	PDA	Moderate	90% tubular
KPC13	KPC	PDA	Moderate/Poor	50% tubular
KPC2	KPC	PDA	Poor	10% tubular
KPC22	KPC	PDA	Moderate/Poor	50% tubular
KPC3	KPC	PDA	Moderate/Poor	20% tubular
KPC17	KPC	PDA	Moderate/Poor	Focus of PDA too small to quantify
KPC18	KPC	PDA	Moderate/Poor	50% tubular
KPC23	KPC	PDA	Moderate/Poor	50% tubular
KPTC12	KPTC	PDA	Moderate	100% ductal
KPTC13	KPTC	PDA	Moderate	90% ductal
KPTC16	KPTC	PDA	Poor	5% ductal
KPTC17	KPTC	PDA	Poor	5% ductal
KPTC19	KPTC	PDA	Moderate	90% ductal
KPTC20	KPTC	PDA	Moderate/Poor	70% ductal

KPTC21	KPTC	PDA	Moderate/Poor	80% ductal
KPTC24	KPTC	PDA	Moderate/Poor	95% ductal
KPTC25	KPTC	PDA	Moderate/Poor	40% ductal
KPTC26	KPTC	PDA	Moderate/Poor	Focus of PDA too small to quantify
KPTC28	KPTC	PDA	Moderate/Poor	50% ductal
KPTC29	KPTC	PDA	Moderate/Poor	50% ductal
KPTC30	KPTC	PDA	Moderate	90% ductal
KPTC31	KPTC	PDA	Moderate	N/A
KPTC32	KPTC	PDA	Moderate/Poor	80% ductal
KPTC33	KPTC	PDA	Moderate	95% ductal
KPTC34	KPTC	PDA	Well/Moderate	95% ductal
KPTC35	KPTC	PDA	Moderate/Poor	80% ductal
KPTC4	KPTC	PDA	Moderate/Poor	70% ductal
KPTC22	KPTC	PDA	Poor	20% ductal
KPTC2	KPTC	PDA	Moderate	90% ductal
KPTC7	KPTC	PDA	Moderate	90% ductal
KPTC10	KPTC	PDA (2 primaries)	Moderate and Poor	95% and 70% ductal
KPTC3	KPTC	PDA	Moderate/Poor	80% ductal
KPTC1	KPTC	PDA	Moderate	90% ductal
KPTC15	KPTC	PDA	Moderate/Poor	50% ductal
KPTC11	KPTC	PDA with minor sarcomatoid component	Moderate	70% ductal
KPTC14	KPTC	PDA with minor sarcomatoid component	Moderate	10% ductal
KPTC18	KPTC	PDA with minor sarcomatoid component	Moderate	5% ductal
KPTC23	KPTC	PDA	Moderate/Poor	60% ductal
KPTC5	KPTC	PDA	Poor	Autolyzed
KPTC6	KPTC	PDA	Moderate/Poor	50% ductal
KPTC8	KPTC	PDA	Moderate	80% ductal
KPTC9	KPTC	PDA	Moderate/Poor	60% ductal

Table 3.5: Subset of Differentially Expressed Secreted Proteins in KPC and KPTC Cell Lines

Protein	Function	Rank Diff	t.stat	p.val
Vascular Cell Adhesion Protein 1 (VCAM1)	Angiogenesis	- 0.064444	- 4.397933	1.32E-05
C-C Chemokine 7 (CXCR4/SDF1)	Chemotactic Cytokine	- 2.641026	- 9.754383	2.78E-14
Collagen alpha-1(VI) chain (COL6A1)	ECM	- 1.419753	- 5.290294	4.85E-07
Growth-regulated alpha protein (CXCL1)	Chemotactic cytokine	- 2.238095	- 5.057773	1.45E-05
Galectin-3 binding protein (LGALS3bp)	ECM/Binds Laminin	- 0.654189	- 5.964684	3.47E-09
Glucose-6-phosphate isomerase (GPI)	Glycolysis	2.369048	16.08217	1.24E-41
Superoxide dismutase (SOD1)	Oxidative Stress	1.885965	12.89282	8.68E-32
Annexin A3 (ANX3)	Inflammation/Angiogenesis	1.614719	10.51269	6.92E-23
Mucin-1 (MUC1)	Intracellular Signaling/Apoptosis	1.952381	5.786547	1.93E-07
Apoptosis regulator BAX	Apoptosis	2.6	5.750236	6.32E-06

The above list includes 10 of the 391 significantly differentially expressed proteins. Secretome data were converted to ranks so as to reduce the influence of such outliers. The negative t-statistics indicate proteins that are expressed in KPC (top 5 proteins in this table), while the positive numbers indicate those that are more highly expressed in KPTC (bottom 5 proteins in this table). The p-values shown for each protein are a reflection of the number of unique peptides contributing information in addition to the size of the t-statistic.

Chapter 4 : Characterization of the Immune Response in PDA Tumors with Abrogated TGFβ Signaling

Introduction

Despite advances in our understanding of the events the give rise to and promote the progression of pancreatic adenocarcinoma (PDA), five-year survival rates for the disease remain abysmally low (119). Treatment options are limited, especially for the majority of patients that are diagnosed with metastatic disease (129; 181). One promising avenue of research is that of cancer immunotherapy. Harnessing the body's own immune system to target and kill tumor cells addresses many of the pitfalls of current therapies, namely their lack of specificity and inability to maintain durable responses (106; 182). Significant challenges for the field exist, as tumor cells and the surrounding microenvironment employ a number of mechanisms that serve as barriers to proposed cancer immunotherapies. Analysis of immune cell subsets in tumor tissues has yielded important insights into many of these mechanisms, and has highlighted the role an immunosuppressive microenvironment plays in aiding tumor growth (75; 76). Improved survival has been noted in patients that develop robust lymphocyte responses in contrast to those whose predominant infiltrate is comprised of tumor-promoting, immunosuppressive cells (54; 89).

In PDA, several groups have documented the inflammatory response at preinvasive and invasive stages in human tissues as well as within animal models of the disease (86; 183; 184). As has been noted in other tumor types, effector lymphocytes are vastly outnumbered by immunosuppressive cell subsets, including T regulatory cells, tumor-associated macrophages, and myeloid-derived suppressor cells (88; 185). Understanding how each of these immune cell populations is recruited into the tumor,

and how they subsequently interact with tumor and stromal cells is critical if we are to overcome the barriers they impose on a productive immune response.

TGFβ, a master regulatory cytokine, is known to be dysregulated in cancer. During early stages of cancer initiation, TGFβ acts to inhibit cell growth by facilitating cell cycle arrest and apoptosis. In later stages of tumor development and invasion, TGFβ exerts tumor-promoting effects including enhancement of cell migration and contributing to the suppressive microenvironment that induces immune tolerance (40; 186). TGFβ suppresses the activities of T cells that would otherwise mediate tumor rejection, and also coordinates the recruitment of myeloid cell populations (including neutrophils and monocytes) (67; 187). It is also essential for the differentiation of T regulatory cells, further inhibiting immune-mediated tumor cell killing (66).

TGFβ signaling is perturbed in the majority of PDA patients (20). Loss of SMAD4 function has been described in greater than 50% of cases, with loss of expression correlating with widely metastatic disease and worse prognosis (28; 35; 66; 120). A smaller subset of patients develop mutations in TGFβR2 (34), and as discussed in the previous chapter, loss of TGFβR2 (as well as decreased TGFβ1 levels) correlate with oligometastatic disease. Given the immunomodulatory functions of the TGFβ pathway, we used transgenic mouse models of PDA to interrogate how immune cell populations change in the context of impaired signaling, and whether such alterations influence metastatic propensity of the primary tumor.

Materials and Methods

Antibodies

Primary antibodies raised against F4/80 (#123110), CD11c (#117309), Gr-1 (#108422), CD45 (#103114), Ly-6C (#128011), I-A/I-E (#107622), CD4 (#100443), CD8a (#100744), CD19 (#115511), NK-1.1 (#108728), and CD25 (#102007) were purchased from BioLegend; I-A/I-E (#11-5321-81) was purchased from eBioscience; CD16/CD32 mouse Fc Block (#553142), CD11b (#561114), Ly-6G (#560599), CD11b (#562317), CD3 (#553063) and FoxP3 (#560402) were purchased from BD Biosciences.

Mouse Strains

The conditional *LSL-KRAS*^{G12D} mice (147), *129S4-Trp53tm2Tyj, B6.129S6-Tgfbr2tm1Hlm and Ptf1a*$^{tm1.1(cre)Cvw}$ mice (150) (described in the previous chapter) were used in accordance with the Johns Hopkins Animal Care and Use Committee regulations. Each of the four strains of mice were backcrossed onto a C57BL/6 background in 4-6 generations using marker assisted selection. Single nucleotide polymorphism genotyping was performed at the DartMouse™ Speed Congenic Core Facility at the Dartmouth Medical School. DartMouse uses the Illumina (San Diego, CA) GoldenGate genotyping assay to analyze 1449 SNPs spread throughout the genome. Mice were determined to be >99% C57Bl/6 prior to cross-breeding to generate KPC and KPTC animals.

Lymphocyte Isolation

Resected pancreatic tumors were minced into 3-5 mm^2 pieces and enzymatically digested with collagenase type IV and hyaluronidase for 1 hour at 37°C. Following digestion, cells were passed through a 70 μM nylon cell strainer (BD Biosciences) and washed in RPMI 1640 media. Splenocytes were also harvested from tumor-bearing and control animals for

flow cytometric analysis. After harvest, spleens were crushed through 70 μM nylon cell strainers, washed in cold phosphate-buffered saline (PBS), and centrifuged at 1400rpm for 10 minutes at 4°C. Cell suspensions were incubated in ACK lysis buffer (Quality Biological) to lyse red blood cells and washed in cold PBS. Cell pellets were resuspended in cold FACs buffer (HBSS, 1% FCS and 0.1% sodium azide) and counted by tryphan blue exclusion prior to staining.

Flow Cytometry Staining

For flow cytometric analysis, splenocytes and TILs (10^6) were first incubated with Fc receptor block (BD Pharmingen) for 5 minutes at 4°C. Cells were incubated for 30 minutes at 4°C with fluorochrome-conjugated antibodies in a volume of 0.1ml (Table 4.1 includes antibody concentrations). For intracellular staining, the Cytofix/Cytoperm Fixation/Permeabilization staining kit (BD Pharmingen) was used. Briefly, cells were fixed for 30 minutes at 4°C, washed with FACs buffer, and permeabilized for 30 minutes at 37°C. After washing in FACs buffer, cells were incubated for 30 minutes at room temperature with fluorochrome-conjugated FoxP3 (Table 4.1) in a volume of 0.1ml. Cells were washed in FACs buffer before acquisition on a LSR-II Flow Cytometer or FACs Aria (BD Bioscience).

Results

Reduced TGFβ Signaling Alters the Immune Response to PDA in a Compound Mutant Mouse Model of PDA

In the previous chapter, we described a novel genetically engineered mouse model of PDA with impaired TGFβ signaling. KPTC mice develop aggressive PDA, but ultimately succumb to oligometastatic disease. Secretome analysis of KPTC and KPC cells highlighted differences in chemokine axes that regulate immune cell trafficking. To assess how these changes influenced the immune cell composition of tumors, we isolated tumor-infiltrating leukocytes from KPC and KPTC tumors and subjected them to fluorescence activated cell sorting analysis.

The four mutant mouse strains used to create KPTC mice are a mix of C57Bl/6 and 129 substrains. To alleviate concerns that strain differences may influence immune infiltrate profiles, each strain was backcrossed to the C57Bl/6 background prior to breeding KPC and KPTC mice. Doing so provided the added benefit that cell lines derived from these tumors could be used for future *in vivo* and i*n vitro* experiments where immune responses are assessed or quantified. To confirm that backcrossing did not alter the phenotype of these animals, we monitored cohorts of mice for survival and metastatic burden. As was seen in mice on a mixed genetic background, loss of one allele of TGFβR2 abolished TGFβ-mediated growth inhibition in PDA. KPTC mice (n = 39) had a median survival of 3.5 months with 100% mortality by 5.3 months (Figure 4.1A). This was significantly shorter than littermate controls (*LSL-KRAS*$^{G12D/+}$*;LSL-Trp53*$^{R172H/+}$*; Ptf1a*$^{Cre/+}$ mice, *KPC*, p = 0.0008). At necropsy, hemorrhagic ascites and obstructive, fibrotic pancreatic tumors were noted. As depicted in Figure 4.1B, KPTC frequently

develop oligometastatic (<10 metastases) disease. When observed, metastases were found in the liver, lungs, and diaphragm of KPTC animals, modeling the spectrum of disease seen in PDA patients.

Total leukocyte infiltrate was evaluated in a small subset of animals using the pan-leukocyte marker, CD45. Leukocyte infiltrate was slightly increased in KPTC mice compared to KPC, however, these differences were not statistically significant (Figure 4.2). Next, we evaluated whether particular immune populations infiltrate preferentially in KPTC tumors. Given that others have shown increased myeloid cell accumulation in response to aberrant TGFβ signaling (67; 68), we used two generalized myeloid cell markers (CD11b and Gr-1) to quantify myeloid infiltrate in KPC and KPTC tumors. Once again, increases in myeloid cells were seen in KPTC mice, but these differences did not quite reach statistical significance (Figure 4.3). Myeloid cells are a heterogeneous population of cells that include macrophages, neutrophils, immature monocytes, and myeloid-derived suppressor cells (MDSCs). MDSCs can be further classified into granulocytic and monocytic subsets based on cell surface marker expression and the pathways they use to mediate their suppressive functions (188). Notable increases in granulocytic MDSCs were seen in KPTC tumors (Figure 4.4A). Additionally, a slight elevation in monocytic MDSCs, and decreased macrophage infiltrate were observed (Figure 4.4B & C).

TGFβ Signaling in Tumor Cells Contributes to an Immunosuppressive Microenvironment by Promoting T Regulatory Cell Accumulation

Lymphoid cells make up a small percentage of the overall immune infiltrate in PDA tumors (184). In our mutant mouse models of PDA, lymphocytes account for 5-8%

of the total leukocyte infiltrate (Figure 4.2 & 4.5). Analysis of T cell subsets showed no appreciable differences in the numbers of infiltrating CD4+ or CD8+ cells in KPTC tumors compared to KPC (Figure 4.5 A & B). Interestingly, we did see a small increase in CD19+ B cells in KPTC mouse tumors, shown in Figure 4.5C.

Despite observing no quantitative changes in CD4+ T cell infiltrate in KPTC mice, we were interested to see whether reduced TGFβ signaling altered the polarization of these T cells. T regulatory cells are a subset of CD4+ T cells that are known to accumulate in early precursor lesions of PDA, acting as barriers towards an effective anti-tumor immune response (66; 88). As shown in Figure 4.6, in sharp contrast to KPC mice, nearly all the KPTC tumors lacked T regulatory cell infiltrate at the time they succumb to disease.

Accumulation of Immune Aggregates in the Primary Tumors of KPTC Mice

Quantitative analysis of tumor infiltrating cells provides useful information about the overall immune response; however, comprehensive analysis includes examination of how these immune cells are dispersed or localized within the tumor microenvironment. We have just begun to address this question, but interesting immune cell localization patterns have become apparent. Foci of immune cells clustered in aggregates have been noted in KPTC tumors (Figure 4.7A & B). In contrast, KPC tumors more frequently exhibit immune infiltrate dispersed throughout the tumor microenvironment (Figure 4.7C). A more thorough examination of the composition of these immune aggregates as well as the localization of key immune cell subsets is ongoing.

Discussion

Given that TGFβ is critical in the regulation of immune responses (69), and that this signaling pathway is often impaired in PDA (20), we questioned how a reduction in TGFβ signaling in the tumor epithelium may influence the immune response during PDA carcinogenesis. Using the conditional mouse model of PDA described in the previous chapter, we profiled key myeloid and lymphoid subsets of cells via fluorescence activating cell sorting.

Notably, we observed a slight increase in overall immune infiltrate in KPTC mouse tumors compared to the tumors of KPC mice. Our sample sizes in these two cohorts are still small, so it is possible that a statistically significant increase in leukocyte infiltrate will be observed as we analyze more animals. Importantly, while the TGFβ signaling pathway is known to control genes that control immune cell trafficking, perturbing this pathway may have more appreciable effects on the types of immune cells that infiltrate tumors (81). Our data indicate that this might be the case, as we observed increases in some immune cell populations (granulocytic MDSCs and B cells) with concomitant decreases in others (macrophages and T regulatory cells). Additionally, our analysis to date has been carried out on moribund mice. Studies done in other mouse models indicate that there are temporal changes in immune cell infiltrate as tumors progress (86), and thus, we have also begun to analyze how immune infiltrate changes as precursor lesions develop and progress into PDA.

As has been reported by others, we observed an increase in myeloid cell accumulation in tumors where one copy of TGFβR2 is inactivated (67). Tumor-infiltrating myeloid cells are a heterogeneous mix of neutrophils, macrophages, and

MDSC populations. In our model, the increase in myeloid infiltrate looks to be attributable to an increase in granulocytic MDSCs. G-MDSCs are appreciated for their striking ability to impede T cell immune responses. Recently, Stromnes et al. reported that G-MDSCs are responsible for suppression of T cell effector functions, and when these cells are depleted from mice bearing PDA tumors, T cell-mediated tumor cell killing activity is restored (189). Additionally, research suggests that G-MDSCs can contribute to tumor progression in other ways, as they secrete a variety of cytokines and chemokines (including TGFβ) that influence processes from angiogenesis to extracellular matrix remodeling (188).

Lymphoid cells are rare in PDA tumors, and the overwhelming majority of infiltrating lymphoid cells are immunosuppressive T regulatory cells (88). In PDA, these cells were found to migrate into early precursor lesions and stay elevated throughout carcinogenesis (86). Like MDSCs, T regulatory cells represent a significant obstacle for a productive anti-tumor immune response. Interestingly, reduced TGFβ signaling in the tumor epithelium resulted in a decreased accumulation of T regulatory cells in our model of PDA. The mechanism behind this finding is still unclear. T regulatory cells need TGFβ for their polarization and homeostasis (66), and it is possible that reduced TGFβ signaling in tumor cells results in less ligand in the surrounding milieu. While we have not examined TGFβ levels in the backcrossed model of mice, we did not observe any differences in ligand expression in the KPTC tumors on a mixed background (Chapter 3, Figure 3.5). Moreover, given the numbers of myeloid cells present that are capable of secreting TGFβ into the tumor microenvironment, it is likely that reduced ligand expression is not the mechanism controlling T regulatory cell accumulation.

Alternatively, altered TGFβ signaling in tumor cells may allow for the expression of genes that influence CD4+ T cell polarization. In addition to T regulatory cells, CD4+ T cells can differentiate into Th1, Th2, or Th17 subsets with differentiation being controlled largely by the surrounding milieu (66). Given that we do not see changes in the total CD4+ T cell population, but do observe decreases in the T regulatory subset, it is likely that another population of CD4+ T cells has increased in KPTC mice. Further studies are planned to look at Th1, Th2 and Th17 T cell populations in these animals. We are also exploring differences in the cytokines known to mediate this polarization, including IFN-γ, IL-4 and IL-6. Finally, it is also possible that reduced TGFβ signaling results in the expression of chemokines known to recruit T regulatory cells to tumors, namely CCL22 and CCL2 (190). Studies to test this mechanism are also planned.

Absolute numbers of immune infiltrate provide valuable information on the immune status of the tumor microenvironment. A high proportion of immunosuppressive cells portends a worse prognosis and complicates the use of immunotherapies in patients (88). With this said, it is also recognized that the localization of immune cells within the tumor stromal network is as important as quantitative data of subset populations (191). Immune cells act locally, and the roles they undertake at the invasive fronts of tumors are likely quite different than the functions they exert within a hypoxic or necrotic region of the mass. Likewise, given tumor heterogeneity, the surrounding milieu that greatly influences immune cell function and survival is going to be distinct in different regions of the tumor. We have just begun to look at immune cell localization in the KPTC model of PDA; however, obvious differences in how leukocytes cluster were observed. Aggregates of what appear to be mostly lymphoid cells were seen in several of the KPTC tumors, but

their exact composition and function has yet to be determined. Interestingly, lymphoid aggregates were recently described as forming in patients who received a GM-CSF-secreting PDAC vaccine. Analysis of these aggregates revealed a predominant Th17 lymphoid signature, and their presence was correlated to better vaccine responses (192). In addition to characterizing these clusters of cells in the KPTC tumor microenvironment, we have also begun to use immunohistochemistry to examine how T regulatory cells and MDSCs are distributed within the tumor. Aside from looking at factors such as localization to the periphery, within the stroma, at invasive fronts, or within these aggregates we are also exploring whether immune cells accumulate preferentially in areas of the tumor that are more well or poorly differentiated. As described in Chapter 3, regions of the tumor that were poorly differentiated had higher levels of TGFβ signaling whereas moderately to well differentiated regions displayed reduced pathway activity.

The data presented in this chapter are preliminary, as we have only analyzed a small subset of animals; however, they are in agreement with previously published reports demonstrating a relationship between altered TGFβ signaling in the tumor and a restructuring of the immune microenvironment (67; 193). The additional experiments described above should help to answer key questions pertaining to the mechanisms that drive the altered immune microenvironment in the context of reduced TGFβ signaling, and how localized immune niches affect processes such as invasion and metastasis.

Figures and Tables

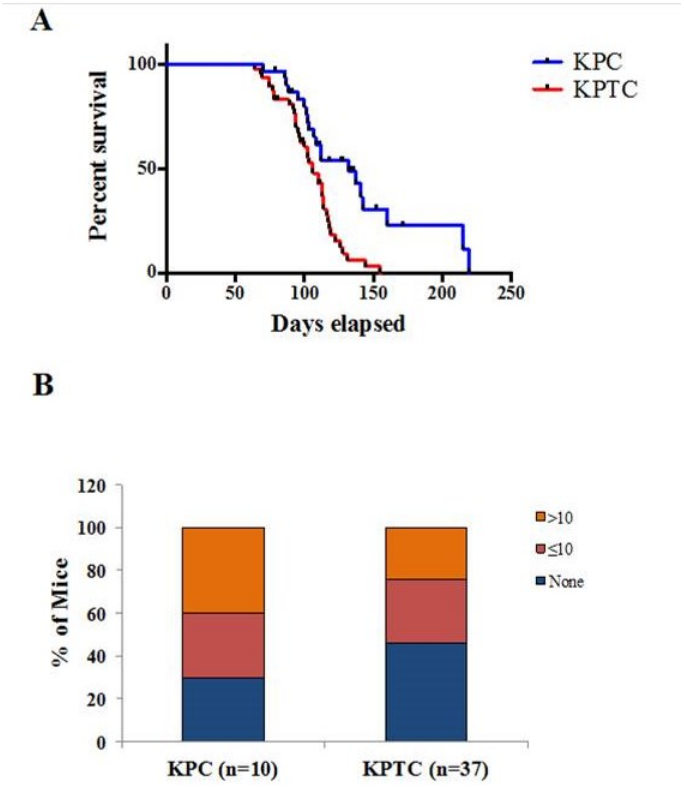

Figure 4-1: Generation and Characterization of Backcrossed KPTC Mice

As described in the Materials and Methods, all four strains of mice were first backcrossed onto a C57Bl/6 background. Compound mutant mice were bred and followed until moribund. (A) Kaplan-Meier survival curves of *KPTC and KPC* mouse cohorts. KPTC mice have a significantly shortened median survival compared to KPC mice (p=0.0008). Medians survival was compared by pair-wise log-rank tests. **(B)** Gross metastatic burdens at necropsy in KPC (n=10) and KPTC mice (n=37).

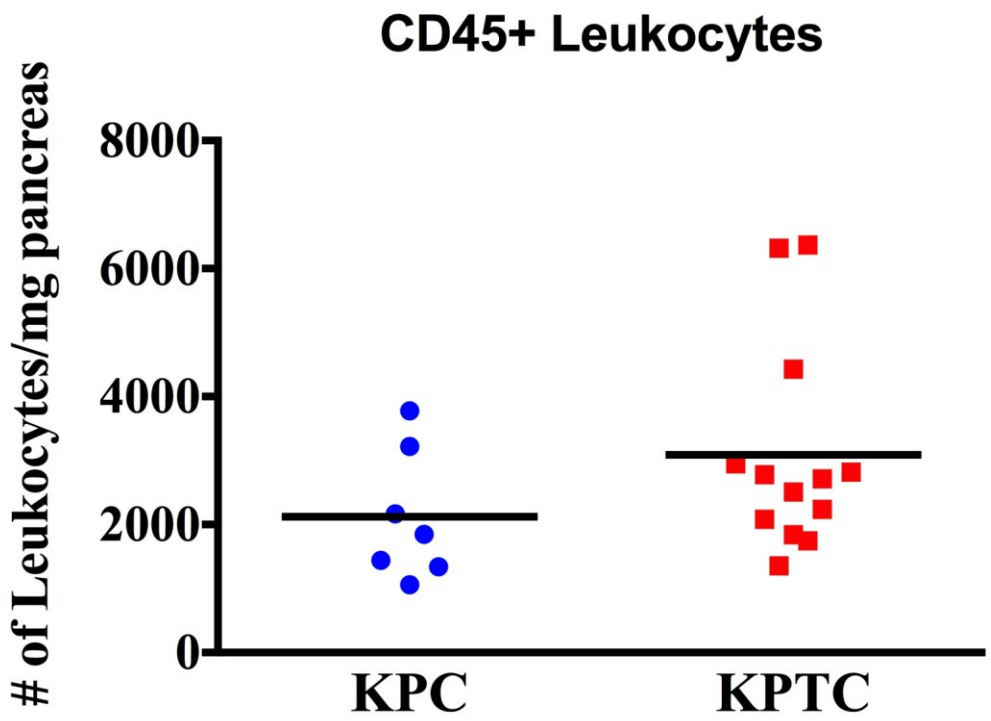

Figure 4-2: Leukocyte Infiltrate in KPTC Mice

Compound mutant mice were allowed to progress until moribund (KPC: n = 7; KPTC: n = 13). At sacrifice, tumors were harvested, digested, and single-cell suspensions were subjected to fluorescence activated cell sorting analysis. Total leukocyte infiltrate was evaluated based on CD45+ expression. Absolute numbers of cells were normalized to tumor weight and compared using a Student's T Test ($p = 0.17$).

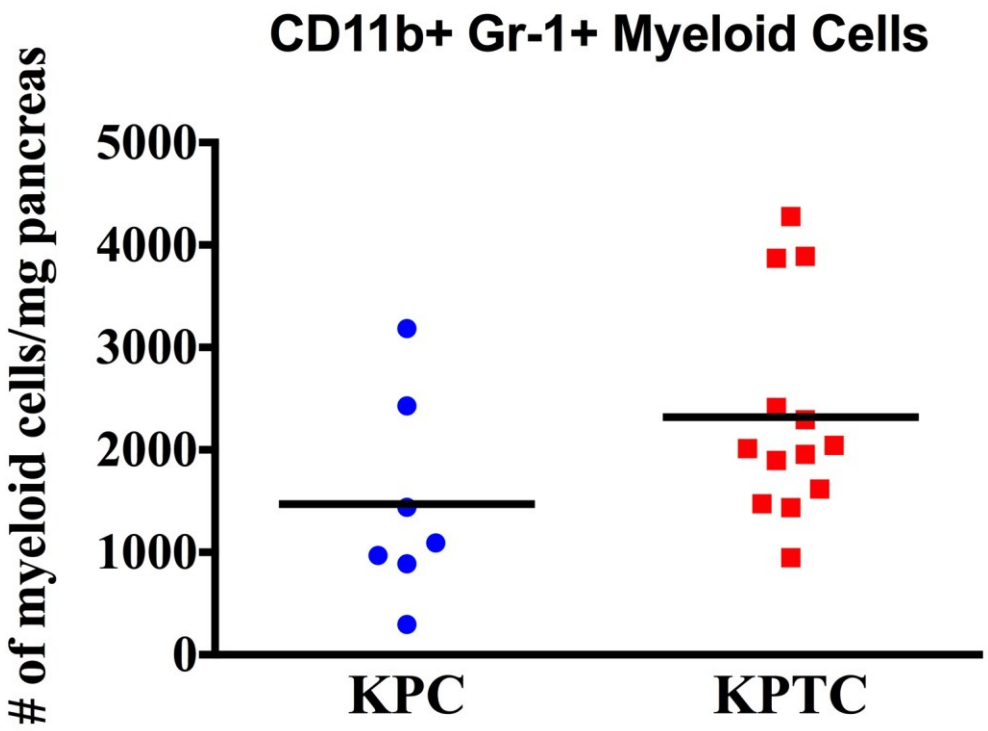

Figure 4-3: Myeloid Cell Infiltrate in KPTC Tumors

Compound mutant mice were allowed to progress until moribund (KPC: n = 7; KPTC: n = 13). At sacrifice, tumors were harvested, digested, and single-cell suspensions were subjected to fluorescence activated cell sorting analysis. Total myeloid infiltrate was evaluated based on CD45+ CD11b+ Gr-1+ expression. Absolute numbers of cells were normalized to tumor weight and compared using a Student's T Test ($p = 0.096$).

Figure 4-4: Myeloid Subset Analysis of KPTC Tumors

Compound mutant mice were allowed to progress until moribund (KPC: n = 7; KPTC: n = 13). At sacrifice, tumors were harvested, digested, and single-cell suspensions were subjected to fluorescence activated cell sorting analysis. **(A)** Granulocytic MDSC infiltrate was characterized as being CD45+ CD11b+ Ly-6G^{hi} Ly-6C^{lo} and MHC II- ($p = 0.10$) **(B)** Monocytic MDSC infiltrate was characterized as being CD45+ CD11b+ Ly-6G^{lo} Ly-6C^{hi} and MHC II- ($p = 0.21$). **(C)** Macrophage infiltrate was characterized as being CD45+ CD11b+ F4/80+ MHC II+ ($p = 0.27$). Absolute numbers of cells were normalized to tumor weight and compared using a Student's T Test.

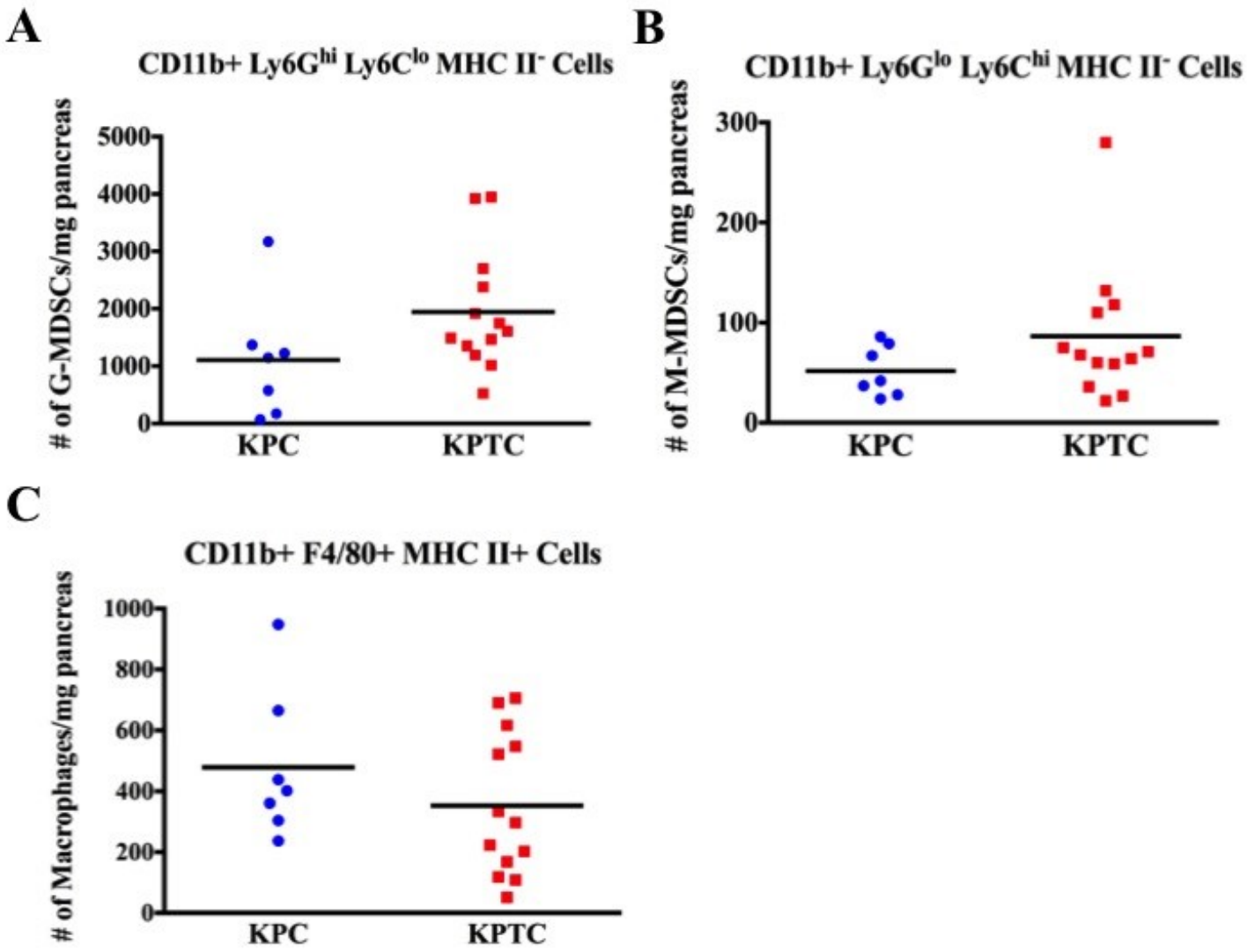
A
CD11b+ Ly6G^hi Ly6C^lo MHC II^- Cells
# of G-MDSCs/mg pancreas
5000
4000
3000
2000
1000
0
KPC
KPTC
B
CD11b+ Ly6G^lo Ly6C^hi MHC II^- Cells
# of M-MDSCs/mg pancreas
300
200
100
0
KPC
KPTC
C
CD11b+ F4/80+ MHC II+ Cells
# of Macrophages/mg pancreas
1000
800
600
400
200
0
KPC
KPTC

Figure 4-5: Lymphoid Infiltrate in KPTC Tumors

Compound mutant mice were allowed to progress until moribund (KPC: n = 7; KPTC: n = 13). At sacrifice, tumors were harvested, digested, and single-cell suspensions were subjected to fluorescence activated cell sorting analysis. **(A)** CD4+ T cells were CD45+ CD3+ CD4+ ($p = 0.84$) **(B)** CD8+ T cells were CD45+ CD3+ CD8+ ($p = 0.65$) **(C)** B cells were CD45+ CD3- CD19+ ($p = 0.38$) Absolute numbers of cells were normalized to tumor weight and compared using a Student's T Test.

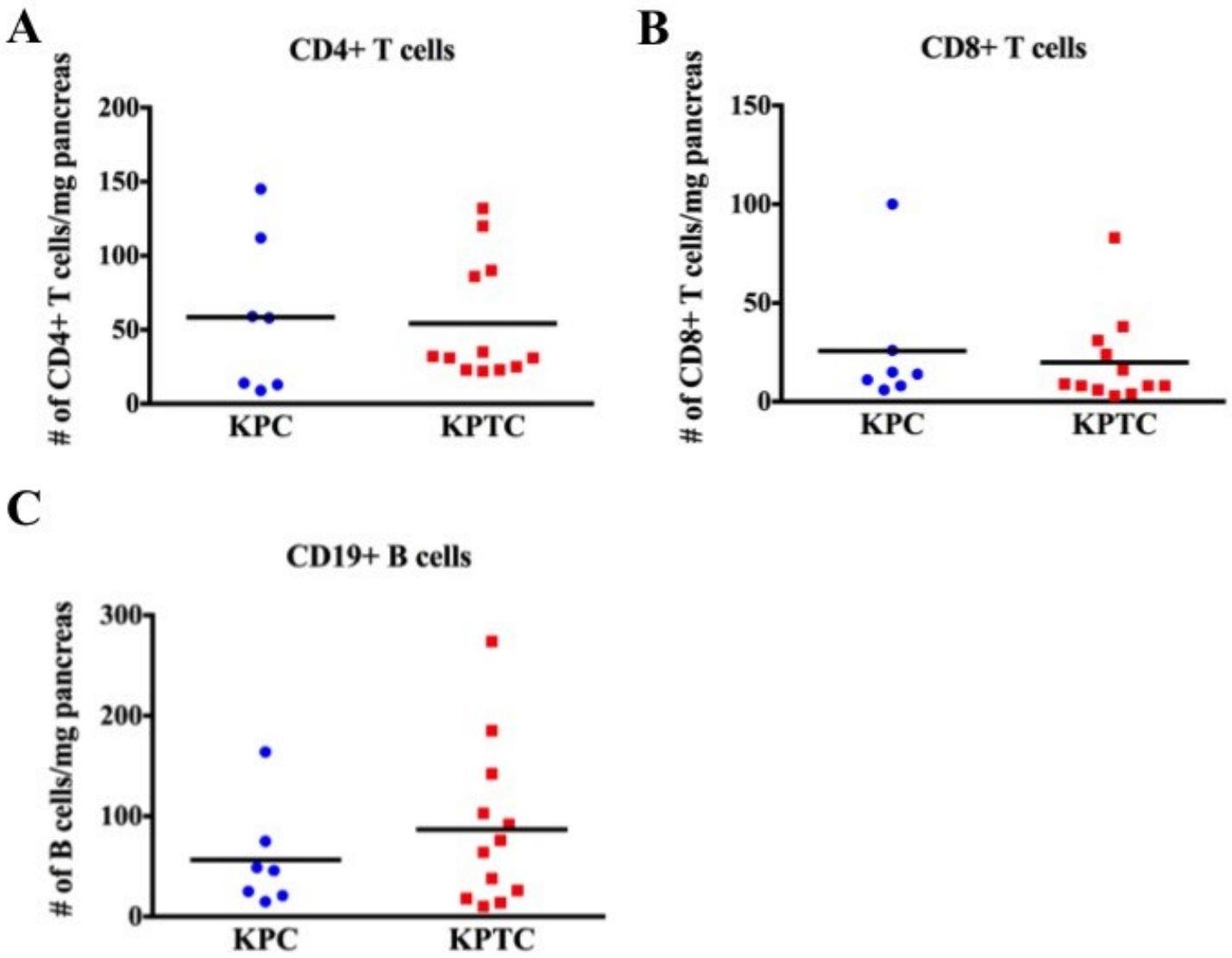
A
CD4+ T cells
# of CD4+ T cells/mg pancreas
200
150
100
50
0
KPC
KPTC
B
CD8+ T cells
# of CD8+ T cells/mg pancreas
150
100
50
0
KPC
KPTC
C
CD19+ B cells
# of B cells/mg pancreas
300
200
100
0
KPC
KPTC

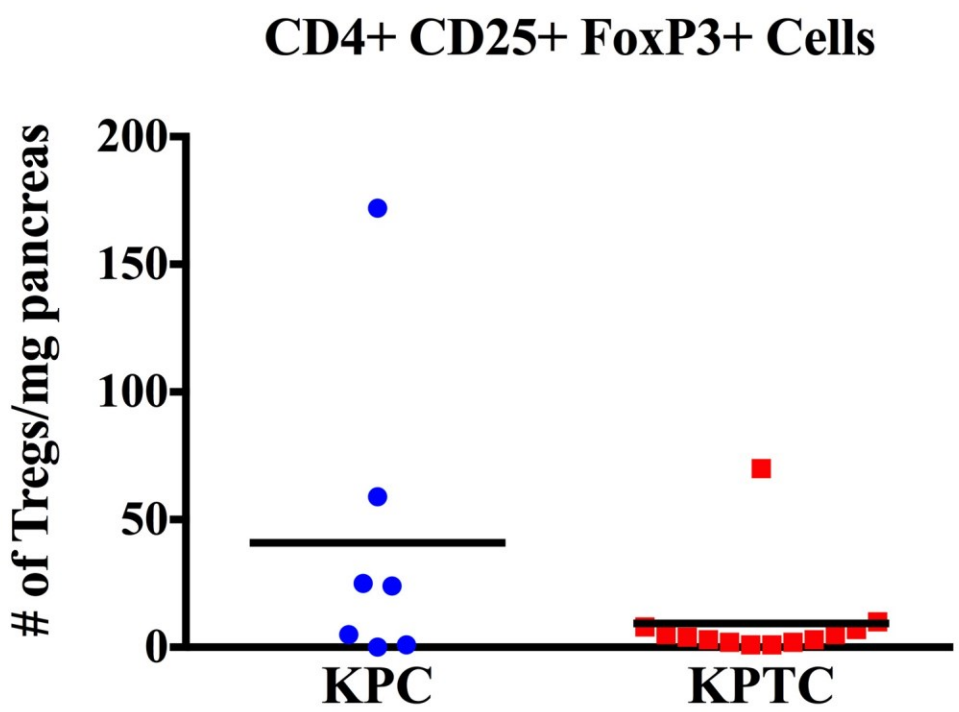

Figure 4-6: T Regulatory Cell Infiltrate in KPTC Tumors

Compound mutant mice were allowed to progress until moribund (KPC: n = 7; KPTC: n = 13). At sacrifice, tumors were harvested, digested, and single-cell suspensions were subjected to fluorescence activated cell sorting analysis. T regulatory cells were characterized as being CD45+ CD4+ CD25+ FoxP3+. Absolute numbers of cells were normalized to tumor weight and compared using a Student's T Test ($p = 0.097$).

Figure 4-7: Immune Aggregates in KPC and KPTC Mouse Tumors

Examples of primary tumor tissues collected at necropsy from KPTC and KPC mice. **(A)** Low-power image of KPTC mouse tumor with clusters of immune aggregates marked with black arrows. **(B)** Example of second KPTC mouse with a focus of immune infiltrates localized to the periphery of the tumor. **(C)** Example of a KPC mouse primary tumor with diffuse immune infiltrate throughout the stroma.

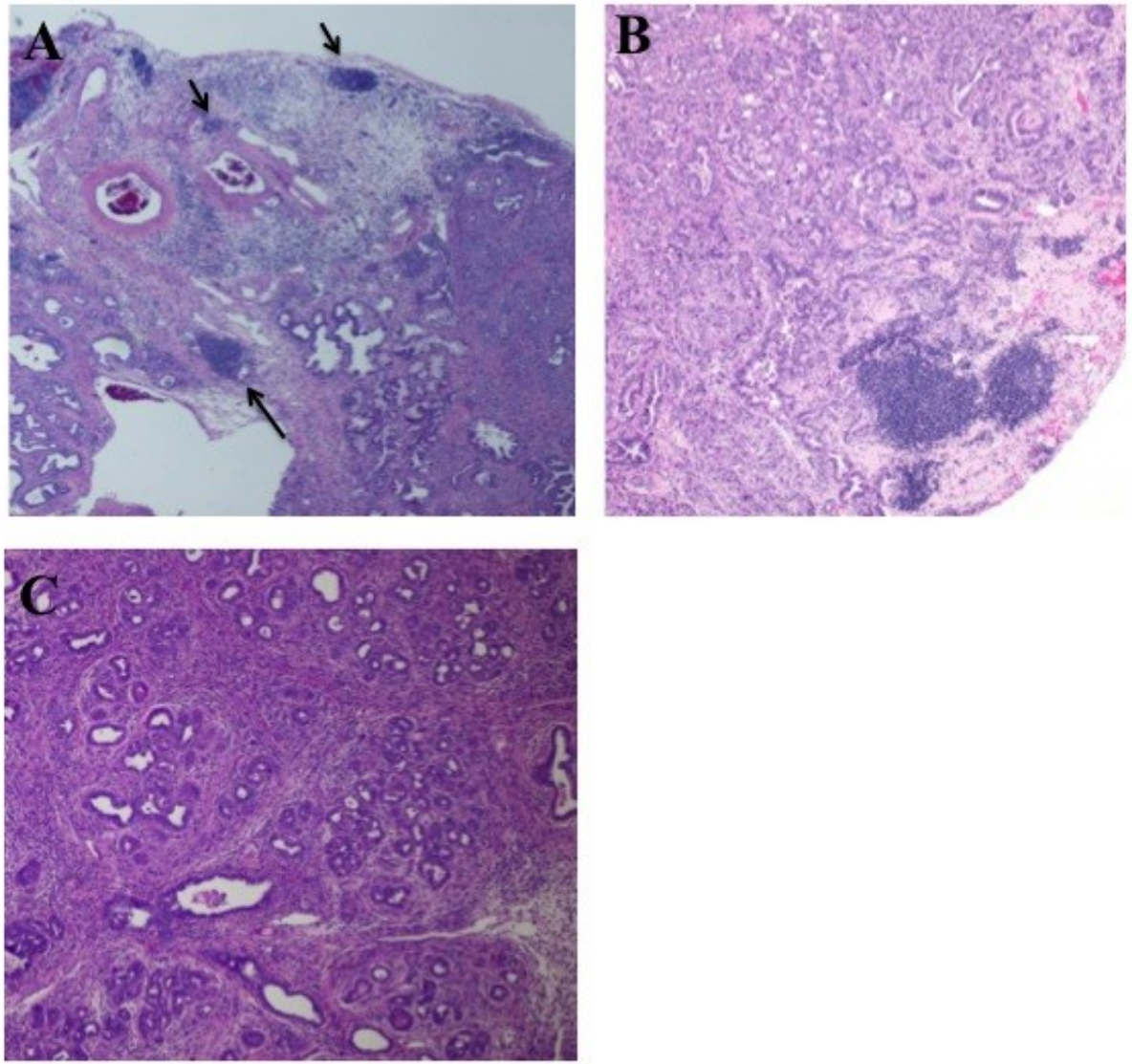
A
B
C

Table 4.1: Antibodies for Flow Cytometry Analysis

Antibody	Clone	Company	Concentration
PE anti-mouse F4/80	BM8	BioLegend	0.2ug/10^6 cells
APC anti-mouse CD11c	N418	BioLegend	0.1ug/10^6 cells
PerCP-Cy5.5 anti-mouse CD11b	M1/70	BD Biosciences	0.05ug/10^6 cells
AF700 anti-mouse GR-1	RB6-865	BioLegend	0.25ug/10^6 cells
PE-Cy7 anti-mouse CD45	30F11	BioLegend	0.008ug/10^6 cells
FITC anti-mouse I-A/I-E	M5/114.15.2	eBioscience	0.18ug/10^6 cells
PE-CF594 anti-mouse CD11b	M1/70	BD Biosciences	0.005ug/10^6 cells
APC anti-mouse Ly-6G	1A8	BD Biosciences	0.1ug/10^6 cells
PerCP-Cy5.5 anti-mouse Ly-6C	HK1.4	BioLegend	0.1ug/10^6 cells
AF700 anti-mouse I-A/I-E	M5/114.15.2	BioLegend	0.18ug/10^6 cells
Brilliant Violet 421 anti-mouse CD4	GK1.5	BioLegend	0.07ug/10^6 cells
PerCP-Cy5.5 anti-mouse NK1.1	PK136	BioLegend	0.4ug/10^6 cells
PE anti-mouse CD3	145-2C11	BD Biosciences	0.4ug/10^6 cells
Brilliant Violet anti-mouse CD8a	53-6.7	BioLegend	0.07ug/10^6 cells
APC anti-mouse CD19	6D5	BioLegend	0.1ug/10^6 cells
PE anti-mouse CD25	PC61	BioLegend	0.1ug/10^6 cells
AF647 anti-mouse FoxP3	MF23	BD Biosciences	0.15ug/10^6 cells

Table 4.2: Primer Sequences for Mouse Genotyping

Primer Name	5'-3' Sequence
Kras G12D Forward	AGCTAGCCACCATGGCTTGAGTAAGTCTGCA
Kras G12D Reverse	CCTTTACAAGCGCACGCAGACTGTAGA
Tp53 R172H Forward	AGCTAGCCACCATGGCTTGAGTAAGTCTGCA
Tp53 R172H Reverse	CTTGGAGACATAGCCACACTG
Tgfbr2 Lox Forward	TAAACAAGGTCCGGAGCCCA
Tgfbr2 Lox Reverse	ACTTCTGCAAGAGGTCCCCT
Ptf1a Cre Forward	ATAGGCTACCTGGCCATGCCC
Ptf1a Cre Reverse	CGGGCTGCAGGAATTCGTCG

Chapter 5 : SMAD4 Loss Alters the Immune Microenvironment in a Murine Orthotopic Model of Pancreatic Adenocarcinoma

Introduction

Whole exome sequencing analysis of human pancreatic tumors has revealed a set of 12 core signaling pathways and processes that are perturbed in the majority of PDA patients (20). One of these pathways, the TGFβ signaling pathway, is a known mediator of critical homeostatic cellular processes including cell survival, differentiation and proliferation (40). The most prevalent alteration observed in this pathway in PDA patients is inactivation of a critical transcription factor, SMAD4. Loss of SMAD4 function, via homozygous deletion or intragenic mutation followed by loss of heterozygosity, occurs in greater than 55% of patients with PDA (24). Importantly, SMAD4 disruption has been correlated to widely metastatic disease and a worse prognosis (27; 28; 120). A small subset of PDA patients harbor inactivating mutations in TGFβ receptor 2 (TGFBR2). Interestingly, unlike what has been observed in SMAD4-deficient tumors, loss of TGFBR2 is associated with a more favorable prognosis compared to those with SMAD4 loss (35). This difference is likely attributable to the effects of SMAD4-independent signaling, which is retained in tumors that lose SMAD4, but lost in those with TGFBR2 inactivation.

In addition to its pivotal role in maintaining cellular homeostatic activities, TGFβ signaling acts as a potent regulator of immune responses, with profound influence on proliferation, differentiation, migration and survival of immune cells (81; 194). Not surprisingly, tumors with mutations in TGFβ pathway components exhibit markedly increased and altered immune profiles that can contribute directly to tumor progression and metastasis. Lu et al. coupled *Ras* pathway activation with TGFBR2 loss in murine head and neck epithelia, which resulted in the formation of metastatic head and neck

squamous cell carcinoma (HNSCC). These tumors produced higher levels of TGFβ1, which contributed to overt changes in stromal architecture and noted increases in neutrophil and macrophage infiltration (195). In a mammary carcinoma model with conditional deletion of TGFBR2, an immature myeloid cell population was found to infiltrate tumors, and in turn, contribute to metastasis by producing matrix metalloproteinases (MMPs) (67). In studies where downstream components of the TGFβ signaling family (namely, SMAD4) were inactivated, similar microenvironmental changes were observed. Using a mouse model of invasive colorectal carcinoma where inactivation of *APC* was coupled with loss of SMAD4 in the intestinal epithelia, Kitamura et al. demonstrated an expansion of immature myeloid cells at the invasive front of tumors. These cells were shown to contribute to tumor invasion via production of MMPs (68). Similarly, Bornstein et al. showed that deletion of SMAD4 in head and neck epithelia resulted in mice that developed HNSCC with increased leukocyte accumulation (193).

In the previous chapter, we examined infiltrating immune population alterations in a transgenic mouse model of PDA where TGFβ signaling was abrogated through conditional inactivation of TGFBR2. Given the complex nature of this signaling pathway, with its canonical and SMAD4-independent arms, we sought to test whether similar immunophenotypic changes are observed in the context of SMAD4 loss. We used shRNA-mediated knockdown to generate SMAD4-deficient PDA tumor cells that were implanted into the pancreata of mice. The resultant tumors were assayed for infiltrating lymphocyte content. Additionally, we utilized adoptive transfer experiments to determine

whether immature myeloid cells derived from mice bearing SMAD4-deficent tumors contribute to metastatic potential.

Materials and Methods

Antibodies

Primary antibodies raised against F4/80 (#123110), CD11c (#117309), Gr-1 (#108422), CD45 (#103114), Ly-6C (#128011), I-A/I-E (#107622), CD4 (#100443), CD8a (#100744), CD19 (#115511), NK-1.1 (#108728), and CD25 (#102007) were purchased from BioLegend; I-A/I-E (#11-5321-81) was purchased from eBioscience; CD16/CD32 mouse Fc Block (#553142), CD11b (#561114), Ly-6G (#560599), CD11b (#562317), CD3 (#553063) and FoxP3 (#560402) were purchased from BD Biosciences. For Western blotting experiments, a primary antibody against SMAD4 (#sc-7966) was purchased from Santa Cruz Biotechnology and a corresponding anti-mouse HRP secondary antibody (NA9314)) was purchased from GE Healthcare UK.

Mouse Strains and Cell Lines

KPC tumor-derived cell lines were a gift from David Tuveson (Cold Spring Harbor Laboratories, Cold Spring Harbor, NY). Cells were cultured in DMEM (GIBCO, Invitrogen Life Technologies, Carlsbad, CA, USA) supplemented with 10% fetal bovine serum (FBS), 100 units/ml penicillin, 100 □g/ml streptomycin and 2 mmol/L L-glutamine at 37 ^{o}C and 5% CO2. For experimental metastasis and adoptive transfer assays, C57Bl/6 male mice aged 5-6 weeks were purchased from Jackson Laboratory (Bar Harbor, ME). Experiments involving animals were carried out in accordance with the Johns Hopkins Animal Care and Use Committee regulations.

shRNA Stable Knockdown

SMAD4 shRNAs (TG501287, Origen) were purchased from Origen. KPC cells were cultured in Dulbecco's modified medium containing 10%FBS. Plasmid DNA transfection

of cells was performed using Attractene reagent (Cat. No., 301005, Qiagen) per the manufacturer's instructions. Forty-eight hours after transfection, cells were passaged into media containing puromycin (5ug/ml) and maintained in selective culture medium until colonies appeared. GFP positive cells were sorted on a FACs Aria (BD Bioscience) and plated in 96-well plates to obtain single cell clones. Clones were grown in DMEM media containing 10% FBS, and inhibition of gene expression by shRNA was assessed by Western blot and quantitative real-time PCR analysis.

Western Blotting

Cell lysates were prepared by suspending cell pellets in RIPA buffer (20 mM Tris, 0.1% SDS, 1% Triton X-100, 1% sodium deoxycholate, pH 7.4) supplemented with protease inhibitor cocktail tablets (Roche diagnostics GmbH, Mannheim, Germany). Equal amounts of proteins were separated on SDS-polyacrylamide gel and transferred onto PVDF membranes (DuPont NEN, Boston, MA). Each membrane was hybridized with primary antibody followed by horseradish peroxidase (HRP)-linked IgG and visualized by the enhanced chemiluminescence (ECL) system (Amersham). Expression of β-actin or GAPDH were used as internal controls.

Quantitative Real-Time PCR

Total RNA was extracted from tissue samples using RNeasy mini Kit (Cat. No., 74104; Qiagen). RNA was treated with DNase I (Invitrogen) to digest remnant genomic DNA. cDNA was synthesized from 0.5 □g of total RNA by the SuperScript Preamplification System (Invitrogen) according to the protocol recommended by the manufacturer. For quantitative PCR, one microgram of RNA per sample was reverse transcribed into cDNA using SuperScriptTMIII Platinum® Two-Step qRT-PCR Kit (Invitrogen) according to

the protocol recommended by the manufacturer. Real-time quantitative RT-PCR analysis was performed using an automated sequence detection instrument (7300 Real Time PCR System, Applied Biosystems, CA, USA) for the real-time monitoring of nucleic acid green dye fluorescence (SYBR®Green, Invitrogen Inc, CA, USA). Relative fold-changes of analyzed gene expression compared to the housekeeping gene β-actin were determined by calculation of the $2^{\Delta\Delta Ct}$. All analyses were performed in triplicate at least 2 times. Primer sequences available in Table 5.2.

Orthotopic Implantation Model

KPC and KPC-SMAD4 knockdown cell cultures were dissociated into single cell suspensions, counted, resuspended in Matrigel (BD Biosciences) and injected into the pancreata of C57Bl/6 mice (5×10^5 cells per mouse). After three weeks the animals were euthanized, tumors and spleens were harvested for immune infiltrate analysis, and numbers of macroscopic metastases were counted.

Lymphocyte Isolation and Flow Cytometry Staining

Resected pancreatic tumors were minced into 3-5 mm^2 pieces and enzymatically digested with collagenase type IV and hyaluronidase for 1 hour at 37°C. Following digestion, cells were passed through a 70 μM nylon cell strainer (BD Biosciences) and washed in RPMI 1640 media. Splenocytes were also harvested from tumor-bearing and control animals for flow cytometric analysis. After harvest, spleens were crushed through 70 μM nylon cell strainers, washed in cold phosphate-buffered saline (PBS), and centrifuged at 1400rpm for 10 minutes at 4°C. Cell suspensions were incubated in ACK lysis buffer (Quality Biological) to lyse red blood cells and washed in cold PBS. Cell pellets were resuspended in cold FACs buffer (HBSS, 1% FCS and 0.1% sodium azide) and counted by tryphan

blue exclusion prior to staining. For flow cytometric analysis, splenocytes and TILs (10^6) were first incubated with Fc receptor block (BD Pharmingen) for 5 minutes at 4°C. Cells were incubated for 30 minutes at 4°C with fluorochrome-conjugated antibodies in a volume of 0.1ml (Table 4.1 includes antibody concentrations). For intracellular staining, the Cytofix/Cytoperm Fixation/Permeabilization staining kit (BD Pharmingen) was used. Briefly, cells were fixed for 30 minutes at 4°C, washed with FACs buffer, and permeabilized for 30 minutes at 37°C. After washing in FACs buffer, cells were incubated for 30 minutes at room temperature with fluorochrome-conjugated FoxP3 (Table 4.1) in a volume of 0.1ml. Cells were washed in FACs buffer before acquisition on a LSR-II Flow Cytometer or FACs Aria (BD Bioscience).

Adoptive Transfer Assay

C57Bl/6 mice were orthotopically implanted with either KPC or KPC-SMAD4 knockdown tumor cells as described above. Three weeks after implantation, $CD45^+$ $Gr\text{-}1^+$ $CD11b^+$ myeloid cells were sorted from the spleens of tumor-bearing mice using a FACs Aria (BD Biosciences). Myeloid cells were washed and mixed with either KPC or KPC-SMAD4 knockdown cells at indicated ratios and implanted orthotopically into the pancreata of C57Bl/6 mice as described above. Myeloid cells sorted from the spleens of non-tumor bearing C57Bl/6 mice served as control cells in all experiments. After three weeks, animals were euthanized, spleens and tumors were harvested for immune infiltrate analysis, and metastases were counted.

Results

Loss of SMAD4 in KPC Tumor Cells Does Not Alter Metastatic Proficiency in an Orthotopic Model of PDA

In the previous chapter, we used a genetically engineered mouse model of PDA with impaired TGFβR2 to assess how tumor immune infiltrate composition changed in response to deficiencies in TGFβ signaling. To determine the extent to which loss of SMAD-dependent TGFβ signaling contributes to changes in immune cell trafficking to PDA tumors, we generated SMAD4-deficient KPC tumor cells that were subsequently implanted into the mouse pancreas. Stable knockdown of SMAD4 was confirmed at both the protein and mRNA level (Figure 5.1 A & B) prior to orthotopic implantation into mice. Four weeks post-implantation, neither of the SMAD4-deficient clones demonstrated differences in tumor size compared to control KPC tumors (Figure 5.2A), suggesting that loss of SMAD4 did not alter tumor proliferation.

Given that loss of SMAD4 is correlated to widely metastatic disease in human PDA patients (28), we next accessed metastatic burden in mice bearing SMAD4-deficient tumors (Figure 5.2B). Interestingly, four weeks post-implantation no differences in metastatic efficiency were observed in any of the SMAD4-deficient clones compared to control KPC tumors. A subset of mice implanted with SMAD4-deficient cells (KPC Clone #1) were followed for an additional two weeks to determine whether mice were succumbing to disease prior to the formation of metastases. As shown in Figure 5.3, a significantly greater number of metastases were found in mice bearing SMAD4 knockout KPC tumors six weeks post implantation. Frequent sites of metastases included the lungs, liver and diaphragm. While we would have liked to have carried out the remaining

experiments at this six-week time point, greater than 85% of the mice (irrespective of which cell line was used and the SMAD4 status of the tumor) died from their tumors within four weeks of injection.

Leukocyte Infiltration is Increased in SMAD4-Deficient Tumors

The TGFβ signaling pathway is known to be important in regulating leukocyte migration, differentiation and survival (54; 63). To determine whether SMAD4 loss augments the immune response in PDA, KPC (control) and SMAD4-deficient tumors were harvested four weeks after orthotopic implantation for immune infiltrate analysis via fluorescence activated cell sorting. The pan-leukocyte marker CD45 was used to quantify the total immune infiltrate in tumors. Leukocytes were increased in both SMAD4-deficient cell lines compared to their mock-transfected KPC controls (Figure 5.4), with more robust differences being noted in KPC2. Because metastatic efficiency differences were observed at a later time point for KPC1 (Figure 5.3), we decided to look at leukocyte infiltrate in a small cohort of mice 6 weeks post-implantation with this cell line. As is shown in Figure 5.5, leukocyte infiltrate was not appreciably altered if KPC1 SMAD4-deficient tumors were allowed to progress an additional two weeks.

SMAD4 Loss in PDA Facilitates Granulocytic Myeloid Derived Suppressor Cell Recruitment into Tumors

With an increase in total leukocyte infiltrate observed, we next examined how individual immune cell populations were altered in response to SMAD4 inactivation. To probe myeloid cell infiltration, we first looked at general myeloid markers: CD11b and Gr-1. An increase in total myeloid infiltration was observed in both SMAD4-deficient tumors; however, neither increase was found to be statistically significant (Figure 5.6A).

CD11b+ Gr-1+ myeloid cells are a heterogeneous population of cells that can include immature monocyte, macrophage, and granulocytic subsets. Additionally, these markers have been described as being expressed on a potent immunosuppressive set of cells known as myeloid-derived suppressor cells (MDSCs) (67). In both humans and mice, two separate subsets of these cells have been described. Mononuclear cell-like MDSCs (M-MDSCs) histologically resemble immature precursors of macrophages while polymorphonuclear or granulocytic cell-like MDSCs (G-MDSCs) histologically resemble neutrophils (196). To address whether SMAD4 loss alters a particular myeloid subset of cells, we phenotyped the CD11b+ Gr-1+ myeloid cells isolated from the tumors of these mice. G-MDSCs, characterized here as Ly-6G^{hi} Ly-6C^{lo}, were found to be increased in SMAD4-deficient tumors (significantly increased in KPC2, Figure 5.6B; $p = 0.008$). Interestingly, M-MDSC infiltrate was found to be elevated in one SMAD4-deficient line (KPC1); however, decreases in the influx of these cells were observed in KPC2 SMAD4 knockout tumors (Figure 5.6C).

CD4+ T Cells are Recruited to KPC SMAD4-Deficient Tumors

MDSCs are characterized by their ability to produce anti-inflammatory cytokines such as TGFβ and IL-10 (67; 197). Additionally, PDA tumors are known to overexpress TGFβ ligand (38), and several groups have observed increased TGFβ ligand production in tumors with defective TGFβ signaling (118; 193). Given the critical role that TGFβ plays in polarizing T cells, especially into T regulatory cells (66), we next examined T cell infiltrate in our KPC tumors with SMAD4 knockdown. As is illustrated in Figure 5.7A, a significant increase in CD4+ T cells was observed in KPC2 SMAD4-deficient tumors compared to control KPC tumors ($p = 0.04$). Further analysis of these CD4+ T

cells revealed that T regulatory cells (defined here as CD4+ CD25+ FoxP3+ cells) were also increased in tumors with SMAD4 loss (Figure 5.7B).

Adoptive Transfer of Myeloid Cells Does Not Alter Metastatic Propensity of KPC Tumors

Myeloid cells can contribute to many processes that are involved in tumor progression, including extracellular matrix remodeling, angiogenesis, and immune cell recruitment (198). It has been reported that macrophages and MSDCs promote metastasis via the secretion of matrix metalloproteinases (67; 68). To test this *in vivo*, we sorted splenic-derived CD11b+ Gr-1+ myeloid cells from the mice bearing implanted KPC tumors, and adoptively transferred these cells with KPC tumor cells into the pancreata of mice. After three weeks, mice were sacrificed and macroscopic metastases were counted. As expected, primary tumor burden was not significantly altered when myeloid cells were implanted with tumor cells (Figure 5.8A). Metastatic burden tended to increase with increasing myeloid cell concentrations, but this finding was not statistically significant (Figure 5.8B).

Discussion

Perturbations to components of the TGFβ pathway in tumor cells can potentiate tumor growth via direct and indirect mechanisms (40). Ablation of TGFβ signaling in tumor cells dramatically alters the tumor microenvironment, which in turn, profoundly influences tumor cell proliferation and survival (69). As an example, studies have shown that impaired TGFβ signaling contributes to extracellular matrix deposition and remodeling, and these stromal cells act as sources of various growth factors and cytokines that fuel tumor cell proliferation (118).

In addition to its well-known functions in controlling key cellular homeostatic mechanisms, the TGFβ signaling pathway is essential for regulating immune cell development, trafficking and function (69; 81). In animal models of head and neck, mammary, and colorectal carcinoma, inactivation of genes in this pathway in tumor cells alters the recruitment of immune cell populations to the tumor (67; 68; 193). In the previous chapter, we examined immune cell infiltrate in the context of TGFβR2 inactivation. In this chapter, I present preliminary data showing that the immune microenvironment in PDA is altered in response to SMAD4 loss.

A conditional murine model of PDA with *Kras* activation coupled to SMAD4 loss resulted in papillary and mucinous precursor lesions that occasionally gave rise to adenocarcinoma (117). As we wanted to study the immune infiltrate in adenocarcinoma, we knocked out SMAD4 in KPC tumor cell lines and utilized an orthotopic implantation model to generate tumors for experimental analysis. Interestingly, only one of the SMAD4-deficient cell lines that we tested yielded an increase in metastatic burden compared to mock-transfected KPC tumor cells. One explanation for this observation is

that the parental KPC cell lines were derived from aggressive tumors harvested from moribund mice. Thus, these cells may already have acquired genetic or epigenetic changes that lend them to be more capable of metastasis, making SMAD4 loss redundant. As mentioned, even the parental (non-transfected) KPC cell lines kill the mice three to four weeks after implantation. The resultant tumor is large and obstructive, which may be killing the mouse before metastases become evident. Finally, it is also possible that screening additional clones might result in identifying SMAD4-deficient lines with increased metastatic propensity.

When analyzing the immune infiltrate, we observed an overall increase in leukocytes in SMAD4-deficient tumors. This is not particularly surprising given that TGFβ signaling regulates the transcription of genes that are necessary for leukocyte trafficking (199). Interestingly, the populations that were most altered in response to SMAD4 loss were regulatory immune cells (MDSCs and T regulatory cells). Others have demonstrated an increase in myeloid cell populations in murine tumor models with impaired TGFβ signaling (67; 68); however, their characterization of these cells has been limited to the general myeloid markers of CD11b and Gr-1. As mentioned, CD11b+ Gr-1+ cells are a heterogeneous population of immune cells that include macrophages, immature monocytes, granulocytes and MDSCs. In our SMAD4-deficient model of PDA, the most significantly altered myeloid subset of cells were granulocytic MDSCs. G-MDSCs are immunosuppressive cells that have also been implicated in promoting angiogenesis and invasion. Importantly, G-MDSCs are functionally and phenotypically distinct from M-MDSCs and macrophages (188; 200), which were not found to be altered in our SMAD4-deficient tumors.

Myeloid cell populations, including MDSCs, are known to contribute to invasion namely through secretion of extracellular matrix remodeling enzymes (188). In our preliminary adoptive transfer experiments, we did not see increased metastasis when tumor cells were co-transplanted with myeloid cells obtained from tumor-bearing mice. One possible explanation for this observation is that we were using myeloid cells sorted from the spleens of tumor-bearing mice, as it was not feasible to sort enough cells directly from tumors. It is not clear whether myeloid cells derived from the spleen possess the same functional capabilities that tumor-derived myeloid cells do. Moreover, we used generalized myeloid markers (rather than specific markers for subsets such as G-MDSCs) when sorting cells. This was also a feasibility issue, as obtaining enough cells for these adoptive transfer experiments is a limiting factor. Additional *in vitro* studies looking at matrix metalloproteinase secretion and/or co-culture invasion assays may help address the pitfalls of our *in vivo* approach.

We also observed a significant increase in CD4+ T cells in SMAD4-deficient tumors. CD4+ T cells differentiate into Th1, Th2, Th17, or T regulatory cells depending on the cytokine milieu. TGFβ ligand is necessary for polarization of both Th17 and T regulatory subsets (66). We did find an increase in T regulatory cells in our SMAD4-deficient tumors; however, they only comprised about 8% of the total CD4+ infiltrate. While not specifically assayed for in our initial characterization of SMAD4-impaired tumors, there is some limited evidence that Th17 cells infiltrate PDA tumors (201). Their functional consequences in the tumor microenvironment are not yet understood. In addition to examining Th17 cells, we also plan to look at TGFβ levels in our SMAD4-deficient tumors. PDA tumors are known to overexpress TGFβ ligand (38), but as

discussed in Chapter 3 (Table 3.2), oligometastatic PDA tumors lack TGFβ ligand expression. Appreciable TGFβ ligand expression in SMAD4 knockout tumors could help to explain the influx of T regulatory cells that we have observed in these tumors.

In summary, although the data presented in this chapter are preliminary, they are in agreement with other studies examining immune infiltrate in SMAD4-deficient tumor models. An increase in leukocyte trafficking (especially of regulatory suppressive subsets of cells) in the context of SMAD4 loss indicates that SMAD-dependent signaling contributes to TGFβ-mediated immunosuppression. Future work to further characterize the immune infiltrate in these tumors in the form of additional subset analysis, TGFβ ligand expression, immune cell localization within tumors, and their functional roles in promoting invasion and metastasis, is necessary. Insight from these studies should help us better understand mechanisms of immune tolerance in the tumor microenvironment, and ultimately allow for better implementation of immunotherapy treatment regimens for PDA patients.

Figures and Tables

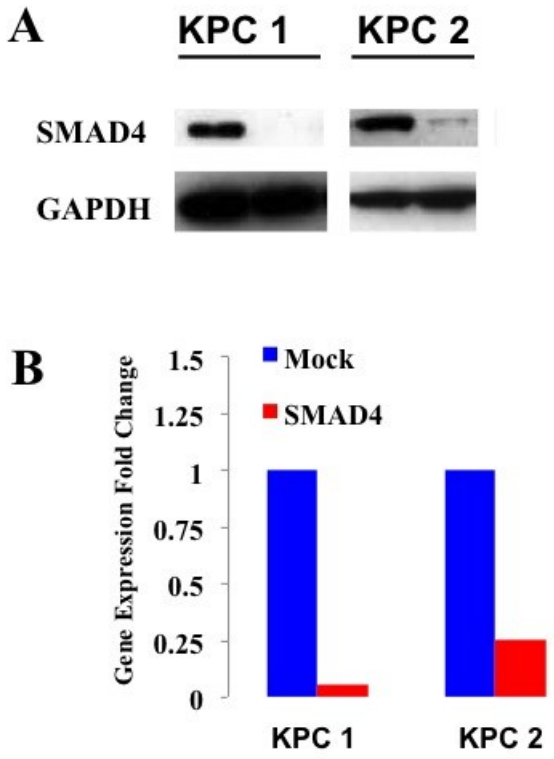

Figure 5-1: SMAD4 Protein and mRNA Expression Following Transfection of KPC Cell Lines with SMAD4 shRNAs.

Two different KPC cell lines were transfected with shRNAs against SMAD4 using Attractene. After puromycin selection and GFP-sorting and plating, single-cell clones were grown to confluency. **(A)** Western blot of protein lysates from representative clones derived from both of the KPC cell lines showing near complete loss of SMAD4 protein expression. **(B)** Expression of SMAD4 was measured by qRT-PCR, normalized to ACTB and expressed as the fold change with respect to cells transfected with the control mock shRNA plasmid.

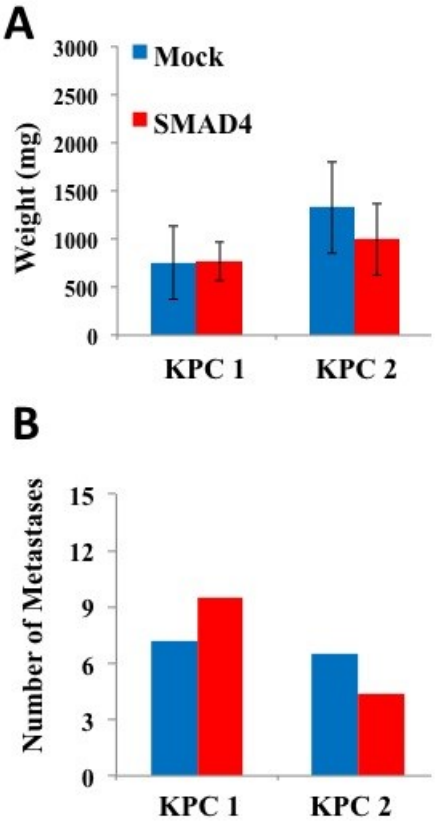

Figure 5-2: Characterization of SMAD4-Deficient KPC Tumor Cells

Four weeks after implanting either SMAD-4 deficient or Mock KPC cells into the pancreata of mice (n=5 or 6 for each cohort), animals were sacrificed and assessed for tumor burden. **(A)** Average tumor size (mg) four weeks post injection. **(B)** Average number of metastases to all sites four weeks post injection. Comparisons were made using a Student's T Test.

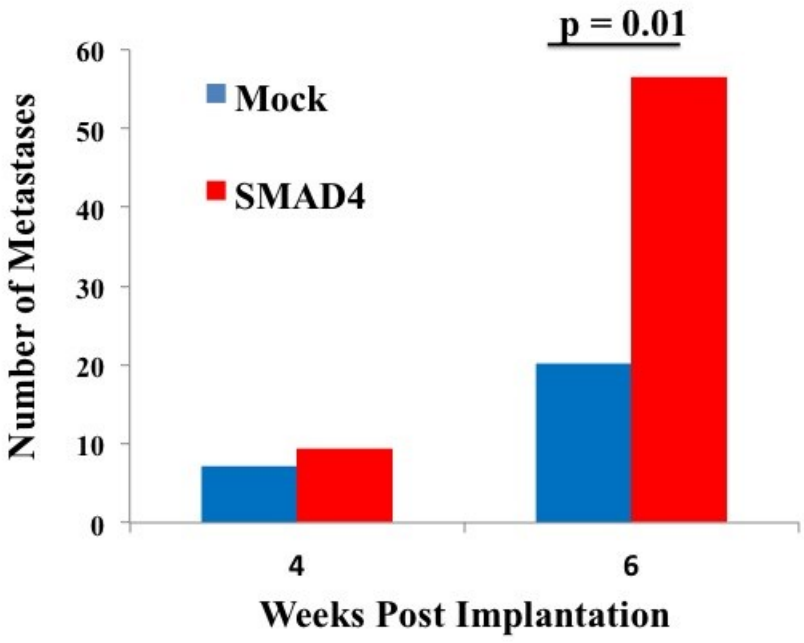

Figure 5-3: Metastatic Burden in SMAD4-Deficient KPC Clone #1 Tumor Cells

Four and six weeks after implanting either SMAD-4 deficient or Mock KPC Clone 1 cells into the pancreata of mice (n = 5 or 6 for each cohort), animals were sacrificed and assessed for tumor burden. Average number of metastases to all sites at four and six weeks post injection were compared using a Student's T Test.

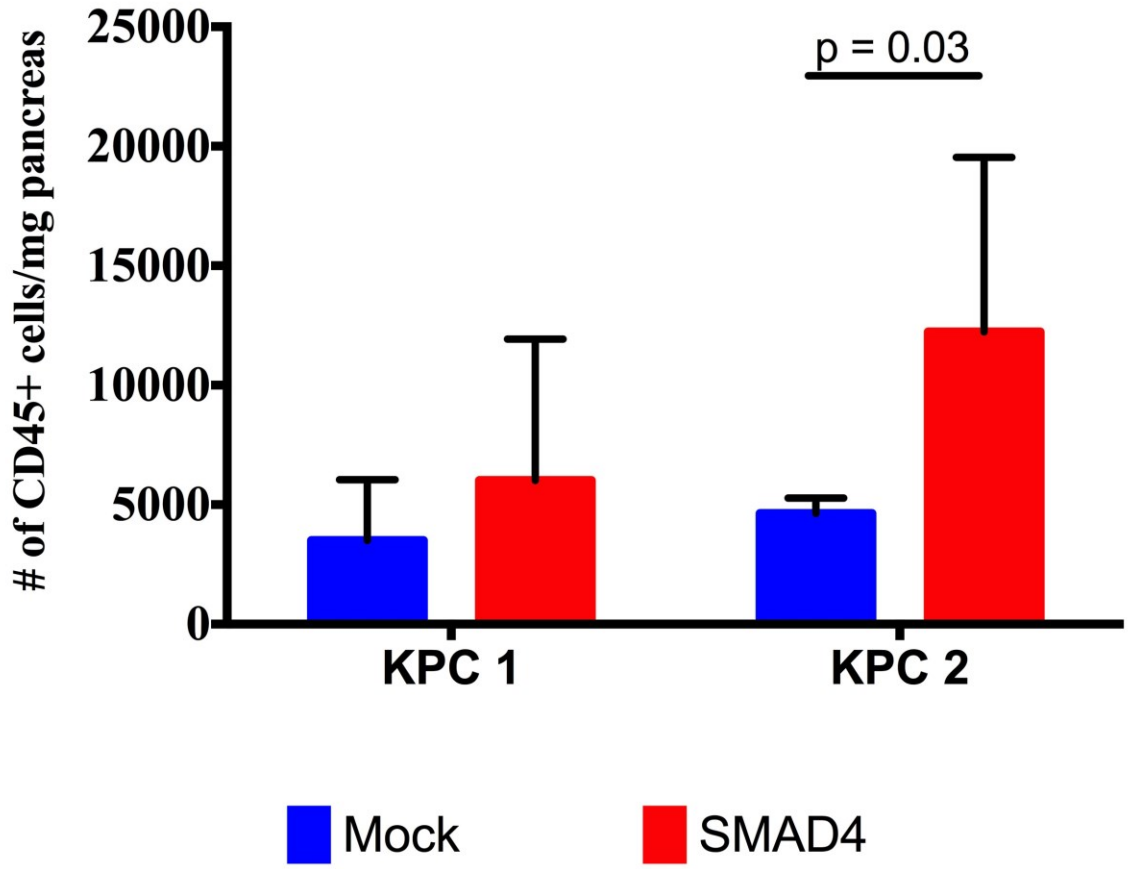

Figure 5-4: Leukocyte Infiltration in KPC vs. SMAD4-Deficient Tumors

Tumor-infiltrating leukocytes were isolated from mice injected with either KPC (mock) or SMAD4-deficient KPC cells four weeks after implantation (n = 4 or 5 for each cohort), and analyzed via fluorescence activated cell sorting. Absolute numbers of cells were normalized to tumor weight and were compared using a Student's T Test.

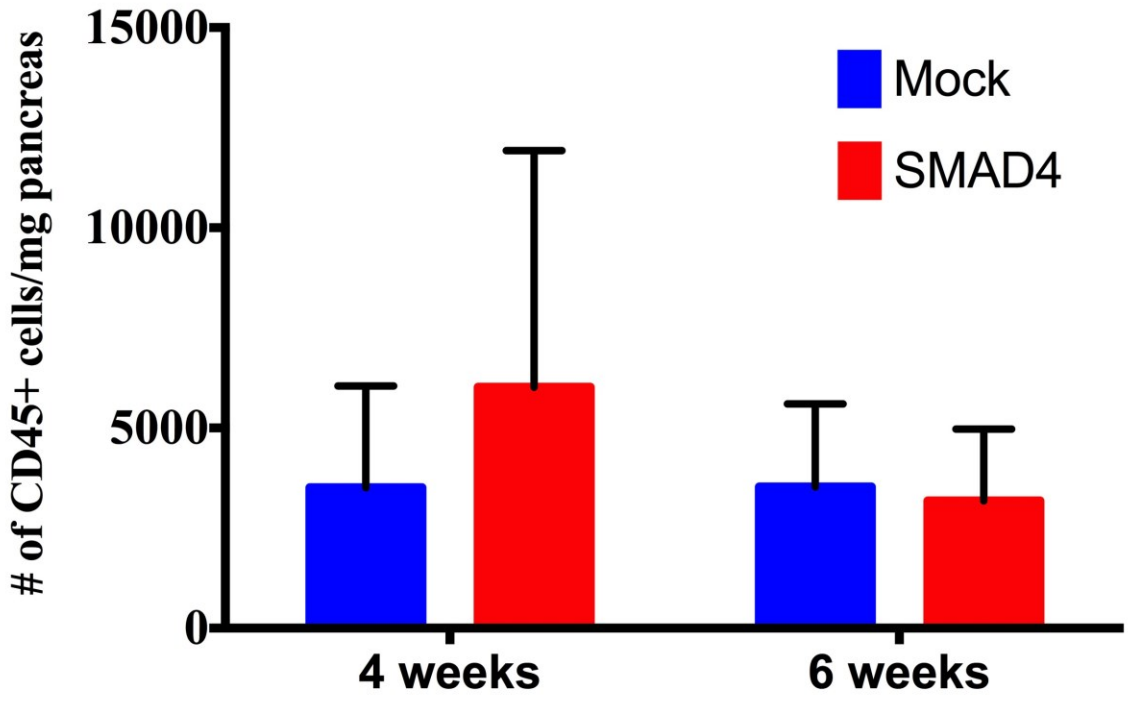

Figure 5-5: Leukocyte Infiltrate in SMAD4-Deficient KPC Clone #1 Tumor Cells

Four and six weeks after implanting either SMAD-4 deficient or Mock KPC Clone 1 cells into the pancreata of mice (n = 4 for each cohort), animals were sacrificed and assessed for CD45+ leukocyte infiltrate. Absolute numbers of cells were normalized to tumor weight and compared using a Student's T Test.

Figure 5-6: Myeloid Infiltrate in KPC vs. SMAD4-Deficient Tumors

Tumor-infiltrating immune cells were isolated from mice injected with either KPC (mock) or SMAD4-deficient KPC cells four weeks after implantation (n = 4 or 5 for each cohort), and analyzed via fluorescence activated cell sorting for myeloid markers. **(A)** Number of myeloid cells (defined as CD45+ CD11b+ Gr-1+) per milligram of tumor tissue. **(B)** Number of granulocytic myeloid derived suppressor cells (G-MDSCS) were defined as CD45+ CD11b+ Ly-6G^{hi} and Ly-6C^{lo} positive. **(C)** Number of monocytic myeloid derived suppressor cells (M-MDSCs) were defined as CD45+ CD11b+ Ly-6G^{lo} and Ly-6C^{hi} positive. Absolute numbers of cells were normalized to tumor weight and compared using a Student's T Test.

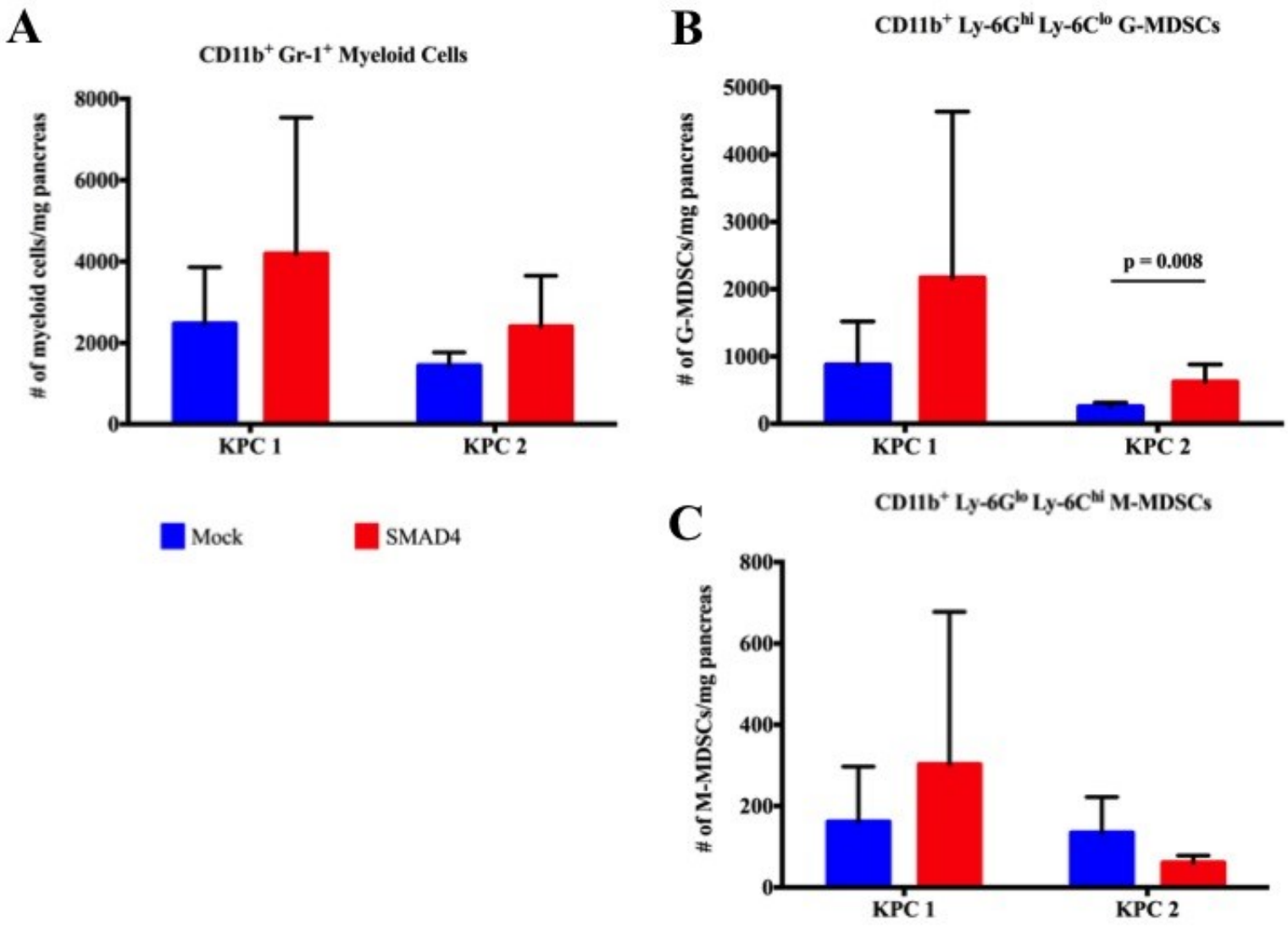
A
CD11b+ Gr-1+ Myeloid Cells
# of myeloid cells/mg pancreas
8000
6000
4000
2000
0
KPC 1
KPC 2
Mock
SMAD4
B
CD11b+ Ly-6Ghi Ly-6Clo G-MDSCs
# of G-MDSCs/mg pancreas
5000
4000
3000
2000
1000
0
p = 0.008
KPC 1
KPC 2
C
CD11b+ Ly-6Glo Ly-6Chi M-MDSCs
# of M-MDSCs/mg pancreas
800
600
400
200
0
KPC 1
KPC 2

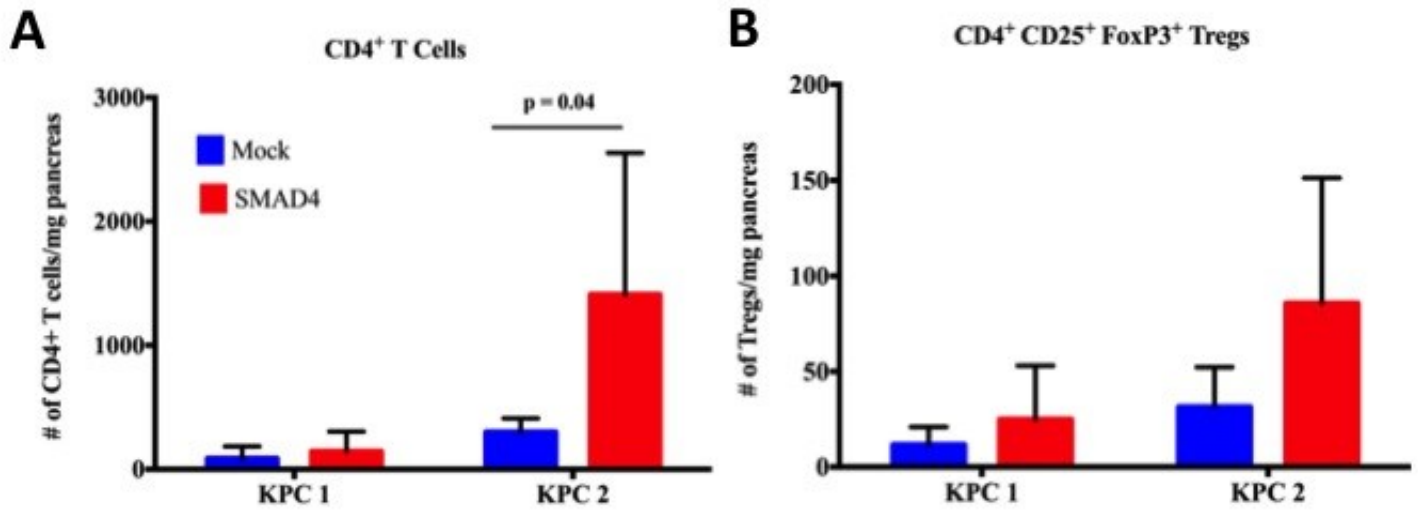

Figure 5-7: CD4+ T Cell Infiltrate in KPC vs. SMAD4-Deficient Tumors

Tumor-infiltrating immune cells were isolated from mice injected with either KPC (mock) or SMAD4-deficient KPC cells four weeks after implantation (n = 4 or 5 for each cohort), and analyzed via fluorescence activated cell sorting for myeloid markers. **(A)** Number of CD4+ T cells (defined as CD45+ CD3+) per milligram of tumor tissue (p = 0.04) **(B)** Number of T regulatory cells (Tregs) were defined as CD45+ CD25+ CD4+ and FoxP3+. Absolute numbers of cells were normalized to tumor weight and compared using a Student's T Test.

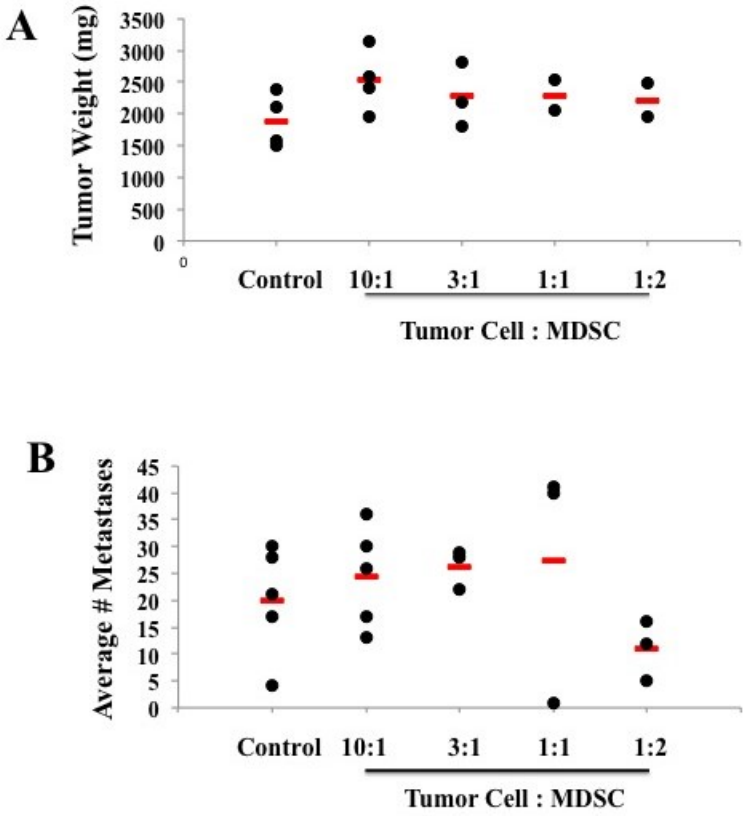

Figure 5-8: Characterization of KPC Tumors Following Adoptive Transfer of CD11b+ Gr-1+ MDSCs

KPC tumor cells were implanted into the pancreata of mice. Three weeks later, spleens were harvested and CD11b+ Gr-1+ myeloid cells were sorted from splenocyte suspensions (donor cells). These myeloid cells were mixed with KPC tumor cells at the indicated ratios and injected into the pancreata of recipient mice (n=3-5 for each cohort). Tumors were allowed to grow for three weeks prior to harvesting for analysis. **(A)** Tumor sizes were compared for each of the indicated ratios of KPC:MDSCs. **(B)** Total number of macroscopic metastases were counted in each animal. Control mice received KPC tumor cells alone.

Table 5.1: Primers Sets for Gene Expression Analysis

Gene	Product Size	5'-3' Sequence
ACTB – Forward	241bp	GGCTGTATTCCCCTCCATCG
ACTB – Reverse		CCAGTTGGTAACAATGCCATGT
SMAD4 – Forward	124bp	CAGCCATAGTGAAGGACTGTTGC
SMAD4 – Reverse		CCTACTTCCAGTCCAGGTGGTA

Chapter 6 : Conclusions and Future Directions

The immune response in cancer is both dynamic and complex. There is compelling evidence to suggest that our immune system can recognize and eliminate nascent transformed cells, and yet during carcinogenesis, tumor cells are able to escape immune detection and proliferate. Similarly, we are beginning to elucidate the mechanisms by which chronic inflammation promote tumor initiation even as countless studies suggest that robust immune responses in patients are correlated with better outcomes (202).

Central to understanding this paradox is an appreciation of the diversity and flexibility of the immune system. The innate and adaptive arms of the immune system are comprised of an array of immune cell subsets with unique and complementary roles designed to protect the host from pathogens, toxins, and neoplastic cells. Immune cells react to such threats by secreting cytokines and chemokines to mediate immune responses, releasing reactive oxygen and nitrogen species to thwart pathogens from multiplying, restructuring the local environment to protect against deleterious consequences of the mediators they release, and by engaging the adaptive arm to develop memory responses for future exposures (203). Unfortunately, tumor cells can utilize these same responses to facilitate their proliferative and metastatic capabilities. As the function and survival of immune cells is a direct consequence of their localized environments, tumor cells can effectively hijack the immune response by shaping the surrounding milieu (126).

The TGFβ signaling pathway has similar, paradoxical roles during carcinogenesis. This pathway is critical for preventing tumor formation by inhibiting cell division and promoting apoptosis. At later stages, TGFβ promotes tumor progression through a number of cell autonomous and cell non-autonomous mechanisms, including regulation of mitogenic factors that promote cell growth, promoting extracellular matrix remodeling, and shaping the tumor

microenvironment to support immunosuppression and tolerance (40). The TGFβ signaling pathway is known to be mutated in the majority of PDA patients, with alterations most commonly observed in SMAD4 (24), and to a lesser extent in TGFβR2 (34). This thesis focuses on understanding how cell autonomous and non-autonomous effects of the TGFβ signaling pathway promote PDA carcinogenesis and metastatic progression. Studies in this dissertation have contributed to understanding TGFβ-mediated PDA carcinogenesis and progression in the following ways:

1) In Chapter 3, we showed that the different metastatic phenotypes of PDA are a result of the activation status of the TGFβ signaling pathway. During carcinogenesis, Tgfβ signaling works to restrain tumor cell proliferation; however, once invasive PDA develops, Tgfβ exerts its tumor-promoting effects. This switch is likely a consequence of acquired mutations that can bypass the effects of TGFβ-mediated growth inhibition (such as in p53). We showed that in contrast to widely metastatic disease, oligometastatic PDA is characterized by reduced expression of key TGFβ pathway components and favorable histologic features. We also described a novel murine model of oligometastatic PDA. This conditional mouse model with *Tgfbr2* haploinsufficiency coupled with $Kras^{G12D}$ and $Trp53^{R172H}$ activation accelerated PDA carcinogenesis, but decreased metastatic efficiency.
2) In Chapters 4 and 5, we highlighted preliminarily evidence to suggest that reduced Tgfβ signaling in tumor cells, via TgfβR2 or SMAD4 inactivation, results in changes to the immune profile in invasive PDA. Importantly, the most substantial differences

were noted in regulatory immune cell populations such as granulocytic MDSCs and T regulatory cells. Although not demonstrated by work done in this thesis, others have shown that these immune cells facilitate tumor progression by promoting immune tolerance.

Additional experiments are underway to confirm that these subsets of immune cells are significantly altered in our murine model and human tissues of oligometastatic PDA. We have also begun to explore the localization of these immune cells within the tumor microenvironment, and the mechanisms by which they are recruited into pancreatic tumors.

Going forward, our novel mouse model of oligometastatic PDA provides researchers with a tool to study the biology of the different metastatic phenotypes of PDA. Understanding the differences between and mechanisms that drive oligometastatic and widely metastatic disease, be they cell autonomous or indirect tumor microenvironmental influences, has the potential to highlight new targets for therapeutic intervention that are so desperately needed to combat this disease.

References

1. Siegel R, Naishadham D, Jemal A. 2012. Cancer statistics, 2012. *CA Cancer J Clin* 62:10-29
2. Bardeesy N, DePinho RA. 2002. Pancreatic cancer biology and genetics. *Nat Rev Cancer* 2:897-909
3. Maitra A, Hruban RH. 2008. Pancreatic cancer. *Annu Rev Pathol* 3:157-88
4. Hruban RH, Adsay NV, Albores-Saavedra J, Compton C, Garrett ES, et al. 2001. Pancreatic intraepithelial neoplasia: a new nomenclature and classification system for pancreatic duct lesions. *Am J Surg Pathol* 25:579-86
5. Matthaei H, Schulick RD, Hruban RH, Maitra A. 2011. Cystic precursors to invasive pancreatic cancer. *Nat Rev Gastroenterol Hepatol* 8:141-50
6. Hruban RH, Takaori K, Klimstra DS, Adsay NV, Albores-Saavedra J, et al. 2004. An illustrated consensus on the classification of pancreatic intraepithelial neoplasia and intraductal papillary mucinous neoplasms. *Am J Surg Pathol* 28:977-87
7. Gaujoux S, Brennan MF, Gonen M, D'Angelica MI, DeMatteo R, et al. 2011. Cystic lesions of the pancreas: changes in the presentation and management of 1,424 patients at a single institution over a 15-year time period. *Journal of the American College of Surgeons* 212:590-600; discussion -3
8. Maitra A, Fukushima N, Takaori K, Hruban RH. 2005. Precursors to invasive pancreatic cancer. *Adv Anat Pathol* 12:81-91
9. van Heek NT, Meeker AK, Kern SE, Yeo CJ, Lillemoe KD, et al. 2002. Telomere shortening is nearly universal in pancreatic intraepithelial neoplasia. *Am J Pathol* 161:1541-7
10. Kanda M, Matthaei H, Wu J, Hong SM, Yu J, et al. 2012. Presence of somatic mutations in most early-stage pancreatic intraepithelial neoplasia. *Gastroenterology* 142:730-3 e9
11. Caldas C, Kern SE. 1995. K-ras mutation and pancreatic adenocarcinoma. *Int J Pancreatol* 18:1-6
12. Schubbert S, Shannon K, Bollag G. 2007. Hyperactive Ras in developmental disorders and cancer. *Nat Rev Cancer* 7:295-308
13. Calhoun ES, Jones JB, Ashfaq R, Adsay V, Baker SJ, et al. 2003. BRAF and FBXW7 (CDC4, FBW7, AGO, SEL10) mutations in distinct subsets of pancreatic cancer: potential therapeutic targets. *Am J Pathol* 163:1255-60
14. Schutte M, Hruban RH, Geradts J, Maynard R, Hilgers W, et al. 1997. Abrogation of the Rb/p16 tumor-suppressive pathway in virtually all pancreatic carcinomas. *Cancer Res* 57:3126-30
15. Caldas C, Hahn SA, da Costa LT, Redston MS, Schutte M, et al. 1994. Frequent somatic mutations and homozygous deletions of the p16 (MTS1) gene in pancreatic adenocarcinoma. *Nat Genet* 8:27-32
16. Larsson LG. 2011. Oncogene- and tumor suppressor gene-mediated suppression of cellular senescence. *Seminars in cancer biology* 21:367-76

17. Rozenblum E, Schutte M, Goggins M, Hahn SA, Panzer S, et al. 1997. Tumor-suppressive pathways in pancreatic carcinoma. *Cancer Res* 57:1731-4
18. Kim WY, Sharpless NE. 2006. The regulation of INK4/ARF in cancer and aging. *Cell* 127:265-75
19. DiGiuseppe JA, Redston MS, Yeo CJ, Kern SE, Hruban RH. 1995. p53-independent expression of the cyclin-dependent kinase inhibitor p21 in pancreatic carcinoma. *Am J Pathol* 147:884-8
20. Jones S, Zhang X, Parsons DW, Lin JC, Leary RJ, et al. 2008. Core signaling pathways in human pancreatic cancers revealed by global genomic analyses. *Science* 321:1801-6
21. Redston MS, Caldas C, Seymour AB, Hruban RH, da Costa L, et al. 1994. p53 mutations in pancreatic carcinoma and evidence of common involvement of homocopolymer tracts in DNA microdeletions. *Cancer Res* 54:3025-33
22. Vogelstein B, Kinzler KW. 2004. Cancer genes and the pathways they control. *Nat Med* 10:789-99
23. Wilentz RE, Iacobuzio-Donahue CA, Argani P, McCarthy DM, Parsons JL, et al. 2000. Loss of expression of Dpc4 in pancreatic intraepithelial neoplasia: evidence that DPC4 inactivation occurs late in neoplastic progression. *Cancer research* 60:2002-6
24. Hahn SA, Schutte M, Hoque AT, Moskaluk CA, da Costa LT, et al. 1996. DPC4, a candidate tumor suppressor gene at human chromosome 18q21.1. *Science* 271:350-3
25. Siegel PM, Massague J. 2003. Cytostatic and apoptotic actions of TGF-beta in homeostasis and cancer. *Nature reviews. Cancer* 3:807-21
26. Dai JL, Bansal RK, Kern SE. 1999. G1 cell cycle arrest and apoptosis induction by nuclear Smad4/Dpc4: phenotypes reversed by a tumorigenic mutation. *Proc Natl Acad Sci U S A* 96:1427-32
27. Tascilar M, Skinner HG, Rosty C, Sohn T, Wilentz RE, et al. 2001. The SMAD4 protein and prognosis of pancreatic ductal adenocarcinoma. *Clin Cancer Res* 7:4115-21
28. Iacobuzio-Donahue CA, Fu B, Yachida S, Luo M, Abe H, et al. 2009. DPC4 gene status of the primary carcinoma correlates with patterns of failure in patients with pancreatic cancer. *Journal of clinical oncology : official journal of the American Society of Clinical Oncology* 27:1806-13
29. Wood LD, Parsons DW, Jones S, Lin J, Sjoblom T, et al. 2007. The genomic landscapes of human breast and colorectal cancers. *Science* 318:1108-13
30. Jones S, Wang TL, Shih Ie M, Mao TL, Nakayama K, et al. 2010. Frequent mutations of chromatin remodeling gene ARID1A in ovarian clear cell carcinoma. *Science* 330:228-31
31. Jones S, Li M, Parsons DW, Zhang X, Wesseling J, et al. 2012. Somatic mutations in the chromatin remodeling gene ARID1A occur in several tumor types. *Hum Mutat* 33:100-3
32. Shain AH, Giacomini CP, Matsukuma K, Karikari CA, Bashyam MD, et al. 2012. Convergent structural alterations define SWItch/Sucrose NonFermentable (SWI/SNF) chromatin remodeler as a central tumor suppressive complex in pancreatic cancer. *Proc Natl Acad Sci U S A* 109:E252-9

33. Friess H, Yamanaka Y, Buchler M, Berger HG, Kobrin MS, et al. 1993. Enhanced expression of the type II transforming growth factor beta receptor in human pancreatic cancer cells without alteration of type III receptor expression. *Cancer research* 53:2704-7
34. Goggins M, Shekher M, Turnacioglu K, Yeo CJ, Hruban RH, Kern SE. 1998. Genetic alterations of the transforming growth factor beta receptor genes in pancreatic and biliary adenocarcinomas. *Cancer research* 58:5329-32
35. Blackford A, Serrano OK, Wolfgang CL, Parmigiani G, Jones S, et al. 2009. SMAD4 gene mutations are associated with poor prognosis in pancreatic cancer. *Clinical cancer research : an official journal of the American Association for Cancer Research* 15:4674-9
36. Kleeff J, Ishiwata T, Maruyama H, Friess H, Truong P, et al. 1999. The TGF-beta signaling inhibitor Smad7 enhances tumorigenicity in pancreatic cancer. *Oncogene* 18:5363-72
37. Kleeff J, Maruyama H, Friess H, Buchler MW, Falb D, Korc M. 1999. Smad6 suppresses TGF-beta-induced growth inhibition in COLO-357 pancreatic cancer cells and is overexpressed in pancreatic cancer. *Biochemical and biophysical research communications* 255:268-73
38. Friess H, Yamanaka Y, Buchler M, Ebert M, Beger HG, et al. 1993. Enhanced expression of transforming growth factor beta isoforms in pancreatic cancer correlates with decreased survival. *Gastroenterology* 105:1846-56
39. Zhang YE. 2009. Non-Smad pathways in TGF-beta signaling. *Cell research* 19:128-39
40. Massague J. 2008. TGFbeta in Cancer. *Cell* 134:215-30
41. Shi Y, Massague J. 2003. Mechanisms of TGF-beta signaling from cell membrane to the nucleus. *Cell* 113:685-700
42. Edlund S, Landstrom M, Heldin CH, Aspenstrom P. 2002. Transforming growth factor-beta-induced mobilization of actin cytoskeleton requires signaling by small GTPases Cdc42 and RhoA. *Molecular biology of the cell* 13:902-14
43. Bhowmick NA, Ghiassi M, Bakin A, Aakre M, Lundquist CA, et al. 2001. Transforming growth factor-beta1 mediates epithelial to mesenchymal transdifferentiation through a RhoA-dependent mechanism. *Molecular biology of the cell* 12:27-36
44. Engel ME, McDonnell MA, Law BK, Moses HL. 1999. Interdependent SMAD and JNK signaling in transforming growth factor-beta-mediated transcription. *The Journal of biological chemistry* 274:37413-20
45. Yue J, Mulder KM. 2000. Activation of the mitogen-activated protein kinase pathway by transforming growth factor-beta. *Methods in molecular biology* 142:125-31
46. Li JM, Nichols MA, Chandrasekharan S, Xiong Y, Wang XF. 1995. Transforming growth factor beta activates the promoter of cyclin-dependent kinase inhibitor p15INK4B through an Sp1 consensus site. *The Journal of biological chemistry* 270:26750-3
47. Datto MB, Li Y, Panus JF, Howe DJ, Xiong Y, Wang XF. 1995. Transforming growth factor beta induces the cyclin-dependent kinase inhibitor p21 through a

p53-independent mechanism. *Proceedings of the National Academy of Sciences of the United States of America* 92:5545-9
48. Wildey GM, Patil S, Howe PH. 2003. Smad3 potentiates transforming growth factor beta (TGFbeta)-induced apoptosis and expression of the BH3-only protein Bim in WEHI 231 B lymphocytes. *The Journal of biological chemistry* 278:18069-77
49. Saltzman A, Munro R, Searfoss G, Franks C, Jaye M, Ivashchenko Y. 1998. Transforming growth factor-beta-mediated apoptosis in the Ramos B-lymphoma cell line is accompanied by caspase activation and Bcl-XL downregulation. *Experimental cell research* 242:244-54
50. Chipuk JE, Bhat M, Hsing AY, Ma J, Danielpour D. 2001. Bcl-xL blocks transforming growth factor-beta 1-induced apoptosis by inhibiting cytochrome c release and not by directly antagonizing Apaf-1-dependent caspase activation in prostate epithelial cells. *The Journal of biological chemistry* 276:26614-21
51. Bhowmick NA, Chytil A, Plieth D, Gorska AE, Dumont N, et al. 2004. TGF-beta signaling in fibroblasts modulates the oncogenic potential of adjacent epithelia. *Science* 303:848-51
52. Balkwill F, Mantovani A. 2001. Inflammation and cancer: back to Virchow? *Lancet* 357:539-45
53. Lu H, Ouyang W, Huang C. 2006. Inflammation, a key event in cancer development. *Molecular cancer research : MCR* 4:221-33
54. Fridman WH, Remark R, Goc J, Giraldo NA, Becht E, et al. 2014. The immune microenvironment: a major player in human cancers. *International archives of allergy and immunology* 164:13-26
55. Lebrun JJ. 2012. The Dual Role of TGF-beta in Human Cancer: From Tumor Suppression to Cancer Metastasis. *ISRN Molecular Biology* 2012:28
56. Thiery JP. 2003. Epithelial-mesenchymal transitions in development and pathologies. *Current opinion in cell biology* 15:740-6
57. Thuault S, Valcourt U, Petersen M, Manfioletti G, Heldin CH, Moustakas A. 2006. Transforming growth factor-beta employs HMGA2 to elicit epithelial-mesenchymal transition. *The Journal of cell biology* 174:175-83
58. Larue L, Bellacosa A. 2005. Epithelial-mesenchymal transition in development and cancer: role of phosphatidylinositol 3' kinase/AKT pathways. *Oncogene* 24:7443-54
59. Zavadil J, Bitzer M, Liang D, Yang YC, Massimi A, et al. 2001. Genetic programs of epithelial cell plasticity directed by transforming growth factor-beta. *Proceedings of the National Academy of Sciences of the United States of America* 98:6686-91
60. Xie L, Law BK, Chytil AM, Brown KA, Aakre ME, Moses HL. 2004. Activation of the Erk pathway is required for TGF-beta1-induced EMT in vitro. *Neoplasia* 6:603-10
61. Wiercinska E, Naber HP, Pardali E, van der Pluijm G, van Dam H, ten Dijke P. 2011. The TGF-beta/Smad pathway induces breast cancer cell invasion through the up-regulation of matrix metalloproteinase 2 and 9 in a spheroid invasion model system. *Breast cancer research and treatment* 128:657-66

62. Zarzynska JM. 2014. Two faces of TGF-beta1 in breast cancer. *Mediators of inflammation* 2014:141747
63. Yang L, Pang Y, Moses HL. 2010. TGF-beta and immune cells: an important regulatory axis in the tumor microenvironment and progression. *Trends in immunology* 31:220-7
64. Thomas DA, Massague J. 2005. TGF-beta directly targets cytotoxic T cell functions during tumor evasion of immune surveillance. *Cancer cell* 8:369-80
65. Dong Y, Tang L, Letterio JJ, Benveniste EN. 2001. The Smad3 protein is involved in TGF-beta inhibition of class II transactivator and class II MHC expression. *Journal of immunology* 167:311-9
66. Josefowicz SZ, Lu LF, Rudensky AY. 2012. Regulatory T cells: mechanisms of differentiation and function. *Annual review of immunology* 30:531-64
67. Yang L, Huang J, Ren X, Gorska AE, Chytil A, et al. 2008. Abrogation of TGF beta signaling in mammary carcinomas recruits Gr-1+CD11b+ myeloid cells that promote metastasis. *Cancer Cell* 13:23-35
68. Kitamura T, Kometani K, Hashida H, Matsunaga A, Miyoshi H, et al. 2007. SMAD4-deficient intestinal tumors recruit CCR1+ myeloid cells that promote invasion. *Nature genetics* 39:467-75
69. Bierie B, Moses HL. 2006. Tumour microenvironment: TGFbeta: the molecular Jekyll and Hyde of cancer. *Nature reviews. Cancer* 6:506-20
70. De Wever O, Mareel M. 2003. Role of tissue stroma in cancer cell invasion. *The Journal of pathology* 200:429-47
71. Kojima Y, Acar A, Eaton EN, Mellody KT, Scheel C, et al. 2010. Autocrine TGF-beta and stromal cell-derived factor-1 (SDF-1) signaling drives the evolution of tumor-promoting mammary stromal myofibroblasts. *Proceedings of the National Academy of Sciences of the United States of America* 107:20009-14
72. Kretzschmar M, Doody J, Timokhina I, Massague J. 1999. A mechanism of repression of TGFbeta/ Smad signaling by oncogenic Ras. *Genes & development* 13:804-16
73. Gomis RR, Alarcon C, Nadal C, Van Poznak C, Massague J. 2006. C/EBPbeta at the core of the TGFbeta cytostatic response and its evasion in metastatic breast cancer cells. *Cancer cell* 10:203-14
74. Jen J, Harper JW, Bigner SH, Bigner DD, Papadopoulos N, et al. 1994. Deletion of p16 and p15 genes in brain tumors. *Cancer research* 54:6353-8
75. Liyanage UK, Moore TT, Joo HG, Tanaka Y, Herrmann V, et al. 2002. Prevalence of regulatory T cells is increased in peripheral blood and tumor microenvironment of patients with pancreas or breast adenocarcinoma. *J Immunol* 169:2756-61
76. Diaz-Montero CM, Salem ML, Nishimura MI, Garrett-Mayer E, Cole DJ, Montero AJ. 2009. Increased circulating myeloid-derived suppressor cells correlate with clinical cancer stage, metastatic tumor burden, and doxorubicin-cyclophosphamide chemotherapy. *Cancer Immunol Immunother* 58:49-59
77. Yang L, Edwards CM, Mundy GR. Gr-1+CD11b+ myeloid-derived suppressor cells: formidable partners in tumor metastasis. *J Bone Miner Res* 25:1701-6
78. Farrow B, Albo D, Berger DH. 2008. The role of the tumor microenvironment in the progression of pancreatic cancer. *The Journal of surgical research* 149:319-28

79. Hartel M, Di Mola FF, Gardini A, Zimmermann A, Di Sebastiano P, et al. 2004. Desmoplastic reaction influences pancreatic cancer growth behavior. *World journal of surgery* 28:818-25
80. Kleeff J, Beckhove P, Esposito I, Herzig S, Huber PE, et al. 2007. Pancreatic cancer microenvironment. *International journal of cancer. Journal international du cancer* 121:699-705
81. Flavell RA, Sanjabi S, Wrzesinski SH, Licona-Limon P. 2010. The polarization of immune cells in the tumour environment by TGFbeta. *Nature reviews. Immunology* 10:554-67
82. Dunn GP, Old LJ, Schreiber RD. 2004. The three Es of cancer immunoediting. *Annual review of immunology* 22:329-60
83. Zea AH, Rodriguez PC, Atkins MB, Hernandez C, Signoretti S, et al. 2005. Arginase-producing myeloid suppressor cells in renal cell carcinoma patients: a mechanism of tumor evasion. *Cancer Res* 65:3044-8
84. Ochoa AC, Zea AH, Hernandez C, Rodriguez PC. 2007. Arginase, prostaglandins, and myeloid-derived suppressor cells in renal cell carcinoma. *Clin Cancer Res* 13:721s-6s
85. Almand B, Clark JI, Nikitina E, van Beynen J, English NR, et al. 2001. Increased production of immature myeloid cells in cancer patients: a mechanism of immunosuppression in cancer. *J Immunol* 166:678-89
86. Clark CE, Hingorani SR, Mick R, Combs C, Tuveson DA, Vonderheide RH. 2007. Dynamics of the immune reaction to pancreatic cancer from inception to invasion. *Cancer research* 67:9518-27
87. Wachsmann MB, Pop LM, Vitetta ES. 2012. Pancreatic ductal adenocarcinoma: a review of immunologic aspects. *Journal of investigative medicine : the official publication of the American Federation for Clinical Research* 60:643-63
88. Hiraoka N, Onozato K, Kosuge T, Hirohashi S. 2006. Prevalence of FOXP3+ regulatory T cells increases during the progression of pancreatic ductal adenocarcinoma and its premalignant lesions. *Clinical cancer research : an official journal of the American Association for Cancer Research* 12:5423-34
89. Fukunaga A, Miyamoto M, Cho Y, Murakami S, Kawarada Y, et al. 2004. CD8+ tumor-infiltrating lymphocytes together with CD4+ tumor-infiltrating lymphocytes and dendritic cells improve the prognosis of patients with pancreatic adenocarcinoma. *Pancreas* 28:e26-31
90. Becht E, Goc J, Germain C, Giraldo NA, Dieu-Nosjean MC, et al. 2014. Shaping of an effective immune microenvironment to and by cancer cells. *Cancer immunology, immunotherapy : CII* 63:991-7
91. Emmrich J, Sparmann G, Hopt U, Lohr M, Liebe S. 1999. Typing of leukocytes in pancreatic tissue surrounding human pancreatic carcinoma. *Annals of the New York Academy of Sciences* 880:171-4
92. Funa K, Nilsson B, Jacobsson G, Alm GV. 1984. Decreased natural killer cell activity and interferon production by leucocytes in patients with adenocarcinoma of the pancreas. *British journal of cancer* 50:231-3
93. Ino Y, Yamazaki-Itoh R, Shimada K, Iwasaki M, Kosuge T, et al. 2013. Immune cell infiltration as an indicator of the immune microenvironment of pancreatic cancer. *British journal of cancer* 108:914-23

94. Wormann SM, Diakopoulos KN, Lesina M, Algul H. 2014. The immune network in pancreatic cancer development and progression. *Oncogene* 33:2956-67
95. Noy R, Pollard JW. 2014. Tumor-associated macrophages: from mechanisms to therapy. *Immunity* 41:49-61
96. Sica A, Larghi P, Mancino A, Rubino L, Porta C, et al. 2008. Macrophage polarization in tumour progression. *Seminars in cancer biology* 18:349-55
97. Gabrilovich DI, Nagaraj S. 2009. Myeloid-derived suppressor cells as regulators of the immune system. *Nat Rev Immunol* 9:162-74
98. Kusmartsev S, Nefedova Y, Yoder D, Gabrilovich DI. 2004. Antigen-specific inhibition of CD8+ T cell response by immature myeloid cells in cancer is mediated by reactive oxygen species. *J Immunol* 172:989-99
99. Ugel S, Delpozzo F, Desantis G, Papalini F, Simonato F, et al. 2009. Therapeutic targeting of myeloid-derived suppressor cells. *Curr Opin Pharmacol* 9:470-81
100. Serafini P, Borrello I, Bronte V. 2006. Myeloid suppressor cells in cancer: recruitment, phenotype, properties, and mechanisms of immune suppression. *Semin Cancer Biol* 16:53-65
101. Leao IC, Ganesan P, Armstrong TD, Jaffee EM. 2008. Effective depletion of regulatory T cells allows the recruitment of mesothelin-specific CD8 T cells to the antitumor immune response against a mesothelin-expressing mouse pancreatic adenocarcinoma. *Clin Transl Sci* 1:228-39
102. Reid MD, Basturk O, Thirabanjasak D, Hruban RH, Klimstra DS, et al. 2011. Tumor-infiltrating neutrophils in pancreatic neoplasia. *Modern pathology : an official journal of the United States and Canadian Academy of Pathology, Inc* 24:1612-9
103. Houghton AM. 2010. The paradox of tumor-associated neutrophils: fueling tumor growth with cytotoxic substances. *Cell cycle* 9:1732-7
104. Bausch D, Pausch T, Krauss T, Hopt UT, Fernandez-del-Castillo C, et al. 2011. Neutrophil granulocyte derived MMP-9 is a VEGF independent functional component of the angiogenic switch in pancreatic ductal adenocarcinoma. *Angiogenesis* 14:235-43
105. Benson DD, Meng X, Fullerton DA, Moore EE, Lee JH, et al. 2012. Activation state of stromal inflammatory cells in murine metastatic pancreatic adenocarcinoma. *American journal of physiology. Regulatory, integrative and comparative physiology* 302:R1067-75
106. Zheng L, Xue J, Jaffee EM, Habtezion A. 2013. Role of immune cells and immune-based therapies in pancreatitis and pancreatic ductal adenocarcinoma. *Gastroenterology* 144:1230-40
107. Hruban RH, Goggins M, Parsons J, Kern SE. 2000. Progression model for pancreatic cancer. *Clinical cancer research : an official journal of the American Association for Cancer Research* 6:2969-72
108. DeCant BT, Principe DR, Guerra C, Pasca di Magliano M, Grippo PJ. 2014. Utilizing past and present mouse systems to engineer more relevant pancreatic cancer models. *Frontiers in physiology* 5:464
109. Fokas E, O'Neill E, Gordon-Weeks A, Mukherjee S, McKenna WG, Muschel RJ. 2015. Pancreatic ductal adenocarcinoma: From genetics to biology to

radiobiology to oncoimmunology and all the way back to the clinic. *Biochimica et biophysica acta* 1855:61-82
110. Kim MP, Evans DB, Wang H, Abbruzzese JL, Fleming JB, Gallick GE. 2009. Generation of orthotopic and heterotopic human pancreatic cancer xenografts in immunodeficient mice. *Nature protocols* 4:1670-80
111. Schutte U, Bisht S, Brossart P, Feldmann G. 2011. Recent developments of transgenic and xenograft mouse models of pancreatic cancer for translational research. *Expert opinion on drug discovery* 6:33-48
112. Capella G, Farre L, Villanueva A, Reyes G, Garcia C, et al. 1999. Orthotopic models of human pancreatic cancer. *Annals of the New York Academy of Sciences* 880:103-9
113. Offield MF, Jetton TL, Labosky PA, Ray M, Stein RW, et al. 1996. PDX-1 is required for pancreatic outgrowth and differentiation of the rostral duodenum. *Development* 122:983-95
114. Krapp A, Knofler M, Ledermann B, Burki K, Berney C, et al. 1998. The bHLH protein PTF1-p48 is essential for the formation of the exocrine and the correct spatial organization of the endocrine pancreas. *Genes & development* 12:3752-63
115. Hingorani SR, Petricoin EF, Maitra A, Rajapakse V, King C, et al. 2003. Preinvasive and invasive ductal pancreatic cancer and its early detection in the mouse. *Cancer cell* 4:437-50
116. Hingorani SR, Wang L, Multani AS, Combs C, Deramaudt TB, et al. 2005. Trp53R172H and KrasG12D cooperate to promote chromosomal instability and widely metastatic pancreatic ductal adenocarcinoma in mice. *Cancer cell* 7:469-83
117. Izeradjene K, Combs C, Best M, Gopinathan A, Wagner A, et al. 2007. Kras(G12D) and Smad4/Dpc4 haploinsufficiency cooperate to induce mucinous cystic neoplasms and invasive adenocarcinoma of the pancreas. *Cancer cell* 11:229-43
118. Ijichi H, Chytil A, Gorska AE, Aakre ME, Fujitani Y, et al. 2006. Aggressive pancreatic ductal adenocarcinoma in mice caused by pancreas-specific blockade of transforming growth factor-beta signaling in cooperation with active Kras expression. *Genes & development* 20:3147-60
119. Howlader. 2011. *SEER Cancer Statistics Review, 1975-2008* . http://seer.cancer.gov/statfacts/html/pancreas.html
120. Biankin AV, Morey AL, Lee CS, Kench JG, Biankin SA, et al. 2002. DPC4/Smad4 expression and outcome in pancreatic ductal adenocarcinoma. *Journal of clinical oncology : official journal of the American Society of Clinical Oncology* 20:4531-42
121. Carlini MJ, De Lorenzo MS, Puricelli L. Cross-talk between Tumor Cells and the Microenvironment at the Metastatic Niche. *Curr Pharm Biotechnol*
122. Kopfstein L, Christofori G. 2006. Metastasis: cell-autonomous mechanisms versus contributions by the tumor microenvironment. *Cell Mol Life Sci* 63:449-68
123. Joyce JA, Pollard JW. 2009. Microenvironmental regulation of metastasis. *Nat Rev Cancer* 9:239-52
124. de Visser KE, Eichten A, Coussens LM. 2006. Paradoxical roles of the immune system during cancer development. *Nat Rev Cancer* 6:24-37

125. Mantovani A, Bottazzi B, Colotta F, Sozzani S, Ruco L. 1992. The origin and function of tumor-associated macrophages. *Immunol Today* 13:265-70
126. Flavell RA, Sanjabi S, Wrzesinski SH, Licona-Limon P. The polarization of immune cells in the tumour environment by TGFbeta. *Nat Rev Immunol* 10:554-67
127. Bronte V, Wang M, Overwijk WW, Surman DR, Pericle F, et al. 1998. Apoptotic death of CD8+ T lymphocytes after immunization: induction of a suppressive population of Mac-1+/Gr-1+ cells. *J Immunol* 161:5313-20
128. Shipley JM, Wesselschmidt RL, Kobayashi DK, Ley TJ, Shapiro SD. 1996. Metalloelastase is required for macrophage-mediated proteolysis and matrix invasion in mice. *Proc Natl Acad Sci U S A* 93:3942-6
129. Sohn TA, Yeo CJ, Cameron JL, Koniaris L, Kaushal S, et al. 2000. Resected adenocarcinoma of the pancreas-616 patients: results, outcomes, and prognostic indicators. *J Gastrointest Surg* 4:567-79
130. Conroy T, Desseigne F, Ychou M, Bouche O, Guimbaud R, et al. 2011. FOLFIRINOX versus gemcitabine for metastatic pancreatic cancer. *The New England journal of medicine* 364:1817-25
131. Von Hoff DD, Ervin T, Arena FP, Chiorean EG, Infante J, et al. 2013. Increased survival in pancreatic cancer with nab-paclitaxel plus gemcitabine. *The New England journal of medicine* 369:1691-703
132. Rahib L, Smith BD, Aizenberg R, Rosenzweig AB, Fleshman JM, Matrisian LM. 2014. Projecting cancer incidence and deaths to 2030: the unexpected burden of thyroid, liver, and pancreas cancers in the United States. *Cancer research* 74:2913-21
133. Stathis A, Moore MJ. 2010. Advanced pancreatic carcinoma: current treatment and future challenges. *Nature reviews. Clinical oncology* 7:163-72
134. Fidler IJ. 2011. The biology of cancer metastasis. *Seminars in cancer biology* 21:71
135. Haeno H, Gonen M, Davis MB, Herman JM, Iacobuzio-Donahue CA, Michor F. 2012. Computational modeling of pancreatic cancer reveals kinetics of metastasis suggesting optimum treatment strategies. *Cell* 148:362-75
136. Yachida S, Jones S, Bozic I, Antal T, Leary R, et al. 2010. Distant metastasis occurs late during the genetic evolution of pancreatic cancer. *Nature* 467:1114-7
137. Rhim AD, Mirek ET, Aiello NM, Maitra A, Bailey JM, et al. 2012. EMT and dissemination precede pancreatic tumor formation. *Cell* 148:349-61
138. Biankin AV, Waddell N, Kassahn KS, Gingras MC, Muthuswamy LB, et al. 2012. Pancreatic cancer genomes reveal aberrations in axon guidance pathway genes. *Nature* 491:399-405
139. Vogelstein B, Papadopoulos N, Velculescu VE, Zhou S, Diaz LA, Jr., Kinzler KW. 2013. Cancer genome landscapes. *Science* 339:1546-58
140. Hruban RH, Maitra A, Kern SE, Goggins M. 2007. Precursors to pancreatic cancer. *Gastroenterology clinics of North America* 36:831-49, vi
141. Berman DM, Karhadkar SS, Maitra A, Montes De Oca R, Gerstenblith MR, et al. 2003. Widespread requirement for Hedgehog ligand stimulation in growth of digestive tract tumours. *Nature* 425:846-51

142. Miyamoto Y, Maitra A, Ghosh B, Zechner U, Argani P, et al. 2003. Notch mediates TGF alpha-induced changes in epithelial differentiation during pancreatic tumorigenesis. *Cancer cell* 3:565-76
143. Son J, Lyssiotis CA, Ying H, Wang X, Hua S, et al. 2013. Glutamine supports pancreatic cancer growth through a KRAS-regulated metabolic pathway. *Nature* 496:101-5
144. Sousa CM, Kimmelman AC. 2014. The complex landscape of pancreatic cancer metabolism. *Carcinogenesis* 35:1441-50
145. Yang A, Rajeshkumar NV, Wang X, Yabuuchi S, Alexander BM, et al. 2014. Autophagy is critical for pancreatic tumor growth and progression in tumors with p53 alterations. *Cancer discovery* 4:905-13
146. Stromnes IM, DelGiorno KE, Greenberg PD, Hingorani SR. 2014. Stromal reengineering to treat pancreas cancer. *Carcinogenesis* 35:1451-60
147. Jackson EL, Willis N, Mercer K, Bronson RT, Crowley D, et al. 2001. Analysis of lung tumor initiation and progression using conditional expression of oncogenic K-ras. *Genes & development* 15:3243-8
148. Olive KP, Tuveson DA, Ruhe ZC, Yin B, Willis NA, et al. 2004. Mutant p53 gain of function in two mouse models of Li-Fraumeni syndrome. *Cell* 119:847-60
149. Chytil A, Magnuson MA, Wright CV, Moses HL. 2002. Conditional inactivation of the TGF-beta type II receptor using Cre:Lox. *Genesis* 32:73-5
150. Kawaguchi Y, Cooper B, Gannon M, Ray M, MacDonald RJ, Wright CV. 2002. The role of the transcriptional regulator Ptf1a in converting intestinal to pancreatic progenitors. *Nature genetics* 32:128-34
151. Erkan M, Adler G, Apte MV, Bachem MG, Buchholz M, et al. 2012. StellaTUM: current consensus and discussion on pancreatic stellate cell research. *Gut* 61:172-8
152. Borromeo MD, Meredith DM, Castro DS, Chang JC, Tung KC, et al. 2014. A transcription factor network specifying inhibitory versus excitatory neurons in the dorsal spinal cord. *Development* 141:2803-12
153. Ignotz RA, Massague J. 1986. Transforming growth factor-beta stimulates the expression of fibronectin and collagen and their incorporation into the extracellular matrix. *The Journal of biological chemistry* 261:4337-45
154. Labelle M, Hynes RO. 2012. The initial hours of metastasis: the importance of cooperative host-tumor cell interactions during hematogenous dissemination. *Cancer discovery* 2:1091-9
155. Pertovaara L, Kaipainen A, Mustonen T, Orpana A, Ferrara N, et al. 1994. Vascular endothelial growth factor is induced in response to transforming growth factor-beta in fibroblastic and epithelial cells. *The Journal of biological chemistry* 269:6271-4
156. Minn AJ, Gupta GP, Siegel PM, Bos PD, Shu W, et al. 2005. Genes that mediate breast cancer metastasis to lung. *Nature* 436:518-24
157. Yi T, Zhai B, Yu Y, Kiyotsugu Y, Raschle T, et al. 2014. Quantitative phosphoproteomic analysis reveals system-wide signaling pathways downstream of SDF-1/CXCR4 in breast cancer stem cells. *Proceedings of the National Academy of Sciences of the United States of America* 111:E2182-90

158. Kouro H, Kon S, Matsumoto N, Miyashita T, Kakuchi A, et al. 2014. The novel alpha4B murine alpha4 integrin protein splicing variant inhibits alpha4 protein-dependent cell adhesion. *The Journal of biological chemistry* 289:16389-98
159. Tsai YP, Yang MH, Huang CH, Chang SY, Chen PM, et al. 2009. Interaction between HSP60 and beta-catenin promotes metastasis. *Carcinogenesis* 30:1049-57
160. Medjkane S, Perez-Sanchez C, Gaggioli C, Sahai E, Treisman R. 2009. Myocardin-related transcription factors and SRF are required for cytoskeletal dynamics and experimental metastasis. *Nature cell biology* 11:257-68
161. Chiu KH, Chang YH, Wu YS, Lee SH, Liao PC. 2011. Quantitative secretome analysis reveals that COL6A1 is a metastasis-associated protein using stacking gel-aided purification combined with iTRAQ labeling. *Journal of proteome research* 10:1110-25
162. Bolignano D, Donato V, Lacquaniti A, Fazio MR, Bono C, et al. 2010. Neutrophil gelatinase-associated lipocalin (NGAL) in human neoplasias: a new protein enters the scene. *Cancer letters* 288:10-6
163. Adrian K, Strouch MJ, Zeng Q, Barron MR, Cheon EC, et al. 2009. Tgfbr1 haploinsufficiency inhibits the development of murine mutant Kras-induced pancreatic precancer. *Cancer research* 69:9169-74
164. Ostapoff KT, Cenik BK, Wang M, Ye R, Xu X, et al. 2014. Neutralizing murine TGFbetaR2 promotes a differentiated tumor cell phenotype and inhibits pancreatic cancer metastasis. *Cancer research* 74:4996-5007
165. Feig C, Jones JO, Kraman M, Wells RJ, Deonarine A, et al. 2013. Targeting CXCL12 from FAP-expressing carcinoma-associated fibroblasts synergizes with anti-PD-L1 immunotherapy in pancreatic cancer. *Proceedings of the National Academy of Sciences of the United States of America* 110:20212-7
166. Jacobetz MA, Chan DS, Neesse A, Bapiro TE, Cook N, et al. 2013. Hyaluronan impairs vascular function and drug delivery in a mouse model of pancreatic cancer. *Gut* 62:112-20
167. Provenzano PP, Cuevas C, Chang AE, Goel VK, Von Hoff DD, Hingorani SR. 2012. Enzymatic targeting of the stroma ablates physical barriers to treatment of pancreatic ductal adenocarcinoma. *Cancer cell* 21:418-29
168. Adorno M, Cordenonsi M, Montagner M, Dupont S, Wong C, et al. 2009. A Mutant-p53/Smad complex opposes p63 to empower TGFbeta-induced metastasis. *Cell* 137:87-98
169. Morton JP, Timpson P, Karim SA, Ridgway RA, Athineos D, et al. 2010. Mutant p53 drives metastasis and overcomes growth arrest/senescence in pancreatic cancer. *Proceedings of the National Academy of Sciences of the United States of America* 107:246-51
170. Weissmueller S, Manchado E, Saborowski M, Morris JPt, Wagenblast E, et al. 2014. Mutant p53 drives pancreatic cancer metastasis through cell-autonomous PDGF receptor beta signaling. *Cell* 157:382-94
171. Yachida S, White CM, Naito Y, Zhong Y, Brosnan JA, et al. 2012. Clinical significance of the genetic landscape of pancreatic cancer and implications for identification of potential long-term survivors. *Clinical cancer research : an official journal of the American Association for Cancer Research* 18:6339-47

172. Jonson T, Heidenblad M, Hakansson P, Gorunova L, Johansson B, et al. 2003. Pancreatic carcinoma cell lines with SMAD4 inactivation show distinct expression responses to TGFB1. *Genes, chromosomes & cancer* 36:340-52
173. Subramanian G, Schwarz RE, Higgins L, McEnroe G, Chakravarty S, et al. 2004. Targeting endogenous transforming growth factor beta receptor signaling in SMAD4-deficient human pancreatic carcinoma cells inhibits their invasive phenotype1. *Cancer research* 64:5200-11
174. Hezel AF, Deshpande V, Zimmerman SM, Contino G, Alagesan B, et al. 2012. TGF-beta and alphavbeta6 integrin act in a common pathway to suppress pancreatic cancer progression. *Cancer research* 72:4840-5
175. Perez-Mancera PA, Guerra C, Barbacid M, Tuveson DA. 2012. What we have learned about pancreatic cancer from mouse models. *Gastroenterology* 142:1079-92
176. Guerra C, Barbacid M. 2013. Genetically engineered mouse models of pancreatic adenocarcinoma. *Molecular oncology* 7:232-47
177. Olive KP, Jacobetz MA, Davidson CJ, Gopinathan A, McIntyre D, et al. 2009. Inhibition of Hedgehog signaling enhances delivery of chemotherapy in a mouse model of pancreatic cancer. *Science* 324:1457-61
178. Ozdemir BC, Pentcheva-Hoang T, Carstens JL, Zheng X, Wu CC, et al. 2014. Depletion of carcinoma-associated fibroblasts and fibrosis induces immunosuppression and accelerates pancreas cancer with reduced survival. *Cancer cell* 25:719-34
179. Kamisawa T, Isawa T, Koike M, Tsuruta K, Okamoto A. 1995. Hematogenous metastases of pancreatic ductal carcinoma. *Pancreas* 11:345-9
180. Mao C, Domenico DR, Kim K, Hanson DJ, Howard JM. 1995. Observations on the developmental patterns and the consequences of pancreatic exocrine adenocarcinoma. Findings of 154 autopsies. *Archives of surgery* 130:125-34
181. Moore MJ. 2005. Brief communication: a new combination in the treatment of advanced pancreatic cancer. *Semin Oncol* 32:5-6
182. Rini B. 2014. Future approaches in immunotherapy. *Seminars in oncology* 41 Suppl 5:S30-40
183. Vonderheide RH, Bayne LJ. 2013. Inflammatory networks and immune surveillance of pancreatic carcinoma. *Current opinion in immunology* 25:200-5
184. Bazhin AV, Shevchenko I, Umansky V, Werner J, Karakhanova S. 2014. Two immune faces of pancreatic adenocarcinoma: possible implication for immunotherapy. *Cancer immunology, immunotherapy : CII* 63:59-65
185. Mielgo A, Schmid MC. 2013. Impact of tumour associated macrophages in pancreatic cancer. *BMB reports* 46:131-8
186. Landskron G, De la Fuente M, Thuwajit P, Thuwajit C, Hermoso MA. 2014. Chronic inflammation and cytokines in the tumor microenvironment. *Journal of immunology research* 2014:149185
187. Ahmadzadeh M, Rosenberg SA. 2005. TGF-beta 1 attenuates the acquisition and expression of effector function by tumor antigen-specific human memory CD8 T cells. *Journal of immunology* 174:5215-23

188. Youn JI, Gabrilovich DI. 2010. The biology of myeloid-derived suppressor cells: the blessing and the curse of morphological and functional heterogeneity. *European journal of immunology* 40:2969-75
189. Stromnes IM, Brockenbrough JS, Izeradjene K, Carlson MA, Cuevas C, et al. 2014. Targeted depletion of an MDSC subset unmasks pancreatic ductal adenocarcinoma to adaptive immunity. *Gut* 63:1769-81
190. Wei S, Kryczek I, Zou W. 2006. Regulatory T-cell compartmentalization and trafficking. *Blood* 108:426-31
191. Halama N, Michel S, Kloor M, Zoernig I, Benner A, et al. 2011. Localization and density of immune cells in the invasive margin of human colorectal cancer liver metastases are prognostic for response to chemotherapy. *Cancer research* 71:5670-7
192. Lutz ER, Wu AA, Bigelow E, Sharma R, Mo G, et al. 2014. Immunotherapy converts nonimmunogenic pancreatic tumors into immunogenic foci of immune regulation. *Cancer immunology research* 2:616-31
193. Bornstein S, White R, Malkoski S, Oka M, Han G, et al. 2009. Smad4 loss in mice causes spontaneous head and neck cancer with increased genomic instability and inflammation. *The Journal of clinical investigation* 119:3408-19
194. Li MO, Wan YY, Sanjabi S, Robertson AK, Flavell RA. 2006. Transforming growth factor-beta regulation of immune responses. *Annual review of immunology* 24:99-146
195. Lu SL, Herrington H, Reh D, Weber S, Bornstein S, et al. 2006. Loss of transforming growth factor-beta type II receptor promotes metastatic head-and-neck squamous cell carcinoma. *Genes & development* 20:1331-42
196. Movahedi K, Guilliams M, Van den Bossche J, Van den Bergh R, Gysemans C, et al. 2008. Identification of discrete tumor-induced myeloid-derived suppressor cell subpopulations with distinct T cell-suppressive activity. *Blood* 111:4233-44
197. Umemura N, Saio M, Suwa T, Kitoh Y, Bai J, et al. 2008. Tumor-infiltrating myeloid-derived suppressor cells are pleiotropic-inflamed monocytes/macrophages that bear M1- and M2-type characteristics. *J Leukoc Biol* 83:1136-44
198. Medina-Echeverz J, Aranda F, Berraondo P. 2014. Myeloid-derived cells are key targets of tumor immunotherapy. *Oncoimmunology* 3:e28398
199. Kim S, Buchlis G, Fridlender ZG, Sun J, Kapoor V, et al. 2008. Systemic blockade of transforming growth factor-beta signaling augments the efficacy of immunogene therapy. *Cancer research* 68:10247-56
200. Martinez FO, Sica A, Mantovani A, Locati M. 2008. Macrophage activation and polarization. *Frontiers in bioscience : a journal and virtual library* 13:453-61
201. He S, Fei M, Wu Y, Zheng D, Wan D, et al. 2011. Distribution and clinical significance of Th17 cells in the tumor microenvironment and peripheral blood of pancreatic cancer patients. *International journal of molecular sciences* 12:7424-37
202. Smyth MJ, Dunn GP, Schreiber RD. 2006. Cancer immunosurveillance and immunoediting: the roles of immunity in suppressing tumor development and shaping tumor immunogenicity. *Advances in immunology* 90:1-50

203. Medler TR, Coussens LM. 2014. Duality of the immune response in cancer: lessons learned from skin. *The Journal of investigative dermatology* 134:E23-8

Curriculum Vitae

Anne M. Macgregor-Das

PERSONAL DATA

Business Address:

Johns Hopkins School of Medicine
Cancer Research Building II, Room 362
1550 Orleans Street
Baltimore, MD 21231

Phone: 410-955-3511
Fax: 410-614-0671
Email: amacgre1@jhmi.edu

ACADEMIC BACKGROUND/EDUCATION

2007 B.S., Microbiology, University of Maryland, College Park, MD
2015 Ph.D., Pathobiology, Department of Pathology, School of Medicine, The Johns Hopkins University School of Medicine, Baltimore, MD

RESEARCH EXPERIENCE

2002-2003 High School Research Program. Johns Hopkins School of Medicine, Baltimore, MD. Advisor: Dr. Leisha Emens

- Clones and expressed VEGF receptor in vaccine cancer cell lines which aided in the analysis of immune responses to a breast cancer vaccine
- Clones and expressed genes important in angiogenesis in tumors for breast cancer vaccine development.

2003-2007 Gemstone Honors Program Research Thesis. The University of Maryland, College Park, MD. Advisor: Dr. Kaci Thompson

- Four-year honors program designed to orient students to team research. Student teams design and complete a research project that culminates with the writing and defense of a thesis.
- My team assessed the reliability of state ballistics identification systems in accurately matching fired ammunition shell markings to their respective weapons

2004-2007 Undergraduate Honors Research Thesis. The University of Maryland, College Park, MD. Advisor: Dr. Louisa Wu

- Isolated and characterized genes that are important in the innate immune antiviral response to *Drosophila X* virus.
- Obtained an HHMI Fellowship to fund research, wrote and defended a thesis for University Honors Program.

2007-2008 Laboratory Technician. The Johns Hopkins School of Medicine, Baltimore, MD. Advisor: Dr. William Baldwin

- Used quantitative RT-PCR to identify potential markers of acute rejection in a rat cardiac transplant model.

2008-2009 Laboratory Technician. The Johns Hopkins School of Medicine, Baltimore, MD. Advisor: Dr. Marc Halushka

- Investigated advanced glycation end product (AGE)-mediated endothelial-mesenchymal transformation in primary human endothelial cells, and their role in diabetes progression

2009-2010 Graduate Laboratory- Rotations (3 mo each). The Johns Hopkins School of Medicine, Baltimore, MD. Advisors: Dr. Richard Roden, Dr. Leisha Emens, Dr. Christine Iacobuzio-Donahue, and Dr. Angelo DeMarzo

2010-2015 Graduate Thesis Research. The Johns Hopkins School of Medicine, Baltimore, MD. Advisor: Dr. Christine Iacobuzio-Donahue

- Created a novel murine model of pancreatic adenocarcinoma to study the role of TGF-beta signaling in PDA metastasis.
- Used this model to investigate how immune populations are altered in the tumor microenvironment in response to impaired TGF-beta signaling in tumor cells.

SCHOLARSHIPS, AWARDS, AND HONORS

2003-2005 Dean's Scholarship, The University of Maryland, College Park
2005-2007 Howard Hughes Undergraduate Fellowship Award
2006 Undergraduate Research Conference Award Biological Sciences, The University of Maryland Baltimore County
2010 Pathobiology Graduate Program Retreat Poster Award
2011-2012 Pathobiology Chief Graduate Student
2013 Pathobiology Graduate Program Retreat Poster Award
2014 Pathobiology Graduate Program Retreat Oral Presentation Award
2014 Pathology Young Investigator Day Poster Award for Translational Research

PUBLICATIONS

Macgregor AM, Eberhart CG, Fraig M, Lu J, Halushka MK. Tissue inhibitor of matrix metalloproteinase-3 levels in the extracellular matrix of lung, kidney, and eye increase with age. J Histochem Cytochem. 2009 Mar; 57(3):207-13.

Halushka MK, Selvin E, Lu J, **Macgregor AM**, Cornish TC. Use of human vascular tissue microarrays for measurement of advanced glycation endproducts. J Histochem Cytochem. 2009 Jun; 57(6):559-66.

Cornish TC, Bagnasco SM, **Macgregor AM**, Lu J, Selvin E, Halushka MK. Glomerular protein levels of matrix metalloproteinase-1 and tissue inhibitor of metalloproteinase-1 are lower in diabetic subjects. J Histochem Cytochem. 2009 Nov; 57(11):995-1001.

Santhanam L, Tuday EC, Webb AK, Dowzicky P, Kim JH, Oh YJ, Sikka G, Kuo M, Halushka MK, **Macgregor AM**, Dunn J, Gutbrod S, Yin D, Shoukas A, Nyhan D, Flavahan NA, Belkin AM, Berkowitz DE. Decreased S-nitrosylation of tissue transglutaminase contributes to age-related increases in vascular stiffness. Circ Res. 2010 Jul 9; 107(1):117-25.

Yachida S, White CM, Naito Y, Zhong Y, Brosnan JA, **Macgregor-Das AM**, Morgan RA, Saunders T, Laheru DA, Herman JM, Hruban RH, Klein AP, Jones S, Velculescu V, Wolfgang CL, Iacobuzio-Donahue CA. Clinical significance of the genetic landscape of pancreatic cancer and implications for identification of potential long-term survivors. Clin Cancer Res. 2012 Nov 15; 18(22):6339-47.

Macgregor-Das AM, Iacobuzio-Donahue CA. Molecular pathways in pancreatic carcinogenesis. J Surg Oncol. 2013, Jan. 107(1):8-14.

Streppel MM, Lata S, Delabastide M, Montgomery EA, Wang JS, Canto MI, **Macgregor-Das AM**, Pai S, Morsink FH, Offerhaus GJ, Antoniou E, Maitra A, McCombie WR. Next-generation sequencing of endoscopic biopsies identifies ARID1A as a tumor-suppressor gene in Barrett's esophagus. Oncogene. 2014 Jan 16; 33(3): 347-57.

ABSTRACTS AND PRESENTATIONS

Macgregor, A., & Wu, L. Identification of novel genes affecting the *Drosophila melanogaster* immune response to DXV. UMBC Undergraduate Research Conference, Baltimore, MD, October 2006.

Macgregor, A. & Wu, L. Identification of novel genes affecting the *D. melanogaster* immune response to DXV. 48th Annual *Drosophila* Research Conference, Philadelphia, PA, March 2007.

Macgregor, A. & Wu, L. Identification of novel antiviral genes affecting the *D.melanogaster* immune response to DXV. National Conference on Undergraduate Research, San Francisco, CA, April 2007.

Wu, L., **Macgregor, A**., Zambon, R., and Tang, J. The Role of RNAi and the Toll Pathway in Antiviral Immune Responses in *Drosophila*. 20th Naito Conference on Innate Immunity in Medicine and Biology, Kanagawa, Japan, October 2007.

Erdinc, M., **Macgregor, A**., Lucas, D.P., Leffell, M.S., Montgomery, R.A., Zachary, A.A., Baldwin, W.M. III, and Wasowska, B.A. IVIg inhibits C1q- and Mannose Binding Lectin (MBL)-dependent deposition of C4d by human alloantibodies. American Transplant Congress, Toronto, May 2008. American J Transpl, 2008, 8, s2: 568.

Halushka, M.K., Cornish, T.C., Lu, J., **Macgregor, A.M**., and Selvin, E. Human Vascular Tissue Microarrays to Investigate Diabetic Vascular Disease. Mid-Atlantic Diabetes Research Symposia, Washington, DC, October 2008.

Macgregor, A., Fox-Talbot, K., Velidedeogiu, E., Baldwin, W.M., and Wasowska, B.A. The Absence of FcγRIII Results in Increased Pro-Inflammatory Response in FcγRIII KO Cardiac Allograft Recipients. American Transplant Congress, Boston, May 2009.

Macgregor-Das, A. and Iacobuzio-Donahue, C. The Role of the Tumor Microenvironment in Pancreatic Cancer Metastasis. Pathobiology Young Investigator Day, Baltimore, April 2014.

TEACHING AND LEADERSHIP

2005-2006	Teaching Assistant Gemstone Program, The University of Maryland College Park
2011-2012	Chief Graduate Student Pathobiology Program, Johns Hopkins School of Medicine

JOHN WILEY AND SONS LICENSE
TERMS AND CONDITIONS

Mar 18, 2015

This Agreement between Anne M Macgregor-Das ("You") and John Wiley and Sons ("John Wiley and Sons") consists of your license details and the terms and conditions provided by John Wiley and Sons and Copyright Clearance Center.

License Number	3592040252566
License date	Mar 18, 2015
Licensed Content Publisher	John Wiley and Sons
Licensed Content Publication	Journal of Surgical Oncology
Licensed Content Title	Molecular pathways in pancreatic carcinogenesis
Licensed Content Author	Anne M. Macgregor-Das,Christine A. Iacobuzio-Donahue
Licensed Content Date	Jul 17, 2012
Pages	7
Type of use	Dissertation/Thesis
Requestor type	Author of this Wiley article
Format	Electronic
Portion	Full article
Will you be translating?	No
Title of your thesis / dissertation	Cell-Autonomous and Non-Autonomous Roles for TGF-beta Signaling in Pancreatic Cancer Metastasis
Expected completion date	Mar 2015
Expected size (number of pages)	162